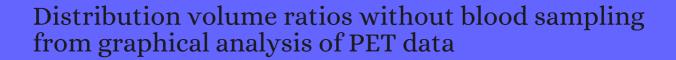
# CITATION REPORT List of articles citing



DOI: 10.1097/00004647-199609000-00008 Journal of Cerebral Blood Flow and Metabolism, 1996, 16, 834-40.

Source: https://exaly.com/paper-pdf/27483984/citation-report.pdf

Version: 2024-04-28

This report has been generated based on the citations recorded by exaly.com for the above article. For the latest version of this publication list, visit the link given above.

The third column is the impact factor (IF) of the journal, and the fourth column is the number of citations of the article.

#	Paper	IF	Citations
1297	Quantitative comparison of 3D and 2D PET with brain studies.		
1296	Parametric imaging of ligand-receptor binding in PET using a simplified reference region model. <b>1997</b> , 6, 279-87		883
1295	Cocaine abusers do not show loss of dopamine transporters with age. <b>1997</b> , 61, 1059-65		35
1294	Concentration and occupancy of dopamine transporters in cocaine abusers with [11C]cocaine and PET. <b>1997</b> , 27, 347-56		43
1293	Age-dependent decline of dopamine D1 receptors in human brain: a PET study. <b>1998</b> , 30, 56-61		175
1292	Positron emission tomography (PET) methodology for small animals and its application in radiopharmaceutical preclinical investigation. <b>1998</b> , 25, 729-32		36
1291	N-[11C]methylspiperone PET, in contrast to [11C]raclopride, fails to detect D2 receptor occupancy by an atypical neuroleptic. <b>1998</b> , 82, 147-60		25
1290	Comparison of FORE, OSEM and SAGE algorithms to 3DRP in 3D PET using phantom and human subject data.		1
1289	Studies of the effects of ECT on the dopamine receptors. <b>1998</b> , 7, S234		
1288	Loss of D2 receptor binding with age in rhesus monkeys: importance of correction for differences in striatal size. <i>Journal of Cerebral Blood Flow and Metabolism</i> , <b>1999</b> , 19, 218-29	7.3	57
1287	Presynaptic and postsynaptic dopaminergic binding densities in the nigrostriatal and mesocortical systems in early Parkinson's disease: a double-tracer positron emission tomography study. <b>1999</b> , 46, 723-31		53
1286	Striatal uptake of a novel PET ligand, [18F]beta-CFT, is reduced in early Parkinson's disease. <b>1999</b> , 31, 119-24		42
1285	Comparison of FORE, OSEM and SAGE algorithms to 3DRP in 3D PET using phantom and human subject data. <b>1999</b> , 46, 1114-1120		10
1284	Access www.neurology.org now for full-text articles. <b>2000</b> , 55, 209		
1283	Dopamine D(2) receptor quantification in extrastriatal brain regions using [(123)I]epidepride with bolus/infusion. <b>2000</b> , 36, 322-9		17
1282	In vivo positron emission tomographic evidence for compensatory changes in presynaptic dopaminergic nerve terminals in Parkinson's disease. <b>2000</b> , 47, 493-503		443
1281	Quantitation of striatal and extrastriatal D-2 dopamine receptors using PET imaging of [(18)F]fallypride in nonhuman primates. <b>2000</b> , 38, 71-9		64

### (2001-2000)

1280	In vivo PET studies of the dopamine D2 receptors in rhesus monkeys with long-term MPTP-induced parkinsonism. <b>2000</b> , 38, 105-13		41
1279	Measurement of striatal and extrastriatal dopamine D1 receptor binding potential with [11C]NNC 112 in humans: validation and reproducibility. <i>Journal of Cerebral Blood Flow and Metabolism</i> , <b>2000</b> , 20, 225-43	7.3	128
1278	Analysis of four dopaminergic tracers kinetics using two different tissue input function methods.  Journal of Cerebral Blood Flow and Metabolism, 2000, 20, 653-60	7.3	19
1277	Modeling dynamic PET-SPECT studies in the wavelet domain. <i>Journal of Cerebral Blood Flow and Metabolism</i> , <b>2000</b> , 20, 879-93	7.3	50
1276	Buprenorphine-induced changes in mu-opioid receptor availability in male heroin-dependent volunteers: a preliminary study. <b>2000</b> , 23, 326-34		98
1275	Measurement of extrastriatal D2-like receptor binding with [11C]FLB 457a test-retest analysis. <b>2000</b> , 27, 1666-73		44
1274	Simplified quantification of dopamine transporters in humans using [99mTc]TRODAT-1 and single-photon emission tomography. <b>2000</b> , 27, 1714-8		28
1273	PET shows that striatal dopamine D1 and D2 receptors are differentially affected in AD. <b>2000</b> , 55, 205-9		62
1272	Access www.neurology.org now for full-text articles. <b>2000</b> , 54, 2251		
1271	[11 C]Flumazenil binding in the medial temporal lobe in patients with temporal lobe epilepsy: correlation with hippocampal MR volumetry, T2 relaxometry, and neuropathology. <b>2000</b> , 54, 2252-60		53
1270	Derivation of [(11)C]WAY-100635 binding parameters with reference tissue models: effect of violations of model assumptions. <b>2000</b> , 27, 487-92		56
1269	Graphical analysis of PET data applied to reversible and irreversible tracers. <b>2000</b> , 27, 661-70		303
1268	PET physiological measurements using constant infusion. <b>2000</b> , 27, 657-60		73
1267	The role of model-based methods in the development of single scan techniques. <b>2000</b> , 27, 637-42		17
1266	D(2) and 5HT(2A) receptor occupancy of different doses of quetiapine in schizophrenia: a PET study. <b>2001</b> , 11, 105-10		112
1265	Expectation and dopamine release: mechanism of the placebo effect in Parkinson's disease. <b>2001</b> , 293, 1164-6		732
1264	Models and methods for derivation of in vivo neuroreceptor parameters with PET and SPECT reversible radiotracers. <b>2001</b> , 28, 595-608		162
1263	Regional mu opioid receptor regulation of sensory and affective dimensions of pain. <b>2001</b> , 293, 311-5		668

1262	Physiological Modelling of Positron Emission Tomography Images. <b>2001</b> , 179-211	2
1261	Analyses of [(18)F]altanserin bolus injection PET data. II: consideration of radiolabeled metabolites in humans. <b>2001</b> , 41, 11-21	47
1260	Effect of endogenous dopamine on extrastriatal [IIIC]FLB 457 binding measured by PET. <b>2001</b> , 41, 87-95	55
1259	Age-related changes of dopamine D1-like and D2-like receptor binding in the F344/N rat striatum revealed by positron emission tomography and in vitro receptor autoradiography. <b>2001</b> , 41, 285-93	45
1258	Biochemical variations in the synaptic level of dopamine precede motor fluctuations in Parkinson's disease: PET evidence of increased dopamine turnover. <b>2001</b> , 49, 298-303	179
1257	Modeling of receptor ligand data in PET and SPECT imaging: a review of major approaches. <b>2001</b> , 11, 30-9	25
1256	A strategy for removing the bias in the graphical analysis method. <i>Journal of Cerebral Blood Flow and Metabolism</i> , <b>2001</b> , 21, 307-20	133
1255	A reversible tracer analysis approach to the study of effective dopamine turnover. <i>Journal of Cerebral Blood Flow and Metabolism</i> , <b>2001</b> , 21, 469-76	57
1254	Imaging human mesolimbic dopamine transmission with positron emission tomography: I. Accuracy and precision of D(2) receptor parameter measurements in ventral striatum. <i>Journal of Cerebral Blood Flow and Metabolism</i> , <b>2001</b> , 21, 1034-57	458
1253	Measurement of cortical dopamine d1 receptor binding with 11C[SCH23390]: a test-retest analysis.  Journal of Cerebral Blood Flow and Metabolism, 2001, 21, 1146-50	26
1252	Apomorphine-induced changes in synaptic dopamine levels: positron emission tomography evidence for presynaptic inhibition. <i>Journal of Cerebral Blood Flow and Metabolism</i> , <b>2001</b> , 21, 1151-9	46
1251	Evaluation of dopamine D-2 receptor occupancy by clozapine, risperidone, and haloperidol in vivo in the rodent and nonhuman primate brain using 18F-fallypride. <b>2001</b> , 25, 476-88	59
1250	mu-Opioid receptors and limbic responses to aversive emotional stimuli. <b>2002</b> , 99, 7084-9	73
1249	Fast formation of statistically reliable FDG parametric images based on clustering and principal components. <b>2002</b> , 47, 455-68	53
1248	Positron emission tomography shows reduced striatal dopamine D1 but not D2 receptors in juvenile neuronal ceroid lipofuscinosis. <b>2002</b> , 33, 138-41	17
1247	Bilateral human fetal striatal transplantation in Huntington's disease. <b>2002</b> , 58, 687-95	208
1246	Human [/sup 123/I]5-I-A-85380 dynamic SPECT studies in normals: kinetic analysis and parametric imaging.	
1245	Serotonin transporter binding in patients with mood disorders: a PET study with [11C](+)McN5652. <b>2002</b> , 51, 715-22	132

1244	Age-related decline of serotonin transporters in living human brain of healthy males. <b>2002</b> , 71, 751-7	68
1243	Monitoring the correction of glycogen storage disease type 1a in a mouse model using [(18)F]FDG and a dedicated animal scanner. <b>2002</b> , 71, 1293-301	9
1242	Improved parametric image generation using spatial-temporal analysis of dynamic PET studies. <b>2002</b> , 15, 697-707	47
1241	Wavelet-aided parametric mapping of cerebral dopamine D2 receptors using the high affinity PET radioligand [11C]FLB 457. <b>2002</b> , 17, 47-60	49
1240	Abstracts. <b>2002</b> , 16, S1-S108	
1239	Positron emission tomography: imaging and quantification of neurotransporter availability. <b>2002</b> , 27, 287-99	83
1238	Cerebral uptake of [ethyl-11C]vinpocetine and 1-[11C]ethanol in cynomolgous monkeys: a comparative preclinical PET study. <b>2002</b> , 29, 753-9	12
1237	Dopamine release in human ventral striatum and expectation of reward. <b>2002</b> , 136, 359-63	275
1236	mu-opioid receptor-mediated antinociceptive responses differ in men and women. <b>2002</b> , 22, 5100-7	297
1235	The impact of prenatal stress, fetal alcohol exposure, or both on development: perspectives from a primate model. <b>2002</b> , 27, 285-98	160
1234	Quantification of [(123)I]PE2I binding to dopamine transporters with SPET. <b>2002</b> , 29, 623-31	13
1233	Quantification of dopamine transporters in the mouse brain using ultra-high resolution single-photon emission tomography. <b>2002</b> , 29, 691-8	76
1232	PET studies on the brain uptake and regional distribution of [11C]vinpocetine in human subjects. <b>2002</b> , 106, 325-32	45
1231	In vivo PET studies of the dopamine D1 receptors in rhesus monkeys with long-term MPTP-induced Parkinsonism. <b>2002</b> , 44, 111-5	11
1230	Density and affinity of the dopamine D2 receptors in aged symptomatic and asymptomatic MPTP-treated monkeys: PET studies with [11C]raclopride. <b>2002</b> , 44, 198-202	34
1229	Mu-receptor agonism with alfentanil increases striatal dopamine D2 receptor binding in man. <b>2002</b> , 45, 25-30	49
1228	Brain imaging of 18F-fallypride in normal volunteers: blood analysis, distribution, test-retest studies, and preliminary assessment of sensitivity to aging effects on dopamine D-2/D-3 receptors. <b>2002</b> , 46, 170-88	223
1227	Increase in dopamine turnover occurs early in Parkinson's disease: evidence from a new modeling approach to PET 18 F-fluorodopa data. <i>Journal of Cerebral Blood Flow and Metabolism</i> , <b>2002</b> , 22, 232-9 $7.3$	101

1226	Quantitative analysis for estimating binding potential of the brain serotonin transporter with [11 C]McN5652. <i>Journal of Cerebral Blood Flow and Metabolism</i> , <b>2002</b> , 22, 490-501	7.3	35
1225	In vivo receptor assay with multiple ligand concentrations: an equilibrium approach. <i>Journal of Cerebral Blood Flow and Metabolism</i> , <b>2002</b> , 22, 1132-41	7.3	32
1224	Positron emission tomography compartmental models: a basis pursuit strategy for kinetic modeling. <i>Journal of Cerebral Blood Flow and Metabolism</i> , <b>2002</b> , 22, 1425-39	7.3	148
1223	Decreased striatal D2 receptor density associated with severe behavioral abnormality in Alzheimer's disease. <b>2003</b> , 17, 567-73		63
1222	Quantification of human brain benzodiazepine receptors using [18F]fluoroethylflumazenil: a first report in volunteers and epileptic patients. <b>2003</b> , 30, 1630-6		12
1221	Chronic subthalamic nucleus stimulation and striatal D2 dopamine receptors in Parkinson's diseaseA [(11)C]-raclopride PET study. <b>2003</b> , 250, 1219-23		44
1220	Deep brain stimulation of the subthalamic nucleus does not increase the striatal dopamine concentration in parkinsonian humans. <b>2003</b> , 18, 41-8		128
1219	Positron emission tomography (PET) advances in neurological applications. 2003, 510, 107-115		1
1218	Age and severity of nigrostriatal damage at onset of Parkinson's disease. <b>2003</b> , 47, 152-8		32
1217	Graphical analysis of 2-[18F]FA binding to nicotinic acetylcholine receptors in rhesus monkey brain. <b>2003</b> , 48, 25-34		76
1216	VMAT2 binding is elevated in dopa-responsive dystonia: visualizing empty vesicles by PET. <b>2003</b> , 49, 20	0-8	61
1215	No association between genotype of the promoter region of serotonin transporter gene and serotonin transporter binding in human brain measured by PET. <b>2003</b> , 48, 184-8		157
1214	In vivo measurement of receptor density and affinity: comparison of the routine sequential method with a nonsequential method in studies of dopamine D2 receptors with [11C]raclopride. <i>Journal of Cerebral Blood Flow and Metabolism</i> , <b>2003</b> , 23, 280-4	7.3	9
1213	Linearized reference tissue parametric imaging methods: application to [11C]DASB positron emission tomography studies of the serotonin transporter in human brain. <i>Journal of Cerebral Blood Flow and Metabolism</i> , <b>2003</b> , 23, 1096-112	7.3	502
1212	Sequential versus nonsequential measurement of density and affinity of dopamine D2 receptors with [11C]raclopride: effect of methamphetamine. <i>Journal of Cerebral Blood Flow and Metabolism</i> , <b>2003</b> , 23, 1489-94	7.3	17
1211	Principles of tracer kinetic analysis. <b>2003</b> , 13, 689-704		12
1210	Linear regression with spatial constraint to generate parametric images of ligand-receptor dynamic PET studies with a simplified reference tissue model. <b>2003</b> , 18, 975-89		104
1209	Presymptomatic diagnosis of experimental Parkinsonism with 123I-PE2I SPECT. <b>2003</b> , 19, 810-6		36

1208 Raclopride studies of dopamine release: dependence on presynaptic integrity. <b>2003</b> , 54, 1193-9	21
1207 Striatal dopamine D1 and D2 receptors in burning mouth syndrome. <b>2003</b> , 101, 149-54	186
1206 Altered dopamine D2 receptor binding in atypical facial pain. <b>2003</b> , 106, 43-8	152
Quantification of brain mu-opioid receptors with [11C]carfentanil: reference-tissue methods. <b>2003</b> , 30, 177-86	56
Small animal imaging with high resolution single photon emission tomography. <b>2003</b> , 30, 889-95	84
1203 A review of graphical methods for tracer studies and strategies to reduce bias. <b>2003</b> , 30, 833-44	67
1202 The use of gene-manipulated mice in the validation of receptor binding radiotracer. <b>2003</b> , 30, 851-60	17
1201 A linear wavelet filter for parametric imaging with dynamic PET. <b>2003</b> , 22, 289-301	56
Regulation of human affective responses by anterior cingulate and limbic mu-opioid neurotransmission. <b>2003</b> , 60, 1145-53	293
1199 [11C]DTBZ-PET correlates of levodopa responses in asymmetric Parkinson's disease. <b>2003</b> , 126, 2648-55	57
1198 A noninvasive LSO-APD blood radioactivity monitor for PET imaging studies. <b>2003</b> , 50, 1457-1461	3
Effects of buprenorphine maintenance dose on mu-opioid receptor availability, plasma concentrations, and antagonist blockade in heroin-dependent volunteers. <b>2003</b> , 28, 2000-9	206
Rank-shaping regularization of exponential spectral analysis for application to functional parametric mapping. <b>2003</b> , 48, 3819-41	33
High levels of serotonin transporter occupancy with low-dose clomipramine in comparative occupancy study with fluvoxamine using positron emission tomography. <b>2003</b> , 60, 386-91	104
1194 Kinetic Modeling in Positron Emission Tomography. <b>2004</b> , 499-540	44
Positron emission tomography receptor assay with multiple ligand concentrations: an equilibrium approach. <b>2004</b> , 385, 169-84	4
Imaging dopamine receptors in the rat striatum with the MicroPET R4: kinetic analysis of [11C]raclopride binding using graphical methods. <b>2004</b> , 385, 213-28	5
Quantitative analysis of dopamine D2 receptor kinetics with small animal positron emission tomography. <b>2004</b> , 385, 228-39	3

1190 Impact of motion correction on parametric images in PET neuroreceptor studies.

1189	Risperidone is effective for wandering and disturbed sleep/wake patterns in Alzheimer's disease. <b>2004</b> , 17, 61-7	41
1188	Brain serotonin transporter binding potential measured with carbon 11-labeled DASB positron emission tomography: effects of major depressive episodes and severity of dysfunctional attitudes. <b>2004</b> , 61, 1271-9	235
1187	Effect of normalization method on image uniformity and binding potential estimates on microPET.	2
1186	Decreased brain dopaminergic transporters in HIV-associated dementia patients. 2004, 127, 2452-8	172
1185		
1184	Limbic reductions of 5-HT1A receptor binding in human temporal lobe epilepsy. <b>2004</b> , 62, 1343-51	147
1183	Evaluation of 5-(2-(4-pyridinyl)vinyl)-6-chloro-3-(1-methyl-2-(S)-pyrrolidinylmethoxy)pyridine and its analogues as PET radioligands for imaging nicotinic acetylcholine receptors. <b>2004</b> , 91, 600-12	16
1182	DRD2 gene transfer into the nucleus accumbens core of the alcohol preferring and nonpreferring rats attenuates alcohol drinking. <b>2004</b> , 28, 720-8	90
1181	Measuring the in vivo binding parameters of [18F]-fallypride in monkeys using a PET multiple-injection protocol. <i>Journal of Cerebral Blood Flow and Metabolism</i> , <b>2004</b> , 24, 309-22	47
1180	Prenatal stress, moderate fetal alcohol, and dopamine system function in rhesus monkeys. <b>2004</b> , 26, 169-78	43
1179	Striatal dopaminergic system in dopa-responsive dystonia: a multi-tracer PET study shows increased D2 receptors. <b>2004</b> , 111, 59-67	30
1178	Evaluation of the use of a standard input function for compartment analysis of [1231]iomazenil data: factors influencing the quantitative results. <b>2004</b> , 18, 563-72	5
1177	In vivo affinity of [18F]fallypride for striatal and extrastriatal dopamine D2 receptors in nonhuman primates. <b>2004</b> , 175, 274-86	54
1176	Non-invasive assessment of distribution volume ratios and binding potential: tissue heterogeneity and interindividually averaged time-activity curves. <b>2004</b> , 31, 564-77	8
1175	MDMA-evoked changes in [11C]raclopride and [11C]NMSP binding in living pig brain. <b>2004</b> , 53, 222-33	34
1174	Imaging brain amyloid in Alzheimer's disease with Pittsburgh Compound-B. <b>2004</b> , 55, 306-19	3088
1173	PET Measurement of rCBF in the presence of a neurochemical tracer. <b>2004</b> , 132, 199-208	12

1172 Fully 4D dynamic image reconstruction by nonlinear constrained programming.

1171	Levodopa-induced changes in synaptic dopamine levels increase with progression of Parkinson's disease: implications for dyskinesias. <b>2004</b> , 127, 2747-54	307
1170	Gradients of dopamine D1- and D2/3-binding sites in the basal ganglia of pig and monkey measured by PET. <b>2004</b> , 22, 1076-1076	
1169	Dopamine transporter density in schizophrenic subjects with and without tardive dyskinesia. <b>2004</b> ,	
1168	[123I]AM281 single-photon emission computed tomography imaging of central cannabinoid CB1 receptors before and after Delta9-tetrahydrocannabinol therapy and whole-body scanning for assessment of radiation dose in tourette patients. <b>2004</b> , 55, 904-15	43
1167	Dopamine transporter density in schizophrenic subjects with and without tardive dyskinesia. <b>2004</b> , 71, 371-5	33
1166	PET imaging of implanted human retinal pigment epithelial cells in the MPTP-induced primate model of Parkinson's disease. <b>2004</b> , 189, 361-8	41
1165	Sensitivity of [11C]N-methylpyrrolidinyl benzilate ([11C]NMPYB) to endogenous acetylcholine: PET imaging vs tissue sampling methods. <b>2004</b> , 31, 393-7	12
1164	Simplified PET measurement for evaluating histamine H1 receptors in human brains using [11C]doxepin. <b>2004</b> , 31, 1005-11	18
1163	Bootstrapped DEPICT for error estimation in PET functional imaging. <b>2004</b> , 21, 1096-104	10
1162	Gradients of dopamine D1- and D2/3-binding sites in the basal ganglia of pig and monkey measured by PET. <b>2004</b> , 22, 1076-83	25
1161	Serotonin transporter occupancy of five selective serotonin reuptake inhibitors at different doses: an [11C]DASB positron emission tomography study. <b>2004</b> , 161, 826-35	399
1160	Limitations of bi-linear regression analysis for the determination of receptor occupancy with positron emission tomography. <b>2004</b> , 25, 451-9	5
1159	Effects of metabolite correction for arterial input function on quantitative receptor images with 11C-flumazenil in clinical positron emission tomography studies. <b>2004</b> , 28, 428-35	15
1158	Quantitative Functional Imaging with Positron Emission Tomography: Principles and Instrumentation. <b>2005</b> , 57-116	1
1157	PET in LRRK2 mutations: comparison to sporadic Parkinson's disease and evidence for presymptomatic compensation. <b>2005</b> , 128, 2777-85	208
1156	MicroPET/sup /spl reg// R4 neuro-imaging in rats and post-mortem measures.	
1155	In-vivo PET imaging of inducible D2R reporter transgene expression using [11C]FLB 457 as reporter probe in living rats. <b>2005</b> , 26, 259-68	12

1154	Development of a simultaneous PET/microdialysis method to identify the optimal dose of 11C-raclopride for small animal imaging. <b>2005</b> , 144, 25-34	35
1153	Kinetic modeling of amyloid binding in humans using PET imaging and Pittsburgh Compound-B.  Journal of Cerebral Blood Flow and Metabolism, <b>2005</b> , 25, 1528-47  7.3	566
1152	Dopamine D(2) receptor availability is associated with subjective responses to alcohol. <b>2005</b> , 29, 965-70	60
1151	Moderate-level prenatal alcohol exposure alters striatal dopamine system function in rhesus monkeys. <b>2005</b> , 29, 1685-97	40
1150	A positron emission tomography (PET) study of cerebral dopamine D2 and serotonine 5-HT2A receptor occupancy in patients treated with cyamemazine (Tercian). <b>2005</b> , 180, 377-84	81
1149	Analysis of neuroreceptor PET-data based on cytoarchitectonic maximum probability maps: a feasibility study. <b>2005</b> , 210, 447-53	9
1148	Decreased prefrontal 5-HT2A receptor binding in subjects at enhanced risk for schizophrenia. <b>2005</b> , 210, 519-23	35
1147	Micropet imaging: in vivo biochemistry in small animals. <b>2005</b> , 112, 319-30	38
1146	Use of reference tissue models for quantification of histamine H1 receptors in human brain by using positron emission tomography and [11c]doxepin. <b>2005</b> , 19, 425-33	16
1145	An internet-based "kinetic imaging system" (KIS) for MicroPET. <b>2005</b> , 7, 330-41	40
1144	Interaction between LSD and dopamine D2/3 binding sites in pig brain. <b>2005</b> , 56, 198-204	18
1143	ntPET: A New Application of PET Imaging for Characterizing the Kinetics of Endogenous Neurotransmitter Release. <b>2005</b> , 4, 7290.2005.05130	45
1142	A new mutation of the tau gene, G303V, in early-onset familial progressive supranuclear palsy. <b>2005</b> , 62, 1444-50	81
1141	Attenuation of fluctuating striatal synaptic dopamine levels in patients with Parkinson disease in response to subthalamic nucleus stimulation: a positron emission tomography study. <b>2005</b> , 103, 968-73	34
1140	Placebo effects mediated by endogenous opioid activity on mu-opioid receptors. <b>2005</b> , 25, 7754-62	607
1139	Kinetic modeling of PET data without blood sampling. <b>2005</b> , 52, 697-702	14
1138	Tracer Kinetic Modeling in PET. <b>2005</b> , 127-159	48
1137	Dopamine transporter positron emission tomography in spinocerebellar ataxias type 1, 2, 3, and 6. <b>2005</b> , 62, 1280-5	81

1136	Regional reductions in serotonin 1A receptor binding in juvenile myoclonic epilepsy. <b>2005</b> , 62, 946-50	56
1135	The influence of measurement uncertainties on the evaluation of the distribution volume ratio and binding potential in rat studies on a microPET R4: a phantom study. <b>2005</b> , 50, 2859-69	10
1134	Wavelet variance components in image space for spatiotemporal neuroimaging data. <b>2005</b> , 25, 159-68	16
1133	Omission of serial arterial blood sampling in neuroreceptor imaging with independent component analysis. <b>2005</b> , 26, 885-90	28
1132	Positron Emission Tomography. <b>2005</b> ,	209
1131	Behavioral response to novelty correlates with dopamine receptor availability in striatum of GEtingen minipigs. <b>2005</b> , 164, 172-7	22
1130	Mapping the amphetamine-evoked dopamine release in the brain of the GEtingen minipig. <b>2005</b> , 65, 1-9	26
1129	The slow and long-lasting blockade of dopamine transporters in human brain induced by the new antidepressant drug radafaxine predict poor reinforcing effects. <b>2005</b> , 57, 640-6	45
1128	Imaging brain mu-opioid receptors in abstinent cocaine users: time course and relation to cocaine craving. <b>2005</b> , 57, 1573-82	138
1127	Effects of tryptophan depletion on the serotonin transporter in healthy humans. <b>2005</b> , 58, 825-30	89
1126	[11C]vinpocetine: a prospective peripheral benzodiazepine receptor ligand for primate PET studies. <b>2005</b> , 229-230, 219-23	37
1125	Neuroreceptor imaging in psychiatry: theory and applications. <b>2005</b> , 67, 385-440	13
1124	Handbook of Biomedical Image Analysis. 2005,	13
1123	MAP-based kinetic analysis for voxel-by-voxel compartment model estimation: detailed imaging of the cerebral glucose metabolism using FDG. <b>2006</b> , 29, 1203-11	10
1122	Effect of age on markers for monoaminergic neurons of normal and MPTP-lesioned rhesus monkeys: a multi-tracer PET study. <b>2006</b> , 30, 26-35	46
1121	High opiate receptor binding potential in the human lateral pain system. <b>2006</b> , 30, 692-9	120
1120	A comparison of recent parametric neuroreceptor mapping approaches based on measurements with the high affinity PET radioligands [11C]FLB 457 and [11C]WAY 100635. <b>2006</b> , 32, 1690-708	63
1119	Multi-resolution Bayesian regression in PET dynamic studies using wavelets. <b>2006</b> , 32, 111-21	36

1118	A1 adenosine receptor PET using [18F]CPFPX: displacement studies in humans. <b>2006</b> , 32, 1100-5	17
1117	Evaluation of voxel-based methods for the statistical analysis of PIB PET amyloid imaging studies in Alzheimer's disease. <b>2006</b> , 33, 94-102	105
1116	An extended simplified reference tissue model for the quantification of dynamic PET with amphetamine challenge. <b>2006</b> , 33, 550-63	37
1115	Acute occupancy of brain serotonin transporter by sertraline as measured by [11C]DASB and positron emission tomography. <b>2006</b> , 59, 821-8	99
1114	D2/D3 dopamine receptor binding with [F-18]fallypride in thalamus and cortex of patients with schizophrenia. <b>2006</b> , 85, 232-44	116
1113	Belief or Need? Accounting for individual variations in the neurochemistry of the placebo effect. <b>2006</b> , 20, 15-26	83
1112	. 2006,	1
1111	Dysregulation of endogenous opioid emotion regulation circuitry in major depression in women. <b>2006</b> , 63, 1199-208	220
1110	Quantitative autoradiography of ligands for dopamine receptors and transporters in brain of GEtingen minipig: comparison with results in vivo. <b>2006</b> , 59, 211-9	24
1109	Therapeutic doses of amphetamine or methylphenidate differentially increase synaptic and extracellular dopamine. <b>2006</b> , 59, 243-51	92
1108	Inhibition of [11C]mirtazapine binding by alpha2-adrenoceptor antagonists studied by positron emission tomography in living porcine brain. <b>2006</b> , 59, 463-71	20
1107	Imaging triiodothyronine binding kinetics in rat brain: a model for studies in human subjects. <b>2006</b> , 60, 212-22	8
1106	Sequential versus nonsequential measurement of density and affinity of dopamine D2 receptors with [11C]raclopride: 2: effects of DAT inhibitors. <i>Journal of Cerebral Blood Flow and Metabolism</i> , 7.3 <b>2006</b> , 26, 28-37	2
1105	Serial microPET measures of the metabolic reaction to a microdialysis probe implant. <b>2006</b> , 155, 272-84	135
1104	[(11)C]d-threo-methylphenidate PET in patients with Parkinson's disease and essential tremor. <b>2006</b> , 113, 187-93	35
1103	Imaging of serotonin transporters and its blockade by citalopram in patients with major depression using a novel SPECT ligand [123I]-ADAM. <b>2006</b> , 113, 659-70	57
1102	Atomoxetine occupies the norepinephrine transporter in a dose-dependent fashion: a PET study in nonhuman primate brain using (S,S)-[18F]FMeNER-D2. <b>2006</b> , 188, 119-27	68
1101	Occupancy of dopamine D(1), D (2) and serotonin (2A) receptors in schizophrenic patients treated with flupentixol in comparison with risperidone and haloperidol. <b>2007</b> , 190, 241-9	42

Oral methylphenidate fails to elicit significant changes in extracellular putaminal dopamine levels in Parkinson's disease patients: positron emission tomographic studies. <b>2006</b> , 21, 970-5	12
Inverse relation between in vivo amyloid imaging load and cerebrospinal fluid Abeta42 in humans. <b>2006</b> , 59, 512-9	1009
1098 In Vivo Radiotracer Imaging. 103-147	
Comparison between the ROI based and pixel based analysis for neuroreceptor studies performed on the high resolution research tomograph (HRRT). <b>2006</b> ,	
Temporal resolution of ntPET using either arterial or reference region-derived plasma input functions. <b>2006</b> , 2006, 2005-8	7
1095 Autosomal dominant dystonia-plus with cerebral calcifications. <b>2006</b> , 67, 620-5	31
1094 Quantitative imaging with the micro-PET small-animal PET tomograph. <b>2006</b> , 73, 191-218	14
1093 Visualizing pathology deposits in the living brain of patients with Alzheimer's disease. <b>2006</b> , 412, 14	<b>14-60</b> 34
The quest for Eldorado: development of radioligands for in vivo imaging of nicotinic acetylcholine receptors in human brain. <b>2006</b> , 12, 3877-900	52
Pronociceptive and antinociceptive effects of estradiol through endogenous opioid neurotransmission in women. <b>2006</b> , 26, 5777-85	234
Variations in the human pain stress experience mediated by ventral and dorsal basal ganglia dopamine activity. <b>2006</b> , 26, 10789-95	226
1089 PET of brain amyloid and tau in mild cognitive impairment. <b>2006</b> , 355, 2652-63	573
Support for dopaminergic hypoactivity in restless legs syndrome: a PET study on D2-receptor binding. <b>2006</b> , 129, 2017-28	193
Increased occupancy of dopamine receptors in human striatum during cue-elicited cocaine craving. <b>2006</b> , 31, 2716-27	244
1086 Concepts of registration and correction of head motion in positron emission tomography. <b>2006</b> , 16,	, 67-74 12
1085 Serotonin 1A receptors in the living brain of Alzheimer's disease patients. <b>2006</b> , 103, 702-7	196
[11C]PIB in a nondemented population: potential antecedent marker of Alzheimer disease. <b>2006</b> , 67, 446-52	893
10 $8_3$ Decreased central mu-opioid receptor availability in fibromyalgia. <b>2007</b> , 27, 10000-6	373

1082	Smoking modulation of mu-opioid and dopamine D2 receptor-mediated neurotransmission in humans. <b>2007</b> , 32, 450-7	105
1081	Longitudinal, quantitative assessment of amyloid, neuroinflammation, and anti-amyloid treatment in a living mouse model of Alzheimer's disease enabled by positron emission tomography. <b>2007</b> , 27, 10957-68	246
1080	11C-PIB PET imaging in Alzheimer disease and frontotemporal lobar degeneration. <b>2007</b> , 68, 1205-12	300
1079	Methods for Parkinson are model PET image analysis with regions of interest. 2007,	2
1078	5-HTT binding in recovered depressed patients and healthy volunteers: a positron emission tomography study with [11C]DASB. <b>2007</b> , 164, 1858-65	62
1077	Movement correction of [18F]FDDNP PET studies for brain amyloid imaging. 2007,	1
1076	A scatter-corrected list-mode reconstruction and a practical scatter/random approximation technique for dynamic PET imaging. <b>2007</b> , 52, 2089-106	12
1075	Placebo effects on human mu-opioid activity during pain. <b>2007</b> , 104, 11056-61	442
1074	Imaging beta-amyloid burden in aging and dementia. <b>2007</b> , 68, 1718-25	883
1073	Sleep deprivation increases A1 adenosine receptor binding in the human brain: a positron emission tomography study. <b>2007</b> , 27, 2410-5	141
1072	Amyloid deposition begins in the striatum of presenilin-1 mutation carriers from two unrelated pedigrees. <b>2007</b> , 27, 6174-84	313
1071	Comparison of simplified methods for quantitative analysis of [18F]FDDNP PET data. 2007,	1
1070	Modulation of dopaminergic and glutamatergic brain function: PET studies on parkinsonian rats. <b>2007</b> , 48, 1147-53	53
1069	Visual assessment versus quantitative assessment of 11C-PIB PET and 18F-FDG PET for detection of Alzheimer's disease. <b>2007</b> , 48, 547-52	172
1068	Molecular imaging with Pittsburgh Compound B confirmed at autopsy: a case report. 2007, 64, 431-4	297
1067	PET imaging of dopamine D2 receptor and transporter availability during acquisition of cocaine self-administration in rhesus monkeys. <b>2007</b> , 1, 33-9	16
1066	Impact of accurate motion-corrected statistical reconstruction on dynamic PET kinetic parameter estimation. <b>2007</b> ,	1
1065	Effect of aging on cerebral A1 adenosine receptors: A [18F]CPFPX PET study in humans. <b>2007</b> , 28, 1914-24	51

### (2007-2007)

1064	Individual differences in reward responding explain placebo-induced expectations and effects. <b>2007</b> , 55, 325-36	354
1063	Simplifications in analyzing positron emission tomography data: effects on outcome measures. <b>2007</b> , 34, 743-56	9
1062	Quantification of alpha4beta2* nicotinic receptors in the rat brain with microPET and 2-[18F]F-A-85380. <b>2007</b> , 34, 1352-62	19
1061	Mapping the amphetamine-evoked changes in [11C]raclopride binding in living rat using small animal PET: modulation by MAO-inhibition. <b>2007</b> , 35, 38-46	30
1060	A systematic comparison of kinetic modelling methods generating parametric maps for [(11)C]-(R)-PK11195. <b>2007</b> , 36, 28-37	33
1059	Using a reference tissue model with spatial constraint to quantify [11C]Pittsburgh compound B PET for early diagnosis of Alzheimer's disease. <b>2007</b> , 36, 298-312	75
1058	Fast and reliable estimation of multiple parametric images using an integrated method for dynamic SPECT. <b>2007</b> , 26, 179-89	9
1057	Effect of measurement uncertainty on region of interest based and parametric binding potential estimates for the high resolution research tomograph (HRRT). <b>2007</b> ,	
1056	Cutting-edge brain imaging with positron emission tomography. 2007, 17, 427-40, viii	6
1055	Cutting-Edge Brain Imaging with Positron Emission Tomography. <b>2007</b> , 2, 91-104	3
1054	Buprenorphine duration of action: mu-opioid receptor availability and pharmacokinetic and behavioral indices. <b>2007</b> , 61, 101-10	8o
1053	Altered central micro-opioid receptor binding after psychological trauma. 2007, 61, 1030-8	93
1052	Novel 5-HTTLPR allele associates with higher serotonin transporter binding in putamen: a [(11)C] DASB positron emission tomography study. <b>2007</b> , 62, 327-31	175
1051	High occupancy of sigma-1 receptors in the human brain after single oral administration of fluvoxamine: a positron emission tomography study using [11C]SA4503. <b>2007</b> , 62, 878-83	101
1050	Imaging of amyloid burden and distribution in cerebral amyloid angiopathy. <b>2007</b> , 62, 229-34	420
1049	Dopamine transporter relation to dopamine turnover in Parkinson's disease: a positron emission tomography study. <b>2007</b> , 62, 468-74	106
1048	Time-course of change in [11C]carfentanil and [11C]raclopride binding potential after a nonpharmacological challenge. <b>2007</b> , 61, 707-14	51
1047	Seeing what Alzheimer saw. <b>2007</b> , 13, 129-31	8

1046	Positron emission tomography displacement sensitivity: predicting binding potential change for positron emission tomography tracers based on their kinetic characteristics. <i>Journal of Cerebral Blood Flow and Metabolism</i> , <b>2007</b> , 27, 606-17	7.3	41
1045	Positron emission tomography quantification of [11C]-(+)-PHNO binding in the human brain. Journal of Cerebral Blood Flow and Metabolism, <b>2007</b> , 27, 857-71	7.3	83
1044	Quantification of dopamine transporter binding using [18F]FP-beta-CIT and positron emission tomography. <i>Journal of Cerebral Blood Flow and Metabolism</i> , <b>2007</b> , 27, 1397-406	7.3	31
1043	In vivo measurement of density and affinity of the monoamine vesicular transporter in a unilateral 6-hydroxydopamine rat model of PD. <i>Journal of Cerebral Blood Flow and Metabolism</i> , <b>2007</b> , 27, 1407-15	7.3	39
1042	Evaluation of methods for generating parametric (R-[11C]PK11195 binding images. <i>Journal of Cerebral Blood Flow and Metabolism</i> , <b>2007</b> , 27, 1603-15	7.3	28
1041	Evaluation of four pyridine analogs to characterize 6-OHDA-induced modulation of mGluR5 function in rat brain using microPET studies. <i>Journal of Cerebral Blood Flow and Metabolism</i> , <b>2007</b> , 27, 1623-31	7.3	15
1040	Consensus nomenclature for in vivo imaging of reversibly binding radioligands. <i>Journal of Cerebral Blood Flow and Metabolism</i> , <b>2007</b> , 27, 1533-9	7.3	1597
1039	The 8th International Conference on Quantification of Brain Function with PET. <i>Journal of Cerebral Blood Flow and Metabolism</i> , <b>2007</b> , 27, PP01-04M-PP10-08U	7.3	
1038	Heterogeneous effects of alcohol on dopamine release in the striatum: a PET study. <b>2007</b> , 31, 965-73		62
1037	Brain serotonin transporter binding in non-depressed patients with Parkinson's disease. <b>2007</b> , 14, 523-8	3	161
1036	Reduced midbrain-pons serotonin transporter binding in patients with obsessive-compulsive disorder. <b>2007</b> , 115, 388-94		29
1035	The physiological and pathophysiological roles of neuronal histamine: an insight from human positron emission tomography studies. <b>2007</b> , 113, 1-15		137
1034	PET kinetic analysispitfalls and a solution for the Logan plot. <b>2007</b> , 21, 1-8		31
1033	Serotonin transporter occupancy of high-dose selective serotonin reuptake inhibitors during major depressive disorder measured with [11C]DASB positron emission tomography. <b>2007</b> , 193, 539-45		46
1032	Test-retest stability of cerebral A1 adenosine receptor quantification using [18F]CPFPX and PET. <b>2007</b> , 34, 1061-70		17
1031	The lack of expression of the peripheral benzodiazepine receptor characterises microglial response in anaplastic astrocytomas. <b>2007</b> , 85, 95-103		23
1030	Voxel-based NK1 receptor occupancy measurements with [(18)F]SPA-RQ and positron emission tomography: a procedure for assessing errors from image reconstruction and physiological modeling. <b>2007</b> , 9, 284-94		5
1029	Distribution volume as an alternative to the binding potential for sigma1 receptor imaging. <b>2007</b> , 21, 533-5		16

### (2008-2008)

1028	Initial comparison of ntPET with microdialysis measurements of methamphetamine-induced dopamine release in rats: support for estimation of dopamine curves from PET data. <b>2008</b> , 10, 67-73	16
1027	Cerebral glucose metabolism and D2/D3 receptor availability in young adults with cannabis dependence measured with positron emission tomography. <b>2008</b> , 197, 549-56	62
1026	Neuroimaging of mirtazapine enantiomers in humans. <b>2008</b> , 200, 273-9	3
1025	Brain mu-opioid receptor binding: relationship to relapse to cocaine use after monitored abstinence. <b>2008</b> , 200, 475-86	52
1024	Cerebral A1 adenosine receptors (A1AR) in liver cirrhosis. 2008, 35, 589-97	27
1023	The ART of loss: Abeta imaging in the evaluation of Alzheimer's disease and other dementias. <b>2008</b> , 38, 1-15	81
1022	PET kinetic analysis: error consideration of quantitative analysis in dynamic studies. <b>2008</b> , 22, 1-11	21
1021	Cancer and blood concentrations of the comutagen harmane in essential tremor. <b>2008</b> , 23, 1747-51	6
1020	Subthalamotomy in cervical dystonia: A case study of lesion location and clinical outcome. <b>2008</b> , 23, 1751-6	8
1019	Intact presupplementary motor area function in early, untreated Parkinson's disease. <b>2008</b> , 23, 1756-9	4
1018	Reversal of head drop after discontinuation of olanzapine in a DLB patient. 2008, 23, 1760-2	5
1017	Hemidystonia secondary to thalamic hemorrhage treated with GPi stimulation. 2008, 23, 1762-6	13
1016	Autonomic dysfunction in different subtypes of multiple system atrophy. <b>2008</b> , 23, 1766-72	30
1015	Ultrasonographic findings of shoulder disorders in patients with Parkinson's disease. <b>2008</b> , 23, 1772-6	15
1014	Elevated serotonin transporter binding in depressed patients with Parkinson's disease: a preliminary PET study with [11C]DASB. <b>2008</b> , 23, 1776-80	130
1013	Psychosis, short stature in benign hereditary chorea: a novel thyroid transcription factor-1 mutation. <b>2008</b> , 23, 1744-7	39
1012	Arm swing is reduced in idiopathic cervical dystonia. <b>2008</b> , 23, 1784-7	18
1011	What relation is there between deep brain stimulation and coping strategies in Parkinson's disease?. <b>2008</b> , 23, 1780-4	11

1010	Dihydrotetrabenazine positron emission tomography imaging in early, untreated Parkinson's disease. <b>2008</b> , 63, 388-94		60
1009	Abeta amyloid and glucose metabolism in three variants of primary progressive aphasia. 2008, 64, 388-4	401	363
1008	Comparison of noninvasive quantification methods of in vivo vesicular acetylcholine transporter using [123I]-IBVM SPECT imaging. <i>Journal of Cerebral Blood Flow and Metabolism</i> , <b>2008</b> , 28, 1624-34	7.3	16
1007	Multiple linear analysis methods for the quantification of irreversibly binding radiotracers. <i>Journal of Cerebral Blood Flow and Metabolism</i> , <b>2008</b> , 28, 1965-77	7.3	10
1006	Noninvasive estimation of normalized distribution volume: application to the muscarinic-2 ligand [(18)F]FP-TZTP. <i>Journal of Cerebral Blood Flow and Metabolism</i> , <b>2008</b> , 28, 420-30	7.3	17
1005	Improving PET receptor binding estimates from Logan plots using principal component analysis. Journal of Cerebral Blood Flow and Metabolism, <b>2008</b> , 28, 852-65	7.3	30
1004	Sensory processing disorder in a primate model: evidence from a longitudinal study of prenatal alcohol and prenatal stress effects. <b>2008</b> , 79, 100-13		42
1003	Functional neuroimaging in multiple sclerosis with radiolabelled glia markers: preliminary comparative PET studies with [11C]vinpocetine and [11C]PK11195 in patients. <b>2008</b> , 264, 9-17		62
1002	What were they thinking? Cognitive states may influence [11C]raclopride binding potential in the striatum. <b>2008</b> , 430, 38-42		17
1001	Midbrain serotonin and striatum dopamine transporter binding in double depression: a one-year follow-up study. <b>2008</b> , 441, 291-5		35
1000	Validation of the reference tissue model for estimation of dopaminergic D2-like receptor binding with [18F](N-methyl)benperidol in humans. <b>2008</b> , 35, 335-41		10
999	Changes in midbrain serotonin transporter availability in atypically depressed subjects after one year of psychotherapy. <b>2008</b> , 32, 229-37		47
998	Estimating neurotransmitter kinetics with ntPET: a simulation study of temporal precision and effects of biased data. <b>2008</b> , 39, 1162-79		16
997	Robust estimation of the arterial input function for Logan plots using an intersectional searching algorithm and clustering in positron emission tomography for neuroreceptor imaging. <b>2008</b> , 40, 26-34		16
996	Associations between dopamine D2-receptor binding and cognitive performance indicate functional compartmentalization of the human striatum. <b>2008</b> , 40, 1287-95		56
995	Measurement of GABAA receptor binding in vivo with [11C]flumazenil: a test-retest study in healthy subjects. <b>2008</b> , 41, 260-9		34
994	Automated system for parametric image analysis in neuroreceptor binding studies with PET. <b>2008</b> , 41, T77		
993	Simplified parametric methods for [11C]PIB studies. <b>2008</b> , 42, 76-86		79

### (2008-2008)

992	Kinetic analyses of [123I]IBZM SPECT for quantification of striatal dopamine D2 receptor binding: a critical evaluation of the single-scan approach. <b>2008</b> , 42, 548-58	15
991	Placebo and nocebo effects are defined by opposite opioid and dopaminergic responses. <b>2008</b> , 65, 220-31	459
990	Automated (11)C-PiB standardized uptake value ratio. <b>2008</b> , 15, 1376-89	17
989	Discovery of (-)-7-methyl-2-exo-[3'-(6-[18F]fluoropyridin-2-yl)-5'-pyridinyl]-7-azabicyclo[2.2.1]heptane, a radiolabeled antagonist for cerebral nicotinic acetylcholine receptor (alpha4beta2-nAChR) with	28
988	Prenatal Stress Influences on Neurobehavior, Stress Reactivity, and Dopaminergic Function in Rhesus Macaques. <b>2008</b> , 231-258	4
987	Voxel-based analysis of 11C-PIB scans for diagnosing Alzheimer's disease. <b>2008</b> , 49, 1262-9	37
986	Novel selective allosteric activator of the M1 muscarinic acetylcholine receptor regulates amyloid processing and produces antipsychotic-like activity in rats. <b>2008</b> , 28, 10422-33	203
985	Seasonal variation in human brain serotonin transporter binding. <b>2008</b> , 65, 1072-8	195
984	Sleep deprivation decreases binding of [11C]raclopride to dopamine D2/D3 receptors in the human brain. <b>2008</b> , 28, 8454-61	148
983	Comparison of 3D-OP-OSEM and 3D-FBP reconstruction algorithms for High-Resolution Research Tomograph studies: effects of randoms estimation methods. <b>2008</b> , 53, 3217-30	28
982	Imaging of opioid receptors in the central nervous system. <b>2008</b> , 131, 1171-96	149
981	Mechanisms of dopaminergic and serotonergic neurotransmission in Tourette syndrome: clues from an in vivo neurochemistry study with PET. <b>2008</b> , 33, 1239-51	200
980	Monoamine oxidase A genotype predicts human serotonin 1A receptor availability in vivo. <b>2008</b> , 28, 11354-9	40
979	Effects of cocaine and MDMA self-administration on serotonin transporter availability in monkeys. <b>2008</b> , 33, 219-25	43
978	Differences in delta- and mu-opioid receptor blockade measured by positron emission tomography in naltrexone-treated recently abstinent alcohol-dependent subjects. <b>2008</b> , 33, 653-65	109
977	Mesolimbic functional magnetic resonance imaging activations during reward anticipation correlate with reward-related ventral striatal dopamine release. <b>2008</b> , 28, 14311-9	376
976	Compartmental modeling of 11C-HOMADAM binding to the serotonin transporter in the healthy human brain. <b>2008</b> , 49, 2018-25	24
975	Post-mortem correlates of in vivo PiB-PET amyloid imaging in a typical case of Alzheimer's disease. <b>2008</b> , 131, 1630-45	714

974	PET amyloid ligand [11C]PIB uptake and cerebrospinal fluid beta-amyloid in mild cognitive impairment. <b>2008</b> , 26, 378-83	84
973	Brain volume decline in aging: evidence for a relation between socioeconomic status, preclinical Alzheimer disease, and reserve. <b>2008</b> , 65, 113-20	158
972	Imaging amyloid deposition in Lewy body diseases. <b>2008</b> , 71, 903-10	376
971	Estimation from PET data of transient changes in dopamine concentration induced by alcohol: support for a non-parametric signal estimation method. <b>2008</b> , 53, 1353-67	9
970	Progression of dopaminergic dysfunction in a LRRK2 kindred: a multitracer PET study. 2008, 71, 1790-5	95
969	Revisiting an old issue: the discrepancy between tissue ratio-derived binding parameters and kinetic modeling-derived parameters after a bolus of the serotonin transporter radioligand 123I-ADAM. <b>2008</b> , 49, 176-8	14
968	Opioid receptor PET reveals the psychobiologic correlates of reward processing. 2008, 49, 1257-61	43
967	Impact of wavelet based denoising of [11C](R)-PK11195 time activity curves on accuracy and precision of kinetic analysis. <b>2008</b> , 35, 5069-78	1
966	. 2008,	
965	Alzheimer disease and cognitive reserve: variation of education effect with carbon 11-labeled Pittsburgh Compound B uptake. <b>2008</b> , 65, 1467-71	163
965 964		163
	Pittsburgh Compound B uptake. <b>2008</b> , 65, 1467-71  Black cohosh has central opioid activity in postmenopausal women: evidence from naloxone	
964	Pittsburgh Compound B uptake. 2008, 65, 1467-71  Black cohosh has central opioid activity in postmenopausal women: evidence from naloxone blockade and positron emission tomography neuroimaging. 2008, 15, 832-40  Timing of moderate level prenatal alcohol exposure influences gene expression of sensory	41
964 963	Pittsburgh Compound B uptake. 2008, 65, 1467-71  Black cohosh has central opioid activity in postmenopausal women: evidence from naloxone blockade and positron emission tomography neuroimaging. 2008, 15, 832-40  Timing of moderate level prenatal alcohol exposure influences gene expression of sensory processing behavior in rhesus monkeys. 2009, 3, 30  Evaluation of two graphical approaches for regional analysis and parametric mapping of dynamic	41
964 963 962	Pittsburgh Compound B uptake. 2008, 65, 1467-71  Black cohosh has central opioid activity in postmenopausal women: evidence from naloxone blockade and positron emission tomography neuroimaging. 2008, 15, 832-40  Timing of moderate level prenatal alcohol exposure influences gene expression of sensory processing behavior in rhesus monkeys. 2009, 3, 30  Evaluation of two graphical approaches for regional analysis and parametric mapping of dynamic [18F]FDDNP PET studies. 2009,  Consideration of optimal time window for Pittsburgh compound B PET summed uptake	8
964 963 962 961	Pittsburgh Compound B uptake. 2008, 65, 1467-71  Black cohosh has central opioid activity in postmenopausal women: evidence from naloxone blockade and positron emission tomography neuroimaging. 2008, 15, 832-40  Timing of moderate level prenatal alcohol exposure influences gene expression of sensory processing behavior in rhesus monkeys. 2009, 3, 30  Evaluation of two graphical approaches for regional analysis and parametric mapping of dynamic [18F]FDDNP PET studies. 2009,  Consideration of optimal time window for Pittsburgh compound B PET summed uptake measurements. 2009, 50, 348-55	41 8 89
964 963 962 961 960	Pittsburgh Compound B uptake. 2008, 65, 1467-71  Black cohosh has central opioid activity in postmenopausal women: evidence from naloxone blockade and positron emission tomography neuroimaging. 2008, 15, 832-40  Timing of moderate level prenatal alcohol exposure influences gene expression of sensory processing behavior in rhesus monkeys. 2009, 3, 30  Evaluation of two graphical approaches for regional analysis and parametric mapping of dynamic [18F]FDDNP PET studies. 2009,  Consideration of optimal time window for Pittsburgh compound B PET summed uptake measurements. 2009, 50, 348-55  11C-PK11195 PET for the in vivo evaluation of neuroinflammation in the rat brain after cortical spreading depression. 2009, 50, 1904-11  Cortical hubs revealed by intrinsic functional connectivity: mapping, assessment of stability, and	41 8 89 30

### (2009-2009)

956	olopatadine, an antihistamine, is reduced after repeated administration of olopatadine. <b>2009</b> , 50, 887-92	11
955	Using cerebral white matter for estimation of nondisplaceable binding of 5-HT1A receptors in temporal lobe epilepsy. <b>2009</b> , 50, 1794-800	10
954	Influence of cognitive status, age, and APOE-4 genetic risk on brain FDDNP positron-emission tomography imaging in persons without dementia. <b>2009</b> , 66, 81-7	52
953	PET demonstrates reduced dopamine transporter expression in PD with dyskinesias. <b>2009</b> , 72, 1211-6	92
952	Episodic memory loss is related to hippocampal-mediated beta-amyloid deposition in elderly subjects. <b>2009</b> , 132, 1310-23	526
951	Dopamine transporters in striatum correlate with deactivation in the default mode network during visuospatial attention. <b>2009</b> , 4, e6102	114
950	Reduced ventrolateral fMRI response during observation of emotional gestures related to the degree of dopaminergic impairment in Parkinson disease. <b>2009</b> , 21, 1321-31	41
949	High occupancy of sigma1 receptors in the human brain after single oral administration of donepezil: a positron emission tomography study using [11C]SA4503. <b>2009</b> , 12, 1127-31	53
948	Longitudinal progression of sporadic Parkinson's disease: a multi-tracer positron emission tomography study. <b>2009</b> , 132, 2970-9	185
947	Pittsburgh compound B imaging and prediction of progression from cognitive normality to symptomatic Alzheimer disease. <b>2009</b> , 66, 1469-75	350
946	Characterization of PiB binding to white matter in Alzheimer disease and other dementias. <b>2009</b> , 50, 198-204	76
945	Cognition, reserve, and amyloid deposition in normal aging. <b>2010</b> , 67, 353-64	246
944	Evidence for modulation of opioidergic activity in central vestibular processing: A [(18)F] diprenorphine PET study. <b>2010</b> , 31, 550-5	14
943	Dose dependency of brain histamine H(1) receptor occupancy following oral administration of cetirizine hydrochloride measured using PET with [11C]doxepin. <b>2009</b> , 24, 540-8	39
942	Cerebrospinal fluid tau and ptau(181) increase with cortical amyloid deposition in cognitively normal individuals: implications for future clinical trials of Alzheimer's disease. <b>2009</b> , 1, 371-80	278
941	Limitations of small animal PET imaging with [18F]FDDNP and FDG for quantitative studies in a transgenic mouse model of Alzheimer's disease. <b>2009</b> , 11, 236-40	77
940	Evaluation of tracer kinetic models for analysis of [18F]FDDNP studies. <b>2009</b> , 11, 322-33	19
939	Amyloid imaging in Alzheimer's disease and other dementias. <b>2009</b> , 3, 246-61	23

937	Measurement of central mu-opioid receptor binding in vivo with PET and [11C]carfentanil: a test-retest study in healthy subjects. <b>2009</b> , 36, 275-86		55
936	Kinetic modelling of [11C]flumazenil using data-driven methods. 2009, 36, 659-70		12
935	Test-retest variability of quantitative [11C]PIB studies in Alzheimer's disease. <b>2009</b> , 36, 1629-38		51
934	Comparative evaluations of norepinephrine transporter radioligands with reference tissue models in rhesus monkeys: (S,S)-[18F]FMeNER-D2 and (S,S)-[11C]MeNER. <b>2009</b> , 36, 1885-91		13
933	Selective serotonin reuptake inhibitor (SSRI) modulation of striatal dopamine measured with [11C]-raclopride and positron emission tomography. <b>2009</b> , 63, 1-6		17
932	Evaluation of the novel 5-HT4 receptor PET ligand [11C]SB207145 in the GEtingen minipig. <i>Journal of Cerebral Blood Flow and Metabolism</i> , <b>2009</b> , 29, 186-96	7.3	49
931	BrainPET Poster Session: Kinetic Modeling. <i>Journal of Cerebral Blood Flow and Metabolism</i> , <b>2009</b> , 29, S312-S328	7.3	
930	BrainPET Poster Session: in vivo Pharmacology and Clinical Applications. <i>Journal of Cerebral Blood Flow and Metabolism</i> , <b>2009</b> , 29, S346-S359	7.3	1
929	Modeling considerations for in vivo quantification of the dopamine transporter using [(11)C]PE2I and positron emission tomography. <i>Journal of Cerebral Blood Flow and Metabolism</i> , <b>2009</b> , 29, 1332-45	7.3	33
928	When what you see isn't what you get: alcohol cues, alcohol administration, prediction error, and human striatal dopamine. <b>2009</b> , 33, 139-49		58
927	The dopaminergic basis of human behaviors: A review of molecular imaging studies. <b>2009</b> , 33, 1109-32		126
926	Striatal dopamine d2/d3 receptor availability is reduced in methamphetamine dependence and is linked to impulsivity. <b>2009</b> , 29, 14734-40		294
925	Behavioral and neurobiological characteristics influencing social hierarchy formation in female cynomolgus monkeys. <b>2009</b> , 158, 1257-65		36
924	Increased brain histamine H1 receptor binding in patients with anorexia nervosa. 2009, 65, 329-35		39
923	Pharmacokinetics and Modeling. <b>2009</b> , 205-214		2
922	Depression and anxiety symptoms are associated with cerebral FDDNP-PET binding in middle-aged and older nondemented adults. <b>2009</b> , 17, 493-502		70
921	Differential FDDNP PET patterns in nondemented middle-aged and older adults. <b>2009</b> , 17, 397-406		14

#### (2010-2009)

Automation of the Logan plot based PiB-PET quantification over multiple subjects and multiple 920 reference regions. 2009, A consistent and efficient graphical analysis method to improve the quantification of reversible 919 43 tracer binding in radioligand receptor dynamic PET studies. 2009, 44, 661-70 The distribution of D2/D3 receptor binding in the adolescent rhesus monkey using small animal PET 918 27 imaging. 2009, 44, 1334-44 [18F]flumazenil binding to central benzodiazepine receptor studies by PET--quantitative analysis 61 917 and comparisons with [11C]flumazenil. 2009, 45, 891-902 Hyperstimulation of striatal D2 receptors with sleep deprivation: Implications for cognitive 916 57 impairment. 2009, 45, 1232-40 Traditional Chinese acupuncture and placebo (sham) acupuncture are differentiated by their 203 effects on mu-opioid receptors (MORs). 2009, 47, 1077-85 Strategies for the generation of parametric images of [11C]PIB with plasma input functions 914 21 considering discriminations and reproducibility. **2009**, 48, 329-38 Fluorine-18 Radiolabeled PET Tracers for Imaging Monoamine Transporters: Dopamine, Serotonin, 16 913 and Norepinephrine. 2009, 4, 101-28 Positron emission tomography measures of endogenous opioid neurotransmission and 78 912 impulsiveness traits in humans. 2009, 66, 1124-34 A study of non-invasive Patlak quantification for experimental whole-body dynamic FDG-PET 911 studies of mice. 2009, 42, 216-221 Quantitative analyses of [IIC]Ro15-4513 binding to subunits of GABAA/benzodiazepine receptor in 910 5 the living human brain. 2009, 30, 872-80 Impact of early life stress on the reinforcing and behavioral-stimulant effects of psychostimulants 909 10 in rhesus monkeys. **2010**, 21, 69-76 908 Paired stereoisomer model for quantifying receptor concentration in vivo. 2010, 37, 1796-806 Pre-clinical detection of Alzheimer's disease using FDG-PET, with or without amyloid imaging. 2010, 187 907 20,843-54 Quantitative analysis of [18F]FDDNP PET using subcortical white matter as reference region. 2010, 906 27 37, 575-88 Visual assessment of [(11)C]PIB PET in patients with cognitive impairment. **2010**, 37, 1141-7 26 905 Differences in D2 dopamine receptor availability and reaction to novelty in socially housed male 904 34 monkeys during abstinence from cocaine. 2010, 208, 585-92 Characterization of the dopamine receptor system in adult rhesus monkeys exposed to cocaine 903 24 throughout gestation. **2010**, 210, 481-8

902	Staging of serotonergic dysfunction in Parkinson's disease: an in vivo 11C-DASB PET study. <b>2010</b> , 40, 216-21		179
901	[Neuroimaging: technical aspects and practice]. <b>2010</b> , 29, 189-210		10
900	Contact with the bone marrow microenvironment readdresses the fate of transplanted hematopoietic stem cells. <b>2010</b> , 38, 968-77		14
899	APOE predicts amyloid-beta but not tau Alzheimer pathology in cognitively normal aging. <b>2010</b> , 67, 122-3	1	618
898	Dopamine turnover increases in asymptomatic LRRK2 mutations carriers. <b>2010</b> , 25, 2717-23		82
897	Amyloid imaging of Lewy body-associated disorders. <b>2010</b> , 25, 2516-23		118
896	Exercise elevates dopamine D2 receptor in a mouse model of Parkinson's disease: in vivo imaging with [II] fallypride. <b>2010</b> , 25, 2777-84		110
895	Dopamine transporter PET in normal aging: dopamine transporter decline and its possible role in preservation of motor function. <b>2010</b> , 64, 146-51		36
894	Positron emission tomography kinetic modeling algorithms for small animal dopaminergic system imaging. <b>2010</b> , 64, 200-8		20
893	Endogenous competition against binding of [(18)F]DMFP and [(18)F]fallypride to dopamine D(2/3) receptors in brain of living mouse. <b>2010</b> , 64, 313-22		44
892	PET studies of D2-receptor binding in striatal and extrastriatal brain regions: Biochemical support in vivo for separate dopaminergic systems in humans. <b>2010</b> , 64, 478-85		15
891	2-adrenergic drugs modulate the binding of [18F]fallypride to dopamine D2/3 receptors in striatum of living mouse. <b>2010</b> , 64, 654-7		7
890	Spinal long-term potentiation is associated with reduced opioid neurotransmission in the rat brain. <b>2010</b> , 30, 285-93		12
889	Measuring drug occupancy in the absence of a reference region: the Lassen plot re-visited. <i>Journal of Cerebral Blood Flow and Metabolism</i> , <b>2010</b> , 30, 46-50	3	197
888	Kinetic modeling of the serotonin 5-HT(1B) receptor radioligand [(11)C]P943 in humans. <i>Journal of Cerebral Blood Flow and Metabolism</i> , <b>2010</b> , 30, 196-210	3	61
887	Measurement of density and affinity for dopamine D(2) receptors by a single positron emission tomography scan with multiple injections of [(11)C]raclopride. <i>Journal of Cerebral Blood Flow and Metabolism</i> , <b>2010</b> , 30, 663-73	3	7
886	In vivo and in vitro validation of reference tissue models for the mGluR(5) ligand [(11)C]ABP688.  Journal of Cerebral Blood Flow and Metabolism, <b>2010</b> , 30, 1538-49	3	51
885	Fetal dopamine receptor characteristics assessed in utero. <i>Journal of Cerebral Blood Flow and Metabolism</i> , <b>2010</b> , 30, 1437-40	3	2

## (2010-2010)

884	PET of brain prion protein amyloid in Gerstmann-Strüssler-Scheinker disease. <b>2010</b> , 20, 419-30	42
883	Serotonin-transporter-linked promoter region polymorphism and serotonin transporter binding in drug-nalle patients with major depression. <b>2010</b> , 64, 387-93	14
882	Positron emission tomography in schizophrenia: a new perspective. <b>2010</b> , 51, 511-20	41
881	Pittsburgh compound B (11C-PIB) and fluorodeoxyglucose (18 F-FDG) PET in patients with Alzheimer disease, mild cognitive impairment, and healthy controls. <b>2010</b> , 23, 185-98	77
880	Serotonergic neurons mediate dyskinesia side effects in Parkinson's patients with neural transplants. <b>2010</b> , 2, 38ra46	231
879	In vivo measurement of vesicular monoamine transporter type 2 density in Parkinson disease with (18)F-AV-133. <b>2010</b> , 51, 223-8	103
878	Scanning rodents on the High Resolution Research Tomograph (HRRT) with point spread function reconstruction: A feasibility study. <b>2010</b> ,	1
877	. 2010,	
876	Central opioidergic neurotransmission in complex regional pain syndrome. <b>2010</b> , 75, 129-36	54
875	Relationship of dementia screening tests with biomarkers of Alzheimer's disease. <b>2010</b> , 133, 3290-300	77
874	Validation of the octamouse for simultaneous 18F-fallypride small-animal PET recordings from 8 mice. <b>2010</b> , 51, 1576-83	23
873	Depressive symptoms in PD correlate with higher 5-HTT binding in raphe and limbic structures. <b>2010</b> , 75, 1920-7	155
872	11C-PIB binding is increased in patients with cerebral amyloid angiopathy-related hemorrhage. <b>2010</b> , 74, 487-93	118
871	Brain serotonin transporter occupancy by oral sibutramine dosed to steady state: a PET study using (11)C-DASB in healthy humans. <b>2010</b> , 35, 741-51	21
870	Dysregulation of regional endogenous opioid function in borderline personality disorder. <b>2010</b> , 167, 925-33	111
869	In vivo amyloid imaging in autopsy-confirmed Parkinson disease with dementia. <b>2010</b> , 74, 77-84	148
868	Brain mu-opioid receptor binding predicts treatment outcome in cocaine-abusing outpatients. <b>2010</b> , 68, 697-703	52
867	18F-fallypride binding potential in patients with schizophrenia compared to healthy controls. <b>2010</b> , 122, 43-52	25

866	Non-motor dopamine withdrawal syndrome after surgery for Parkinson's disease: predictors and underlying mesolimbic denervation. <b>2010</b> , 133, 1111-27	381
865	Dynamic PET denoising with HYPR processing. <b>2010</b> , 51, 1147-54	88
864	Plaque and tangle imaging and cognition in normal aging and Alzheimer's disease. <b>2010</b> , 31, 1669-78	83
863	Basal opioid receptor binding is associated with differences in sensory perception in healthy human subjects: a [18F]diprenorphine PET study. <b>2010</b> , 49, 731-7	32
862	FDDNP binding using MR derived cortical surface maps. <b>2010</b> , 49, 240-8	18
861	Uptake and binding of the serotonin 5-HT1A antagonist [18F]-MPPF in brain of rats: effects of the novel P-glycoprotein inhibitor tariquidar. <b>2010</b> , 49, 1406-15	41
860	Simplified quantification of 5-HT2A receptors in the human brain with [11C]MDL 100,907 PET and non-invasive kinetic analyses. <b>2010</b> , 50, 984-93	19
859	Simplified parametric methods for [18F]FDDNP studies. <b>2010</b> , 49, 433-41	5
858	Movement correction method for human brain PET images: application to quantitative analysis of dynamic 18F-FDDNP scans. <b>2010</b> , 51, 210-8	31
857	Elevated plasma prolactin in abstinent methamphetamine-dependent subjects. <b>2011</b> , 37, 62-7	7
856	Molecular Imaging. <b>2011</b> ,	2
855	Age and disease related changes in the translocator protein (TSPO) system in the human brain: positron emission tomography measurements with [11C]vinpocetine. <b>2011</b> , 56, 1111-21	72
854	Effect of oxybutynin and imidafenacin on central muscarinic receptor occupancy and cognitive function: a monkey PET study with [(11)C](+)3-MPB. <b>2011</b> , 58, 1-9	20
853	EAmyloid affects frontal and posterior brain networks in normal aging. <b>2011</b> , 54, 1887-95	90
852	Synthesis, characterization, and monkey positron emission tomography (PET) studies of [18F]Y1-973, a PET tracer for the neuropeptide Y Y1 receptor. <b>2011</b> , 54, 2635-42	29
851	Where in-vivo imaging meets cytoarchitectonics: the relationship between cortical thickness and neuronal density measured with high-resolution [18F]flumazenil-PET. <b>2011</b> , 56, 951-60	96
850	In vivo positron emission tomographic imaging of glial responses to amyloid-beta and tau pathologies in mouse models of Alzheimer's disease and related disorders. <b>2011</b> , 31, 4720-30	111

### (2011-2011)

848	Association of harm avoidance with dopamine D2/3 receptor availability in striatal subdivisions: a high resolution PET study. <b>2011</b> , 87, 164-7	30
847	Insulin resistance influences central opioid activity in polycystic ovary syndrome. <b>2011</b> , 95, 2494-8	13
846	Differential effects of cocaine and MDMA self-administration on cortical serotonin transporter availability in monkeys. <b>2011</b> , 61, 245-51	21
845	An in vivo comparison of cis- and trans-[18F]mefway in the nonhuman primate. <b>2011</b> , 38, 925-32	15
844	[18F]Fluoroazabenzoxazoles as potential amyloid plaque PET tracers: synthesis and in vivo evaluation in rhesus monkey. <b>2011</b> , 38, 1193-203	19
843	Optimal scanning time window for 18F-FP-(+)-DTBZ (18F-AV-133) summed uptake measurements. <b>2011</b> , 38, 1149-55	21
842	Effects of age on dopamine D2 receptor availability in striatal subdivisions: a high-resolution positron emission tomography study. <b>2011</b> , 21, 885-91	19
841	Increase in hypothalamic aromatase in macaque monkeys treated with anabolic-androgenic steroids: PET study with [11C]vorozole. <b>2011</b> , 22, 326-30	7
840	Antipsychotic-associated mental side effects and their relationship to dopamine D2 receptor occupancy in striatal subdivisions: a high-resolution PET study with [11C]raclopride. <b>2011</b> , 31, 507-11	19
839	Role of family history for Alzheimer biomarker abnormalities in the adult children study. <b>2011</b> , 68, 1313-9	46
838	Amyloid-Dand glucose metabolism in Alzheimer's disease. <b>2011</b> , 26 Suppl 3, 105-16	19
837	Midbrain serotonin transporters in de novo and L-DOPA-treated patients with early Parkinson's diseasea [123 I]-ADAM SPECT study. <b>2011</b> , 18, 750-5	9
836	Positron emission tomography imaging of mu- and delta-opioid receptor binding in alcohol-dependent and healthy control subjects. <b>2011</b> , 35, 2162-73	75
835	The use of alternative forms of graphical analysis to balance bias and precision in PET images.  Journal of Cerebral Blood Flow and Metabolism, <b>2011</b> , 31, 535-46	15
834	Silent cortical neuronal damage in atherosclerotic disease of the major cerebral arteries. <i>Journal of Cerebral Blood Flow and Metabolism</i> , <b>2011</b> , 31, 953-61	25
833	Quantitative analysis of [11C]AZ10419369 binding to 5-HT1B receptors in human brain. <i>Journal of Cerebral Blood Flow and Metabolism</i> , <b>2011</b> , 31, 113-23	68
832	Serotonergic mediated body mass index changes in Parkinson's disease. <b>2011</b> , 43, 609-15	36
831	Face-name associative memory performance is related to amyloid burden in normal elderly. <b>2011</b> , 49, 2776-83	145

830	Naloxone-induced cortisol predicts mu opioid receptor binding potential in specific brain regions of healthy subjects. <b>2011</b> , 36, 1453-9	27
829	PET kinetics of radiolabeled antidepressant, [N-methyl-11C]mirtazapine, in the human brain. <b>2011</b> , 1, 36	2
828	In vivo positron emission tomography imaging with [IIIC]ABP688: binding variability and specificity for the metabotropic glutamate receptor subtype 5 in baboons. <b>2011</b> , 38, 1083-94	47
827	Active cyamemazine metabolites in patients treated with cyamemazine (Tercian (): influence on cerebral dopamine D2 and serotonin 5-HT (2A) receptor occupancy as measured by positron emission tomography (PET). <b>2011</b> , 217, 315-21	3
826	Validation of reference tissue modelling for [11C]flumazenil positron emission tomography following head injury. <b>2011</b> , 25, 396-405	16
825	Test-retest variability of [IIIC]raclopride-binding potential in nontreatment-seeking alcoholics. <b>2011</b> , 65, 553-61	22
824	In vivo kinetics of [F-18]MEFWAY: a comparison with [C-11]WAY100635 and [F-18]MPPF in the nonhuman primate. <b>2011</b> , 65, 592-600	35
823	Validation of reference tissue model of PET ligand [IIC]+3-MPB for the muscarinic cholinergic receptor in the living brain of conscious monkey. <b>2011</b> , 65, 548-51	5
822	Striatal and extrastriatal microPET imaging of D2/D3 dopamine receptors in rat brain with [Æ]fallypride and [Æ]desmethoxyfallypride. <b>2011</b> , 65, 778-87	30
821	Imaging of alcohol-induced dopamine release in rats:preliminary findings with [(11) C]raclopride PET. <b>2011</b> , 65, 929-37	5
820	Specific 42 nicotinic acetylcholine receptor binding of [F-18]nifene in the rhesus monkey. 2011, 65, 1309-18	27
819	Decreased striatal dopamine receptor binding in primary focal dystonia: a D2 or D3 defect?. <b>2011</b> , 26, 100-6	36
818	Practical synthesis of precursor of [N-methyl-11C]vorozole, an efficient PET tracer targeting aromatase in the brain. <b>2011</b> , 19, 1464-70	22
817	Assessment of i.p. injection of [18F]fallypride for behavioral neuroimaging in rats. <b>2011</b> , 196, 70-5	8
816	Selective neuronal damage and Wisconsin Card Sorting Test performance in atherosclerotic occlusive disease of the major cerebral artery. <b>2011</b> , 82, 150-6	14
815	Using positron emission tomography and Carbon 11-labeled Pittsburgh Compound B to image Brain Fibrillar Eamyloid in adults with down syndrome: safety, acceptability, and feasibility. <b>2011</b> , 68, 890-6	57
814	Reference tissue modeling with parameter coupling: application to a study of SERT binding in HIV. <b>2011</b> , 56, 2499-513	4
813	Relationships between Emyloid and functional connectivity in different components of the default mode network in aging. <b>2011</b> , 21, 2399-407	229

812	PET of (R)-11C-rolipram binding to phosphodiesterase-4 is reproducible and sensitive to increased norepinephrine in the rat heart. <b>2011</b> , 52, 263-9		16	
811	Comparison of analytical platforms for cerebrospinal fluid measures of ﷺ Table 1-42, total tau, and p-tau181 for identifying Alzheimer disease amyloid plaque pathology. <b>2011</b> , 68, 1137-44		138	
810	Early 11C-PIB frames and 18F-FDG PET measures are comparable: a study validated in a cohort of AD and FTLD patients. <b>2011</b> , 52, 173-9		60	
809	Molecular Brain Imaging of Personality Traits in Nonhuman Primates: A Study of the Common Marmoset. <b>2011</b> , 389-406		2	
808	From Genes to Animal Behavior. <b>2011</b> ,		3	
807	Protein binding in patients with late-life depression. <b>2011</b> , 68, 1143-50		60	
806	Longitudinal evolution of compensatory changes in striatal dopamine processing in Parkinson's disease. <b>2011</b> , 134, 3290-8		102	
805	Human dosimetry and preliminary tumor distribution of 18F-fluoropaclitaxel in healthy volunteers and newly diagnosed breast cancer patients using PET/CT. <b>2011</b> , 52, 1339-45		25	
804	In vivo variation in metabotropic glutamate receptor subtype 5 binding using positron emission tomography and [11C]ABP688. <i>Journal of Cerebral Blood Flow and Metabolism</i> , <b>2011</b> , 31, 2169-80	7.3	59	
803	Validation and quantification of [18F]altanserin binding in the rat brain using blood input and reference tissue modeling. <i>Journal of Cerebral Blood Flow and Metabolism</i> , <b>2011</b> , 31, 2334-42	7.3	19	
802	Quantitative, preclinical PET of translocator protein expression in glioma using 18F-N-fluoroacetyl-N-(2,5-dimethoxybenzyl)-2-phenoxyaniline. <b>2011</b> , 52, 107-14		54	
801	Noninvasive nuclear imaging enables the in vivo quantification of striatal dopamine receptor expression and raclopride affinity in mice. <b>2011</b> , 52, 1133-41		26	
800	11C-(R)-PK11195 PET imaging of microglial activation and response to minocycline in zymosan-treated rats. <b>2011</b> , 52, 257-62		21	
799	Muscarinic receptor occupancy and cognitive impairment: a PET study with [11C](+)3-MPB and scopolamine in conscious monkeys. <b>2011</b> , 36, 1455-65		21	
798	11C-Acetate PET/CT in localized prostate cancer: a study with MRI and histopathologic correlation. <b>2012</b> , 53, 538-45		111	
797	Relationship between dose, drug levels, and D2 receptor occupancy for the atypical antipsychotics risperidone and paliperidone. <b>2012</b> , 341, 81-9		19	
796	Methodology Poster Abstracts. Journal of Cerebral Blood Flow and Metabolism, 2012, 32, S128-S191	7.3	2	
795	Quantification of ligand PET studies using a reference region with a displaceable fraction: application to occupancy studies with [(11)C]-DASB as an example. <i>Journal of Cerebral Blood Flow and Metabolism</i> <b>2012</b> 32 70-80	7.3	28	

794	Chronic Litetrahydrocannabinol exposure induces a sensitization of dopamine D/Liteceptors in the mesoaccumbens and nigrostriatal systems. <b>2012</b> , 37, 2355-67	41
793	Measurement of 5-HT(1A) receptor density and in-vivo binding parameters of [(18)F]mefway in the nonhuman primate. <i>Journal of Cerebral Blood Flow and Metabolism</i> , <b>2012</b> , 32, 1546-58	12
792	Chronic treatment with extended release methylphenidate does not alter dopamine systems or increase vulnerability for cocaine self-administration: a study in nonhuman primates. <b>2012</b> , 37, 2555-65	42
791	Serotonin neuron loss and nonmotor symptoms continue in Parkinson's patients treated with dopamine grafts. <b>2012</b> , 4, 128ra41	92
790	PET imaging of 40* nicotinic acetylcholine receptors: quantitative analysis of 18F-nifene kinetics in the nonhuman primate. <b>2012</b> , 53, 1471-80	22
789	In vivo dopamine transporter imaging in a unilateral 6-hydroxydopamine rat model of Parkinson disease using 11C-methylphenidate PET. <b>2012</b> , 53, 813-22	14
788	Feasibility and dosimetry studies for 18F-NOS as a potential PET radiopharmaceutical for inducible nitric oxide synthase in humans. <b>2012</b> , 53, 994-1001	22
787	Assessment of striatal dopamine D2/D3 receptor availability with PET and 18F-desmethoxyfallypride: comparison of imaging protocols suited for clinical routine. <b>2012</b> , 53, 1558-64	2
786	Association of lifetime cognitive engagement and low Eamyloid deposition. 2012, 69, 623-29	225
7 <sup>8</sup> 5	Using Pittsburgh Compound B for in vivo PET imaging of fibrillar amyloid-beta. <b>2012</b> , 64, 27-81	66
784	Pattern of cardiac sympathetic denervation in idiopathic Parkinson disease studied with 11C hydroxyephedrine PET. <b>2012</b> , 265, 240-7	27
7 <sup>8</sup> 3	Alcohol consumption induces endogenous opioid release in the human orbitofrontal cortex and nucleus accumbens. <b>2012</b> , 4, 116ra6	148
782	Antiparkinsonian mechanism of electroconvulsive therapy in MPTP-lesioned non-human primates. <b>2012</b> , 9, 128-38	6
781	Prediction of cognitive decline by positron emission tomography of brain amyloid and tau. <b>2012</b> , 69, 215-22	59
780	Improved tumor contrast achieved by single time point dual-reporter fluorescence imaging. <b>2012</b> , 17, 066001	45
779	Subacute ischemic stroke is associated with focal 11C PiB positron emission tomography retention but not with global neocortical Aldeposition. <b>2012</b> , 43, 1341-6	29
778	PET evidence for a role for striatal dopamine in the attentional blink: functional implications. <b>2012</b> , 24, 1932-40	36
777	Irrational choice under uncertainty correlates with lower striatal D(2/3) receptor binding in rats. <b>2012</b> , 32, 15450-7	67

776	Differential modulation of the default mode network via serotonin-1A receptors. <b>2012</b> , 109, 2619-24	92
775	Evidence that sleep deprivation downregulates dopamine D2R in ventral striatum in the human brain. <b>2012</b> , 32, 6711-7	151
774	Quantitative preclinical imaging of TSPO expression in glioma using N,N-diethyl-2-(2-(4-(2-18F-fluoroethoxy)phenyl)-5,7-dimethylpyrazolo[1,5-a]pyrimidin-3-yl)acetamide. <b>2012</b> , 53, 287-94	54
773	PET and MRI reveal early evidence of neurodegeneration in spinocerebellar ataxia type 17. <b>2012</b> , 53, 1074-80	37
772	Clinical validation of 18F-AZD4694, an amyloid-Especific PET radioligand. <b>2012</b> , 53, 415-24	172
771	Dissociative changes in the Bmax and KD of dopamine D2/D3 receptors with aging observed in functional subdivisions of the striatum: a revisit with an improved data analysis method. <b>2012</b> , 53, 805-12	10
770	Relative equilibrium plot improves graphical analysis and allows bias correction of standardized uptake value ratio in quantitative 11C-PiB PET studies. <b>2012</b> , 53, 622-8	14
769	Subjective cognition and amyloid deposition imaging: a Pittsburgh Compound B positron emission tomography study in normal elderly individuals. <b>2012</b> , 69, 223-9	220
768	AlDeposition in aging is associated with increases in brain activation during successful memory encoding. <b>2012</b> , 22, 1813-23	105
767	Advantages of a dual-tracer model over reference tissue models for binding potential measurement in tumors. <b>2012</b> , 57, 6647-59	24
766	Recent software developments and applications in functional imaging. 2012, 13, 2166-81	1
765	Parametric [11C]flumazenil images. <b>2012</b> , 33, 422-30	9
764	Immediate effects of tDCS on the Eppioid system of a chronic pain patient. <b>2012</b> , 3, 93	67
763	Positron emission tomography study of the effects of tryptophan depletion on brain serotonin(2) receptors in subjects recently remitted from major depression. <b>2012</b> , 69, 601-9	14
762	Self-reported memory impairment and brain PET of amyloid and tau in middle-aged and older adults without dementia. <b>2012</b> , 24, 1076-84	22
761	Prediction of cognitive decline based on hemispheric cortical surface maps of FDDNP PET. <b>2012</b> , 61, 749-60	10
760	In vivo quantification of tumor receptor binding potential with dual-reporter molecular imaging. <b>2012</b> , 14, 584-92	82
759	Subjective cognitive complaints and amyloid burden in cognitively normal older individuals. <b>2012</b> , 50, 2880-2886	318

758	Development of N-[4-[6-(isopropylamino)pyrimidin-4-yl]-1,3-thiazol-2-yl]-N-methyl-4-[11C]methylbenzamide for positron emission tomography imaging of metabotropic glutamate 1 receptor in monkey brain.	28
757	<b>2012</b> , 55, 11042-51  Cognition, glucose metabolism and amyloid burden in Alzheimer's disease. <b>2012</b> , 33, 215-25	108
756	Cerebrovascular disease, Emyloid, and cognition in aging. <b>2012</b> , 33, 1006.e25-36	88
755	Coronary risk correlates with cerebral amyloid deposition. <b>2012</b> , 33, 1979-87	55
754	Toward a multifactorial model of Alzheimer disease. <b>2012</b> , 33, 2262-71	42
753	Effects of age and Eamyloid on cognitive changes in normal elderly people. <b>2012</b> , 33, 2746-55	34
752	Simplified quantification and whole-body distribution of [18F]FE-PE2I in nonhuman primates: prediction for human studies. <b>2012</b> , 39, 295-303	13
751	Tobacco smoking produces greater striatal dopamine release in G-allele carriers with mu opioid receptor A118G polymorphism. <b>2012</b> , 38, 236-40	35
750	Alamyloid deposition in patients with Parkinson disease at risk for development of dementia. <b>2012</b> , 79, 1161-7	84
749	PET amyloid-beta imaging in preclinical Alzheimer's disease. <b>2012</b> , 1822, 370-9	102
749 748	PET amyloid-beta imaging in preclinical Alzheimer's disease. <b>2012</b> , 1822, 370-9  A study of non-invasive Patlak quantification for whole-body dynamic FDG-PET studies of mice. <b>2012</b> , 7, 438-446	102
	A study of non-invasive Patlak quantification for whole-body dynamic FDG-PET studies of mice.	
748	A study of non-invasive Patlak quantification for whole-body dynamic FDG-PET studies of mice. <b>2012</b> , 7, 438-446  Not quite PIB-positive, not quite PIB-negative: slight PIB elevations in elderly normal control	6
748 747	A study of non-invasive Patlak quantification for whole-body dynamic FDG-PET studies of mice.  2012, 7, 438-446  Not quite PIB-positive, not quite PIB-negative: slight PIB elevations in elderly normal control subjects are biologically relevant. 2012, 59, 1152-60  In vivo quantification of dopamine transporters in mice with unilateral 6-OHDA lesions using	6
748 747 746	A study of non-invasive Patlak quantification for whole-body dynamic FDG-PET studies of mice.  2012, 7, 438-446  Not quite PIB-positive, not quite PIB-negative: slight PIB elevations in elderly normal control subjects are biologically relevant. 2012, 59, 1152-60  In vivo quantification of dopamine transporters in mice with unilateral 6-OHDA lesions using [11C]methylphenidate and PET. 2012, 59, 2413-22  Quantitative PET analyses of regional [11C]PE2I binding to the dopamine transporterapplication	6 116
748 747 746 745	A study of non-invasive Patlak quantification for whole-body dynamic FDG-PET studies of mice.  2012, 7, 438-446  Not quite PIB-positive, not quite PIB-negative: slight PIB elevations in elderly normal control subjects are biologically relevant. 2012, 59, 1152-60  In vivo quantification of dopamine transporters in mice with unilateral 6-OHDA lesions using [11C]methylphenidate and PET. 2012, 59, 2413-22  Quantitative PET analyses of regional [11C]PE2I binding to the dopamine transporterapplication to juvenile myoclonic epilepsy. 2012, 59, 3582-93  Comparative evaluation of Logan and relative-equilibrium graphical methods for parametric	6 116 16 27
748 747 746 745 744	A study of non-invasive Patlak quantification for whole-body dynamic FDG-PET studies of mice.  2012, 7, 438-446  Not quite PIB-positive, not quite PIB-negative: slight PIB elevations in elderly normal control subjects are biologically relevant. 2012, 59, 1152-60  In vivo quantification of dopamine transporters in mice with unilateral 6-OHDA lesions using [11C]methylphenidate and PET. 2012, 59, 2413-22  Quantitative PET analyses of regional [11C]PE2I binding to the dopamine transporterapplication to juvenile myoclonic epilepsy. 2012, 59, 3582-93  Comparative evaluation of Logan and relative-equilibrium graphical methods for parametric imaging of dynamic [18F]FDDNP PET determinations. 2012, 60, 241-51  Combining image-derived and venous input functions enables quantification of serotonin-1A	6 116 16 27 4

### (2012-2012)

740	[18F]desmethoxyfallypride as a novel PET radiotracer for quantitative in vivo dopamine D2/D3 receptor imaging in rat models of neurodegenerative diseases. <b>2012</b> , 39, 1077-80	9
739	Evolution of microglial activation in ischaemic core and peri-infarct regions after stroke: a PET study with the TSPO molecular imaging biomarker [((11))C]vinpocetine. <b>2012</b> , 320, 110-7	59
738	Quantitative assessment of dynamic PET imaging data in cancer imaging. <b>2012</b> , 30, 1203-15	58
737	Quantification of Neuroreceptors and Neurotransporters. <b>2012</b> , 149-161	1
736	Scanning rats on the high resolution research tomograph (HRRT): a comparison study with a dedicated micro-PET. <b>2012</b> , 39, 5073-83	16
735	Reduced basal ganglia Eppioid receptor availability in trigeminal neuropathic pain: a pilot study. <b>2012</b> , 8, 74	41
734	Quantitative analysis and comparison study of [18F]AlF-NOTA-PRGD2, [18F]FPPRGD2 and [68Ga]Ga-NOTA-PRGD2 using a reference tissue model. <b>2012</b> , 7, e37506	41
733	Reduction of [11C](+)3-MPB binding in brain of chronic fatigue syndrome with serum autoantibody against muscarinic cholinergic receptor. <b>2012</b> , 7, e51515	30
732	Visualising neuroinflammation in post-stroke patients: a comparative PET study with the TSPO molecular imaging biomarkers [11C]PK11195 and [11C]vinpocetine. <b>2012</b> , 5, 19-28	37
731	Automated VOI Analysis in FDDNP PET Using Structural Warping: Validation through Classification of Alzheimer's Disease Patients. <b>2012</b> , 2012, 512069	3
730	Dynamic PET and Optical Imaging and Compartment Modeling using a Dual-labeled Cyclic RGD Peptide Probe. <b>2012</b> , 2, 746-56	28
729	GABA(A) receptors in visual and auditory cortex and neural activity changes during basic visual stimulation. <b>2012</b> , 6, 337	15
728	Cerebral amyloid deposition and serotoninergic innervation in Parkinson disease. 2012, 69, 1628-31	12
727	Improved kinetic analysis of dynamic PET data with optimized HYPR-LR. <b>2012</b> , 39, 3319-31	29
726	Nicotinic acetylcholine receptors in rat forebrain that bind <b>IB</b> -nifene: relating PET imaging, autoradiography, and behavior. <b>2012</b> , 66, 418-34	22
725	Test-retest stability of cerebral mGluR[quantification using [[[]C]ABP688 and positron emission tomography in rats. <b>2012</b> , 66, 552-60	30
724	Characterization of extrastriatal D2 in vivo specific binding of [H](N-methyl)benperidol using PET. <b>2012</b> , 66, 770-80	34
723	Brain amyloid and cognition in Lewy body diseases. <b>2012</b> , 27, 965-73	128

722	Assessment of dementia risk in aging adults using both FDG-PET and FDDNP-PET imaging. <b>2012</b> , 27, 1017-27	6
721	Symptoms of rapid eye movement sleep behavior disorder are associated with cholinergic denervation in Parkinson disease. <b>2012</b> , 71, 560-8	170
720	Importance of quantification for the analysis of PET data in oncology: review of current methods and trends for the future. <b>2012</b> , 14, 131-46	73
719	Decreased microglial activation in MS patients treated with glatiramer acetate. <b>2012</b> , 259, 1199-205	68
718	Serotonergic modulation of receptor occupancy in rats treated with L-DOPA after unilateral 6-OHDA lesioning. <b>2012</b> , 120, 806-17	35
717	[18F]Fallypride PET measurement of striatal and extrastriatal dopamine D 2/3 receptor availability in recently abstinent alcoholics. <b>2012</b> , 17, 490-503	44
716	Dopamine pathway loss in nucleus accumbens and ventral tegmental area predicts apathetic behavior in MPTP-lesioned monkeys. <b>2012</b> , 236, 190-7	50
715	Characterisation of [IIC]PR04.MZ in Papio anubis baboon: a selective high-affinity radioligand for quantitative imaging of the dopamine transporter. <b>2012</b> , 22, 679-82	6
714	Model-independent plot of dynamic PET data facilitates data interpretation and model selection. <b>2012</b> , 295, 1-8	1
713	Serotonin transporter binding after recovery from bulimia nervosa. <b>2012</b> , 45, 345-52	17
712	Early AD pathology in a [C-11]PiB-negative case: a PiB-amyloid imaging, biochemical, and immunohistochemical study. <b>2012</b> , 123, 433-47	74
711	Introduction to the analysis of PET data in oncology. <b>2013</b> , 40, 419-36	4
710	Modeling of PET data in CNS drug discovery and development. <b>2013</b> , 40, 267-79	28
709	Evaluation of serotonin 5-HT(1A) receptors in rodent models using [III] mefway PET. 2013, 67, 596-608	18
708	Quantitative positron emission tomography imaging of angiogenesis in rats with forelimb ischemia using (68)Ga-NOTA-c(RGDyK). <b>2013</b> , 16, 837-46	12
707	PET imaging of the brain serotonin transporters (SERT) with N,N-dimethyl-2-(2-amino-4-[18F]fluorophenylthio)benzylamine (4-[18F]-ADAM) in humans: a preliminary study. <b>2013</b> , 40, 115-24	23
706	Analysis of 5-HT(2A) receptor binding with [(11)C]MDL 100907 in rats: optimization of kinetic modeling. <b>2013</b> , 15, 730-8	6
705	Suitability of [18F]altanserin and PET to determine 5-HT2A receptor availability in the rat brain: in vivo and in vitro validation of invasive and non-invasive kinetic models. <b>2013</b> , 15, 456-67	9

### (2013-2013)

704	GABA(A) receptor imaging with positron emission tomography in the human newborn: a unique binding pattern. <b>2013</b> , 48, 459-62	12
703	Longitudinal assessment of cerebral Emyloid deposition in mice overexpressing Swedish mutant Emyloid precursor protein using 18F-florbetaben PET. <b>2013</b> , 54, 1127-34	65
702	Thalamic cholinergic innervation and postural sensory integration function in Parkinson's disease. <b>2013</b> , 136, 3282-9	105
701	Frontotemporal network connectivity during memory encoding is increased with aging and disrupted by beta-amyloid. <b>2013</b> , 33, 18425-37	47
700	Dopamine asymmetries predict orienting bias in healthy individuals. <b>2013</b> , 23, 2899-904	39
699	Prenatal stress induces increased striatal dopamine transporter binding in adult nonhuman primates. <b>2013</b> , 74, 502-10	19
698	Concordance between in vivo and postmortem measurements of cholinergic denervation in rats using PET with [18F]FEOBV and choline acetyltransferase immunochemistry. <b>2013</b> , 3, 70	12
697	Imaging the role of GABA in movement disorders. <b>2013</b> , 13, 385	16
696	Noninvasive k3 estimation method for slow dissociation PET ligands: application to [11C]Pittsburgh compound B. <b>2013</b> , 3, 76	
695	Amyloid imaging in clinical trials. <b>2013</b> , 5, 36	14
695 694	Amyloid imaging in clinical trials. 2013, 5, 36  Microglial activation in Alzheimer's disease: an (R)-[IIC]PK11195 positron emission tomography study. 2013, 34, 128-36	14
	Microglial activation in Alzheimer's disease: an (R)-[IIC]PK11195 positron emission tomography	
694	Microglial activation in Alzheimer's disease: an (R)-[IIIC]PK11195 positron emission tomography study. <b>2013</b> , 34, 128-36  Amyloid is linked to cognitive decline in patients with Parkinson disease without dementia. <b>2013</b> ,	126
694 693	Microglial activation in Alzheimer's disease: an (R)-[IIC]PK11195 positron emission tomography study. 2013, 34, 128-36  Amyloid is linked to cognitive decline in patients with Parkinson disease without dementia. 2013, 80, 85-91  Waluation quantitative prliminaire du 18F-FDDNP en TEP/TDM dans la maladie d'Alzheimer, en	126
694 693 692	Microglial activation in Alzheimer's disease: an (R)-[IIC]PK11195 positron emission tomography study. 2013, 34, 128-36  Amyloid is linked to cognitive decline in patients with Parkinson disease without dementia. 2013, 80, 85-91  Waluation quantitative prliminaire du 18F-FDDNP en TEP/TDM dans la maladie dAlzheimer, en utilisant difffientes rigions de rffience. 2013, 37, 578-585  Lack of endogenous opioid release during sustained visceral pain: a [11C]carfentanil PET study.	126
694 693 692	Microglial activation in Alzheimer's disease: an (R)-[ITC]PK11195 positron emission tomography study. 2013, 34, 128-36  Amyloid is linked to cognitive decline in patients with Parkinson disease without dementia. 2013, 80, 85-91  Waluation quantitative prliminaire du 18F-FDDNP en TEP/TDM dans la maladie dAlzheimer, en utilisant diffEentes rgions de rfEence. 2013, 37, 578-585  Lack of endogenous opioid release during sustained visceral pain: a [11C]carfentanil PET study. 2013, 154, 2072-2077  Grey matter density and GABAA binding potential show a positive linear relationship across cortical	126 124 9
<ul><li>694</li><li>693</li><li>692</li><li>691</li><li>690</li></ul>	Microglial activation in Alzheimer's disease: an (R)-[ITC]PK11195 positron emission tomography study. 2013, 34, 128-36  Amyloid is linked to cognitive decline in patients with Parkinson disease without dementia. 2013, 80, 85-91  Waluation quantitative prliminaire du 18F-FDDNP en TEP/TDM dans la maladie delzheimer, en utilisant difffientes rijions de riffience. 2013, 37, 578-585  Lack of endogenous opioid release during sustained visceral pain: a [11C]carfentanil PET study. 2013, 154, 2072-2077  Grey matter density and GABAA binding potential show a positive linear relationship across cortical regions. 2013, 235, 226-31  Graphic plot analysis for estimating binding potential of translocator protein (TSPO) in positron	126 124 9

686	Effects of acute detoxification of the herbal blend 'Spice Gold' on dopamine D2/3 receptor availability: a [18F]fallypride PET study. <b>2013</b> , 23, 1606-10	30
685	In vivo evaluation of [(123)I]MNI-420: a novel single photon emission computed tomography radiotracer for imaging of adenosine 2A receptors in brain. <b>2013</b> , 40, 403-9	14
684	The effect of amyloid Ibn cognitive decline is modulated by neural integrity in cognitively normal elderly. <b>2013</b> , 9, 687-698.e1	55
683	Diabetes is associated with postural instability and gait difficulty in Parkinson disease. <b>2013</b> , 19, 522-6	65
682	EAmyloid and postural instability and gait difficulty in Parkinson's disease at risk for dementia. <b>2013</b> , 28, 296-301	66
681	Alzheimer's disease neurodegenerative biomarkers are associated with decreased cognitive function but not Eamyloid in cognitively normal older individuals. <b>2013</b> , 33, 5553-63	113
680	Gender differences in cholinergic and dopaminergic deficits in Parkinson disease. 2013, 120, 1421-4	13
679	Early deficits in declarative and procedural memory dependent behavioral function in a transgenic rat model of Huntington's disease. <b>2013</b> , 239, 15-26	19
678	Measuring dopaminergic function in the 6-OHDA-lesioned rat: a comparison of PET and microdialysis. <b>2013</b> , 3, 69	14
677	Diverging patterns of amyloid deposition and hypometabolism in clinical variants of probable Alzheimer's disease. <b>2013</b> , 136, 844-58	235
676	Amyloid-[positron emission tomography imaging probes: a critical review. 2013, 36, 613-31	56
675	Serotonergic loss in motor circuitries correlates with severity of action-postural tremor in PD. <b>2013</b> , 80, 1850-5	76
674	Principal component analysis of PiB distribution in Parkinson and Alzheimer diseases. <b>2013</b> , 81, 520-7	32
673	The aging brain and cognition: contribution of vascular injury and alto mild cognitive dysfunction. <b>2013</b> , 70, 488-95	98
672	Reference region approaches in PET: a comparative study on multiple radioligands. <i>Journal of Cerebral Blood Flow and Metabolism</i> , <b>2013</b> , 33, 888-97	48
671	First experience of 18F-alfatide in lung cancer patients using a new lyophilized kit for rapid radiofluorination. <b>2013</b> , 54, 691-8	134
670	Preclinical Alzheimer disease and risk of falls. <b>2013</b> , 81, 437-43	53
669	Effects of anesthesia and species on the uptake or binding of radioligands in vivo in the GEtingen minipig. <b>2013</b> , 2013, 808713	16

## (2013-2013)

668	Reference region automatic extraction in dynamic [(11)C]PIB. <i>Journal of Cerebral Blood Flow and Metabolism</i> , <b>2013</b> , 33, 1725-31	7.3	18
667	Kinetic modeling, test-retest, and dosimetry of 123I-MNI-420 in humans. <b>2013</b> , 54, 1760-7		14
666	Synthesis and evaluation of 18F-FE-PEO in rodents: an 18F-labeled full agonist for opioid receptor imaging. <b>2013</b> , 54, 299-305		18
665	Longitudinal amyloid imaging in mouse brain with 11C-PIB: comparison of APP23, Tg2576, and APPswe-PS1dE9 mouse models of Alzheimer disease. <b>2013</b> , 54, 1434-41		61
664	Head-to-head comparison of 11C-PiB and 18F-AZD4694 (NAV4694) for Eamyloid imaging in aging and dementia. <b>2013</b> , 54, 880-6		121
663	Associations between Alzheimer disease biomarkers, neurodegeneration, and cognition in cognitively normal older people. <b>2013</b> , 70, 1512-9		119
662	Nonlinear spatio-temporal filtering of dynamic PET data using a four-dimensional Gaussian filter and expectation-maximization deconvolution. <b>2013</b> , 58, 1151-68		3
661	Assessment of cellular proliferation in tumors by PET using 18F-ISO-1. <b>2013</b> , 54, 350-7		64
660	Longitudinal amyloid imaging using 11C-PiB: methodologic considerations. <b>2013</b> , 54, 1570-6		115
659	Metabolism of epidermal growth factor receptor targeting probe [11C]PD153035: impact on biodistribution and tumor uptake in rats. <b>2013</b> , 54, 1804-11		5
658	Dynamic dual-tracer MRI-guided fluorescence tomography to quantify receptor density in vivo. <b>2013</b> , 110, 9025-30		67
657	Denicotinized versus average nicotine tobacco cigarette smoking differentially releases striatal dopamine. <b>2013</b> , 15, 11-21		20
656	A comparison of D2 receptor specific binding in obese and normal-weight individuals using PET with (N-[(11)C]methyl)benperidol. <b>2013</b> , 67, 748-56		66
655	Validation of nigrostriatal positron emission tomography measures: critical limits. <b>2013</b> , 73, 390-6		55
654	The influence of time sampling on parameters in the Logan plot. <b>2013</b> ,		
653	Catechol-O-methyltransferase genotype modulates opioid release in decision circuitry. <b>2013</b> , 6, 400-3		11
652	individual variation in sleep quality and duration is related to cerebral mu opioid receptor binding potential during tonic laboratory pain in healthy subjects. <b>2013</b> , 14, 1882-92		21
651	Alterations in endogenous opioid functional measures in chronic back pain. <b>2013</b> , 33, 14729-37		42

650	In-vivo measurement of LDOPA uptake, dopamine reserve and turnover in the rat brain using [18F]FDOPA PET. <i>Journal of Cerebral Blood Flow and Metabolism</i> , <b>2013</b> , 33, 59-66	21
649	The simplified reference tissue model with 18F-fallypride positron emission tomography: choice of reference region. <b>2013</b> , 12,	14
648	Molecular Imaging PET and SPECT Approaches for Improving Productivity of Antipsychotic Drug Discovery and Development. <b>2013</b> , 20, 378-388	6
647	Treadmill exercise elevates striatal dopamine D2 receptor binding potential in patients with early Parkinson's disease. <b>2013</b> , 24, 509-14	139
646	Postmortem 3-D brain hemisphere cortical tau and amyloid-[pathology mapping and quantification as a validation method of neuropathology imaging. <b>2013</b> , 36, 261-74	26
645	Vascular risk and FDDNP-PET influence cognitive performance. <b>2013</b> , 35, 147-57	3
644	Associations between white matter hyperintensities and hamyloid on integrity of projection, association, and limbic fiber tracts measured with diffusion tensor MRI. <b>2013</b> , 8, e65175	63
643	Quantitative analysis of PiB-PET with FreeSurfer ROIs. <b>2013</b> , 8, e73377	126
642	PET imaging of neuropathology in tauopathies: progressive supranuclear palsy. <b>2013</b> , 36, 145-53	82
641	How to Study Smoking and Drinking with PET. 2013,	2
640	Human Brain Imaging of Adenosine Receptors. <b>2014</b> , 161-186	
639	Differential dopamine receptor occupancy underlies L-DOPA-induced dyskinesia in a rat model of Parkinson's disease. <b>2014</b> , 9, e90759	14
638	Mu Opioid Receptor Binding Correlates with Nicotine Dependence and Reward in Smokers. <b>2014</b> , 9, e113694	32
637	Quantitative preclinical PET imaging: opportunities and challenges. <b>2014</b> , 2,	37
636	Imaging Brain Metabolism and Pathology in Alzheimer's Disease with Positron Emission Tomography. <b>2014</b> , 4,	11
635	Functional brain imaging and its application to uncover mechanisms driving food intake in humans. <b>2014</b> , 4,	2
634	Physiological Modelling of Positron Emission Tomography Images. <b>2014</b> , 417-448	1
633	In vivo quantification of cerebral translocator protein binding in humans using 6-chloro-2-(4'-123I-iodophenyl)-3-(N,N-diethyl)-imidazo[1,2-a]pyridine-3-acetamide SPECT. <b>2014</b> , 55, 1966-72	14

632	Bilastine vs. hydroxyzine: occupation of brain histamine H1 -receptors evaluated by positron emission tomography in healthy volunteers. <b>2014</b> , 78, 970-80	42
631	Test-retest variability of adenosine A2A binding in the human brain with (11)C-TMSX and PET. <b>2014</b> , 4, 76	13
630	Noninvasive quantification of metabotropic glutamate receptor type 1 with [IIC]ITDM: a small-animal PET study. <i>Journal of Cerebral Blood Flow and Metabolism</i> , <b>2014</b> , 34, 606-12	17
629	Radiosynthesis and validation of III-FP-CMT, a phenyltropane with superior properties for imaging the dopamine transporter in living brain. <i>Journal of Cerebral Blood Flow and Metabolism</i> , <b>2014</b> , 34, 1148-36	13
628	Effects of Beta-Amyloid on Resting State Functional Connectivity Within and Between Networks Reflect Known Patterns of Regional Vulnerability. <b>2016</b> , 26, 695-707	63
627	First-in-human evaluation of 18F-mefway, a PET radioligand specific to serotonin-1A receptors. <b>2014</b> , 55, 1973-9	13
626	Human Brain Imaging of Dopamine Transporters. <b>2014</b> , 203-240	4
625	Comparison of methods for evaluating radiolabelled Annexin A5 uptake in pre-clinical PET oncological studies. <b>2014</b> , 41, 793-800	4
624	Is verbal episodic memory in elderly with amyloid deposits preserved through altered neuronal function?. <b>2014</b> , 24, 2210-8	30
623	Love to win or hate to Lose? Asymmetry of dopamine D2 receptor binding predicts sensitivity to reward versus punishment. <b>2014</b> , 26, 1039-48	47
622	Greater medial temporal hypometabolism and lower cortical amyloid burden in ApoE4-positive AD patients. <b>2014</b> , 85, 266-73	40
621	Serotonergic mechanisms responsible for levodopa-induced dyskinesias in Parkinson's disease patients. <b>2014</b> , 124, 1340-9	172
620	Cortical thickness mediates the effect of Emyloid on episodic memory. <b>2014</b> , 82, 761-7	33
619	Amyloid imaging with carbon 11-labeled Pittsburgh compound B for traumatic brain injury. <b>2014</b> , 71, 23-31	112
618	Carboxyfullerene neuroprotection postinjury in Parkinsonian nonhuman primates. <b>2014</b> , 76, 393-402	50
617	Recent advances in parametric neuroreceptor mapping with dynamic PET: basic concepts and graphical analyses. <b>2014</b> , 30, 733-54	7
616	Localized prostate cancer detection with 18F FACBC PET/CT: comparison with MR imaging and histopathologic analysis. <b>2014</b> , 270, 849-56	122
615	Association of adenosine receptor gene polymorphisms and in vivo adenosine A1 receptor binding in the human brain. <b>2014</b> , 39, 2989-99	20

614	Expioid activation in the midbrain during migraine allodynia - brief report II. <b>2014</b> , 1, 445-50	17
613	Association of Expioid Activation in the Prefrontal Cortex with Spontaneous Migraine Attacks - Brief Report I. <b>2014</b> , 1, 439-444	24
612	Cortical dopamine release during a behavioral response inhibition task. <b>2014</b> , 68, 266-74	30
611	Behavioral deficits and striatal DA signaling in LRRK2 p.G2019S transgenic rats: a multimodal investigation including PET neuroimaging. <b>2014</b> , 4, 483-98	27
610	Dopamine Receptors and Dopamine Release. <b>2014</b> , 289-339	1
609	Dopamine D(2/3) receptor availability and human cognitive impulsivity: a high-resolution positron emission tomography imaging study with [TC]raclopride. <b>2014</b> , 26, 35-42	18
608	Human brain imaging of ∄ nAChR with [(18)F]ASEM: a new PET radiotracer for neuropsychiatry and determination of drug occupancy. <b>2014</b> , 16, 730-8	57
607	Assessment of cerebral dopamine D 2/3 formula-receptors in patients with bilateral vestibular failure. <b>2014</b> , 24, 403-13	8
606	External awareness and GABAa multimodal imaging study combining fMRI and [18F]flumazenil-PET. <b>2014</b> , 35, 173-84	26
605	Covarying alterations in Aldeposition, glucose metabolism, and gray matter volume in cognitively normal elderly. <b>2014</b> , 35, 297-308	66
604	FAAH selectively influences placebo effects. <b>2014</b> , 19, 385-91	64
603	Risky driving and pedunculopontine nucleus-thalamic cholinergic denervation in Parkinson disease. <b>2014</b> , 20, 13-6	7
602	Biodistribution studies of two 18F-labeled pyridinylphenyl amides as subtype selective radioligands for the dopamine D3 receptor. <b>2014</b> , 41, 223-8	13
601	PET imaging with [II] fluoroethoxybenzovesamicol ([II] FEOBV) following selective lesion of cholinergic pedunculopontine tegmental neurons in rat. 2014, 41, 96-101	16
600	In vivo PET quantification of the dopamine transporter in rat brain with [Æ]LBT-999. <b>2014</b> , 41, 106-13	14
599	Dopaminergic manipulations and its effects on neurogenesis and motor function in a transgenic mouse model of Huntington's disease. <b>2014</b> , 66, 19-27	12
598	History of childhood adversity is positively associated with ventral striatal dopamine responses to amphetamine. <b>2014</b> , 231, 2417-33	73
597	Direct characterization of arterial input functions by fluorescence imaging of exposed carotid artery to facilitate kinetic analysis. <b>2014</b> , 16, 488-94	4

596	Evaluation of safety and tolerability, pharmacokinetics, and pharmacodynamics of BMS-820836 in healthy subjects: a placebo-controlled, ascending single-dose study. <b>2014</b> , 231, 2299-310	11
595	Tumor endothelial marker imaging in melanomas using dual-tracer fluorescence molecular imaging. <b>2014</b> , 16, 372-82	15
594	Diagnostic utility of amyloid PET in cerebral amyloid angiopathy-related symptomatic intracerebral hemorrhage. <i>Journal of Cerebral Blood Flow and Metabolism</i> , <b>2014</b> , 34, 753-8	42
593	Accounting for pharmacokinetic differences in dual-tracer receptor density imaging. <b>2014</b> , 59, 2341-51	19
592	Advanced age, cardiovascular risk burden, and timed up and go test performance in Parkinson disease. <b>2014</b> , 69, 1569-75	10
591	Imaging nicotine- and amphetamine-induced dopamine release in rhesus monkeys with [(11)C]PHNO vs [(11)C]raclopride PET. <b>2014</b> , 39, 866-74	36
590	Association of gray matter atrophy with age, Eamyloid, and cognition in aging. <b>2014</b> , 24, 1609-18	52
589	A possible mechanism of the nucleus accumbens and ventral pallidum 5-HT1B receptors underlying the antidepressant action of ketamine: a PET study with macaques. <b>2014</b> , 4, e342	55
588	Longitudinal PET-MRI reveals Emyloid deposition and rCBF dynamics and connects vascular amyloidosis to quantitative loss of perfusion. <b>2014</b> , 20, 1485-92	87
587	Gene-environment interactions: lifetime cognitive activity, APOE genotype, and ⊞myloid burden. <b>2014</b> , 34, 8612-7	93
586	In Vivo Brain Imaging in Animal Models: A Focus on PET and MRI. <b>2014</b> , 149-166	
585	In vivo evaluation of 18F-MNI698: an 18F-labeled radiotracer for imaging of serotonin 4 receptors in brain. <b>2014</b> , 55, 858-64	15
584	Simultaneous fMRI-PET of the opioidergic pain system in human brain. <b>2014</b> , 102 Pt 2, 275-82	43
583	Umbilical Cord Blood Banking and Transplantation. 2014,	1
582	Synthesis and evaluation of (13)N-labelled azo compounds for Eamyloid imaging in mice. <b>2014</b> , 16, 538-49	14
581	Deriving physiological information from PET images: from SUV to compartmental modelling. <b>2014</b> , 2, 239-251	21
580	In vivo PET imaging of beta-amyloid deposition in mouse models of Alzheimer's disease with a high specific activity PET imaging agent [(18)F]flutemetamol. <b>2014</b> , 4, 37	19
579	Modifiable cardiovascular risk factors and axial motor impairments in Parkinson disease. <b>2014</b> , 82, 1514-20	58

578	Neural compensation in older people with brain amyloid-Ideposition. <b>2014</b> , 17, 1316-8	123
577	In vivo imaging of histone deacetylases (HDACs) in the central nervous system and major peripheral organs. <b>2014</b> , 57, 7999-8009	61
576	In vivo imaging of human cholinergic nerve terminals with (-)-5-(18)F-fluoroethoxybenzovesamicol: biodistribution, dosimetry, and tracer kinetic analyses. <b>2014</b> , 55, 396-404	83
575	Discovery and development of 11C-Lu AE92686 as a radioligand for PET imaging of phosphodiesterase10A in the brain. <b>2014</b> , 55, 1513-8	31
574	Reproducibility of non-invasive a1 adenosine receptor quantification in the rat brain using [(18)F]CPFPX and positron emission tomography. <b>2014</b> , 16, 699-709	11
573	Neurobiology of placebo effects: expectations or learning?. <b>2014</b> , 9, 1013-21	37
572	Neuroinflammation in Patients with Chronic Fatigue Syndrome/Myalgic Encephalomyelitis: An IIC-(R)-PK11195 PET Study. <b>2014</b> , 55, 945-50	179
571	Spinal cord dopamine D2/D3 receptors: in vivo and ex vivo imaging in the rat using (18)F/(11)C-fallypride. <b>2014</b> , 41, 841-7	6
570	11C-cetrozole: an improved C-11C-methylated PET probe for aromatase imaging in the brain. <b>2014</b> , 55, 852-7	25
569	Surface-based partial-volume correction for high-resolution PET. <b>2014</b> , 102 Pt 2, 674-87	17
568	Neuroprotective pathways: lifestyle activity, brain pathology, and cognition in cognitively normal older adults. <b>2014</b> , 35, 1873-82	82
567	Characterization of [(11)C]Cimbi-36 as an agonist PET radioligand for the 5-HT(2A) and 5-HT(2C) receptors in the nonhuman primate brain. <b>2014</b> , 84, 342-53	48
566	Serotonin 2A receptor agonist binding in the human brain with [IIC]Cimbi-36. <i>Journal of Cerebral Blood Flow and Metabolism</i> , <b>2014</b> , 34, 1188-96	68
565	Quantification of dopamine transporter density with [18F]FECNT PET in healthy humans. <b>2014</b> , 41, 217-22	10
564	Psychological well-being and regional brain amyloid and tau in mild cognitive impairment. <b>2014</b> , 22, 362-9	7
563	Basal Eppioid receptor availability in the amygdala predicts the inhibition of pain-related brain activity during heterotopic noxious counter-stimulation. <b>2014</b> , 81-82, 78-84	14
562	In vivo measures of nigrostriatal neuronal response to unilateral MPTP treatment. <b>2014</b> , 1571, 49-60	8
561	Kinetic modeling in pre-clinical positron emission tomography. <b>2014</b> , 24, 274-85	13

## (2015-2014)

560	Parallel ICA of FDG-PET and PiB-PET in three conditions with underlying Alzheimer's pathology. <b>2014</b> , 4, 508-16	41
559	Quantification of GABAA receptors in the rat brain with [(123)I]Iomazenil SPECT from factor analysis-denoised images. <b>2014</b> , 41, 186-95	13
558	Amyloid burden and neural function in people at risk for Alzheimer's Disease. <b>2014</b> , 35, 576-84	117
557	[H]Altanserin and small animal PET: impact of multidrug efflux transporters on ligand brain uptake and subsequent quantification of 5-HTA receptor densities in the rat brain. <b>2014</b> , 41, 1-9	11
556	Evaluation of P-glycoprotein (abcb1a/b) modulation of [(18)F]fallypride in MicroPET imaging studies. <b>2014</b> , 84, 152-8	9
555	Extrastriatal dopaminergic changes in Parkinson's disease patients with impulse control disorders. <b>2014</b> , 85, 23-30	35
554	D2 receptor occupancy following lurasidone treatment in patients with schizophrenia or schizoaffective disorder. <b>2014</b> , 19, 176-81	16
553	3D-neuronavigation in vivo through a patient's brain during a spontaneous migraine headache. <b>2014</b> ,	9
552	Dual-tracer receptor concentration imaging using tracers with different tissue delivery kinetics. <b>2014</b> ,	
551	A modified simplified reference tissue model for the quantification of dopamine D2/3 receptors with [18F]fallypride images. <b>2014</b> , 13,	2
551 550		2 23
	with [18F]fallypride images. 2014, 13,  Alzheimer disease biomarkers, attentional control, and semantic memory retrieval: Synergistic and mediational effects of biomarkers on a sensitive cognitive measure in non-demented older adults.	
550	with [18F]fallypride images. 2014, 13,  Alzheimer disease biomarkers, attentional control, and semantic memory retrieval: Synergistic and mediational effects of biomarkers on a sensitive cognitive measure in non-demented older adults. 2015, 29, 368-81  Characterization of brain mGluR5 binding in a pilot study of late-life major depressive disorder	23
550 549	with [18F]fallypride images. 2014, 13,  Alzheimer disease biomarkers, attentional control, and semantic memory retrieval: Synergistic and mediational effects of biomarkers on a sensitive cognitive measure in non-demented older adults. 2015, 29, 368-81  Characterization of brain mGluR5 binding in a pilot study of late-life major depressive disorder using positron emission tomography and [IIC]ABP688. 2015, 5, e693	<sup>2</sup> 3
550 549 548	with [18F]fallypride images. 2014, 13,  Alzheimer disease biomarkers, attentional control, and semantic memory retrieval: Synergistic and mediational effects of biomarkers on a sensitive cognitive measure in non-demented older adults. 2015, 29, 368-81  Characterization of brain mGluR5 binding in a pilot study of late-life major depressive disorder using positron emission tomography and [IIIC]ABP688. 2015, 5, e693  Exploring the effects of coexisting amyloid in subcortical vascular cognitive impairment. 2015, 15, 197	23 27 7
<ul><li>550</li><li>549</li><li>548</li><li>547</li></ul>	with [18F] fally pride images. 2014, 13,  Alzheimer disease biomarkers, attentional control, and semantic memory retrieval: Synergistic and mediational effects of biomarkers on a sensitive cognitive measure in non-demented older adults. 2015, 29, 368-81  Characterization of brain mGluR5 binding in a pilot study of late-life major depressive disorder using positron emission tomography and [IIC] ABP688. 2015, 5, e693  Exploring the effects of coexisting amyloid in subcortical vascular cognitive impairment. 2015, 15, 197  Challenges of quantification of TSPO in the human brain. 2015, 3, 403-416  In vivo quantification of the [(11)C]DASB binding in the normal canine brain using positron emission	23 27 7
<ul><li>550</li><li>549</li><li>548</li><li>547</li><li>546</li></ul>	with [18F]fallypride images. 2014, 13,  Alzheimer disease biomarkers, attentional control, and semantic memory retrieval: Synergistic and mediational effects of biomarkers on a sensitive cognitive measure in non-demented older adults. 2015, 29, 368-81  Characterization of brain mGluR5 binding in a pilot study of late-life major depressive disorder using positron emission tomography and [ITC]ABP688. 2015, 5, e693  Exploring the effects of coexisting amyloid in subcortical vascular cognitive impairment. 2015, 15, 197  Challenges of quantification of TSPO in the human brain. 2015, 3, 403-416  In vivo quantification of the [(11)C]DASB binding in the normal canine brain using positron emission tomography. 2015, 11, 308	23 27 7 15

542	In Vivo Quantification of 5-HT2A Brain Receptors in Mdr1a KO Rats with 123I-R91150 Single-Photon Emission Computed Tomography. <b>2015</b> , 14,		5
541	GABAA receptor deficits predict recovery in patients with disorders of consciousness: A preliminary multimodal [(11) C]Flumazenil PET and fMRI study. <b>2015</b> , 36, 3867-77		6
540	Quantitative graphical analysis of simultaneous dynamic PET/MRI for assessment of prostate cancer. <b>2015</b> , 40, e236-40		9
539	Modeling clustered activity increase in amyloid-beta positron emission tomographic images with statistical descriptors. <b>2015</b> , 10, 759-70		4
538	Positron Emission Tomography (PET): Quantification and Kinetic Modeling. 2015,		1
537	Quantitative amyloid imaging using image-derived arterial input function. <b>2015</b> , 10, e0122920		20
536	Novel Histone Deacetylase Class IIa Selective Substrate Radiotracers for PET Imaging of Epigenetic Regulation in the Brain. <b>2015</b> , 10, e0133512		16
535	Dissociable rate-dependent effects of oral methylphenidate on impulsivity and D2/3 receptor availability in the striatum. <b>2015</b> , 35, 3747-55		40
534	Improved factor analysis of dynamic PET images to estimate arterial input function and tissue curves. <b>2015</b> ,		
533	Existing Pittsburgh Compound-B positron emission tomography thresholds are too high: statistical and pathological evaluation. <b>2015</b> , 138, 2020-33		227
532	Low Dopamine D2/D3 Receptor Availability is Associated with Steep Discounting of Delayed Rewards in Methamphetamine Dependence. <b>2015</b> , 18, pyu119		47
531	Performance of 11C-Pittsburgh Compound B PET Binding Potential Images in the Detection of Amyloid Deposits on Equivocal Static Images. <b>2015</b> , 56, 1910-5		17
530	[(18)F]FPEB and [(18)F]FDEGPECO comparative study of mGlu5 quantification in rodent brain. <b>2015</b> , 98, 103-7		3
529	Automated reference region extraction and population-based input function for brain [(11)C]TMSX PET image analyses. <i>Journal of Cerebral Blood Flow and Metabolism</i> , <b>2015</b> , 35, 157-65	3	30
528	Relationship between in vivo receptor occupancy and efficacy of metabotropic glutamate receptor subtype 5 allosteric modulators with different in vitro binding profiles. <b>2015</b> , 40, 755-65		36
527	Low amyloid-Ideposition correlates with high education in cognitively normal older adults: a pilot study. <b>2015</b> , 30, 919-26		16
526	Test-retest reliability of (11)C-ORM-13070 in PET imaging of 望C-adrenoceptors in vivo in the human brain. <b>2015</b> , 42, 120-7		128
525	Chronic Back Pain Is Associated with Alterations in Dopamine Neurotransmission in the Ventral Striatum. <b>2015</b> , 35, 9957-65		94

#### (2015-2015)

524	2015, 36, 2568-76	129
523	Preclinical evaluation of a promising C-11 labeled PET tracer for imaging phosphodiesterase 10A in the brain of living subject. <b>2015</b> , 121, 253-62	15
522	Resting-state synchrony between the retrosplenial cortex and anterior medial cortical structures relates to memory complaints in subjective cognitive impairment. <b>2015</b> , 36, 2145-52	26
521	Methamphetamine-sensitized rats show augmented dopamine release to methylphenidate stimulation: a positron emission tomography using [18F]fallypride. <b>2015</b> , 232, 92-7	2
520	Endogenous Opioid Mechanisms Are Implicated in Obesity and Weight Loss in Humans. <b>2015</b> , 100, 3193-201	33
519	The simplified reference tissue model: model assumption violations and their impact on binding potential. <i>Journal of Cerebral Blood Flow and Metabolism</i> , <b>2015</b> , 35, 304-11	69
518	PET Quantification of Tau Pathology in Human Brain with 11C-PBB3. <b>2015</b> , 56, 1359-65	77
517	Quantification of [(11)C]PIB PET for imaging myelin in the human brain: a test-retest reproducibility study in high-resolution research tomography. <i>Journal of Cerebral Blood Flow and Metabolism</i> , <b>2015</b> , 35, 1771-82	43
516	Pharmacokinetic Modeling of Dynamic PET. <b>2015</b> , 209-215	
515	Caffeine increases striatal dopamine D2/D3 receptor availability in the human brain. <b>2015</b> , 5, e549	79
514	The role of pallidal serotonergic function in Parkinson's disease dyskinesias: a positron emission tomography study. <b>2015</b> , 36, 1736-1742	39
513	Radiosynthesis and in vivo evaluation of two imidazopyridineacetamides, [(11)C]CB184 and [ (11)C]CB190, as a PET tracer for 18 kDa translocator protein: direct comparison with [ (11)C](R)-PK11195. <b>2015</b> , 29, 325-35	16
512	Imaging pulmonary inducible nitric oxide synthase expression with PET. <b>2015</b> , 56, 76-81	29
511	Predicting amyloid status in corticobasal syndrome using modified clinical criteria, magnetic resonance imaging and fluorodeoxyglucose positron emission tomography. <b>2015</b> , 7, 8	27
510	Quantitative Evaluation of Tumor Early Response to a Vascular-Disrupting Agent with Dynamic PET. <b>2015</b> , 17, 865-73	4
509	Quantitative Analysis of III-(E)-N-(3-Iodoprop-2-Enyl)-2ECarbofluoroethoxy-3E(4'-Methyl-Phenyl) Nortropane Binding to the Dopamine Transporter in Parkinson Disease. <b>2015</b> , 56, 714-20	37
508	Characterization in humans of 18F-MNI-444, a PET radiotracer for brain adenosine 2A receptors. <b>2015</b> , 56, 586-91	38
507	No parkinsonism in SCA2 and SCA3 despite severe neurodegeneration of the dopaminergic substantia nigra. <b>2015</b> , 138, 3316-26	41

506	An exploratory efficacy study of the amyloid imaging agent [(18)F]flutemetamol in Japanese Subjects. <b>2015</b> , 29, 391-9		2
505	Immediate and Persistent Effects of Salvinorin A on the Kappa Opioid Receptor in Rodents, Monitored In Vivo with PET. <b>2015</b> , 40, 2865-72		13
504	Quantitative imaging of protein targets in the human brain with PET. 2015, 60, R363-411		42
503	Imaging neuroinflammation in multiple sclerosis using TSPO-PET. <b>2015</b> , 3, 461-473		32
502	Clustering-initiated factor analysis application for tissue classification in dynamic brain positron emission tomography. <i>Journal of Cerebral Blood Flow and Metabolism</i> , <b>2015</b> , 35, 1104-11	7.3	2
501	Quantitative positron emission tomography of mGluR5 in rat brain with [(18) F]PSS232 at minimal invasiveness and reduced model complexity. <b>2015</b> , 133, 330-42		21
500	Quantification of blood flow-dependent component in estimates of beta-amyloid load obtained using quasi-steady-state standardized uptake value ratio. <i>Journal of Cerebral Blood Flow and Metabolism</i> , <b>2015</b> , 35, 1485-93	7-3	24
499	Quantitative kinetic analysis of PET amyloid imaging agents [(11)C]BF227 and [(18)F]FACT in human brain. <b>2015</b> , 42, 734-44		7
498	Parametric imaging and quantitative analysis of the PET amyloid ligand [(18)F]flutemetamol. <b>2015</b> , 121, 184-92		17
497	EAmyloid binding in elderly subjects with declining or stable episodic memory function measured with PET and [IIIC]AZD2184. <b>2015</b> , 42, 1507-11		4
496	Effects of Silexan on the serotonin-1A receptor and microstructure of the human brain: a randomized, placebo-controlled, double-blind, cross-over study with molecular and structural neuroimaging. <b>2014</b> , 18,		36
495	Non-exercise physical activity attenuates motor symptoms in Parkinson disease independent from nigrostriatal degeneration. <b>2015</b> , 21, 1227-31		11
494	Quantitative in vivo cell-surface receptor imaging in oncology: kinetic modeling and paired-agent principles from nuclear medicine and optical imaging. <b>2015</b> , 60, R239-69		68
493	Quantification of EAmyloidosis and rCBF with Dedicated PET, 7 T MR Imaging, and High-Resolution Microscopic MR Imaging at 16.4 T in APP23 Mice. <b>2015</b> , 56, 1593-9		9
492	FDG-PET Contributions to the Pathophysiology of Memory Impairment. <b>2015</b> , 25, 326-55		17
491	Human serotonin transporter availability predicts fear conditioning. <b>2015</b> , 98, 515-9		9
490	Noninvasive blood-free full quantification of positron emission tomography radioligand binding. Journal of Cerebral Blood Flow and Metabolism, <b>2015</b> , 35, 148-56	7.3	8
489	Partial volume correction in quantitative amyloid imaging. <b>2015</b> , 107, 55-64		138

## (2016-2015)

488	Dynamic interactions between plasma IL-1 family cytokines and central endogenous opioid neurotransmitter function in humans. <b>2015</b> , 40, 554-65		18
487	Deficit in sustained attention following selective cholinergic lesion of the pedunculopontine tegmental nucleus in rat, as measured with both post-mortem immunocytochemistry and in vivo PET imaging with [I]fluoroethoxybenzovesamicol. 2015, 278, 107-14		24
486	Insulin resistance predicts brain amyloid deposition in late middle-aged adults. <b>2015</b> , 11, 504-510.e1		147
485	Quantitative Amyloid Imaging in Autosomal Dominant Alzheimer's Disease: Results from the DIAN Study Group. <b>2016</b> , 11, e0152082		31
484	Dynamic PET Measures of Tau Accumulation in Cognitively Normal Older Adults and Alzheimer's Disease Patients Measured Using [18F] THK-5351. <b>2016</b> , 11, e0158460		65
483	Imaging Central Nervous System Demyelination and Remyelination by Positron-Emission Tomography. <b>2016</b> , 2, 93-98		5
482	Interpreting DTBZ binding data in rodent: Inherent variability and compensation. 2016, 70, 147-52		5
481	High amyloid-Ideposition related to depressive symptoms in older individuals with normal cognition: a pilot study. <b>2016</b> , 31, 920-8		31
480	Oral Abstracts. Journal of Cerebral Blood Flow and Metabolism, 2016, 36, 1-173	7.3	4
479	Dopamine D1 signaling organizes network dynamics underlying working memory. <b>2016</b> , 2, e1501672		41
479 478	Dopamine D1 signaling organizes network dynamics underlying working memory. <b>2016</b> , 2, e1501672  Comparison of [C]TZ1964B and [F]MNI659 for PET imaging brain PDE10A in nonhuman primates. <b>2016</b> , 4, e00253		41
	Comparison of [C]TZ1964B and [F]MNI659 for PET imaging brain PDE10A in nonhuman primates.		
478	Comparison of [C]TZ1964B and [F]MNI659 for PET imaging brain PDE10A in nonhuman primates. <b>2016</b> , 4, e00253		4
478 477	Comparison of [C]TZ1964B and [F]MNI659 for PET imaging brain PDE10A in nonhuman primates.  2016, 4, e00253  PET Imaging of Tau Deposition in the Aging Human Brain. 2016, 89, 971-982  Noninvasive evaluation of nicotinic acetylcholine receptor availability in mouse brain using		4 619
478 477 476	Comparison of [C]TZ1964B and [F]MNI659 for PET imaging brain PDE10A in nonhuman primates. 2016, 4, e00253  PET Imaging of Tau Deposition in the Aging Human Brain. 2016, 89, 971-982  Noninvasive evaluation of nicotinic acetylcholine receptor availability in mouse brain using single-photon emission computed tomography with [(123)I]5IA. 2016, 43, 372-8		4 619 6
478 477 476 475	Comparison of [C]TZ1964B and [F]MNI659 for PET imaging brain PDE10A in nonhuman primates. 2016, 4, e00253  PET Imaging of Tau Deposition in the Aging Human Brain. 2016, 89, 971-982  Noninvasive evaluation of nicotinic acetylcholine receptor availability in mouse brain using single-photon emission computed tomography with [(123)I]5IA. 2016, 43, 372-8  PET-CT and PET-MRI in Neurology. 2016,  Modifiable Risk Factors and Brain Positron Emission Tomography Measures of Amyloid and Tau in		<ul><li>4</li><li>619</li><li>6</li><li>2</li></ul>
478 477 476 475 474	Comparison of [C]TZ1964B and [F]MNI659 for PET imaging brain PDE10A in nonhuman primates. 2016, 4, e00253  PET Imaging of Tau Deposition in the Aging Human Brain. 2016, 89, 971-982  Noninvasive evaluation of nicotinic acetylcholine receptor availability in mouse brain using single-photon emission computed tomography with [(123)I]5IA. 2016, 43, 372-8  PET-CT and PET-MRI in Neurology. 2016,  Modifiable Risk Factors and Brain Positron Emission Tomography Measures of Amyloid and Tau in Nondemented Adults with Memory Complaints. 2016, 24, 729-37  Progressive Cortical Neuronal Damage and Chronic Hemodynamic Impairment in Atherosclerotic		4 619 6 2 38

470	Nicotine-specific and non-specific effects of cigarette smoking on endogenous opioid mechanisms. <b>2016</b> , 69, 69-77	23
469	Increased Seasonal Variation in Serotonin Transporter Binding in Seasonal Affective Disorder. <b>2016</b> , 41, 2447-54	26
468	Dynamic relationships between age, amyloid-Ideposition, and glucose metabolism link to the regional vulnerability to Alzheimer's disease. <b>2016</b> , 139, 2275-89	48
467	Serotonin transporter binding is reduced in seasonal affective disorder following light therapy. <b>2016</b> , 134, 410-419	23
466	Impact of spillover from white matter by partial volume effect on quantification of amyloid deposition with [C]PiB PET. <b>2016</b> , 143, 316-324	23
465	Intranasal Opioid Administration in Rhesus Monkeys: PET Imaging and Antinociception. <b>2016</b> , 359, 366-373	18
464	Tau Positron Emission Tomographic Imaging in the Lewy Body Diseases. <b>2016</b> , 73, 1334-1341	138
463	Dynamic Imaging of Individual Remyelination Profiles in Multiple Sclerosis. <b>2016</b> , 79, 726-738	101
462	Baseline symptom severity predicts serotonin transporter change during psychotherapy in patients with major depression. <b>2016</b> , 70, 34-41	6
461	In vivo quantifying molecular specificity of Cy5.5-labeled cyclic 9-mer peptide probe with dynamic fluorescence imaging. <b>2016</b> , 7, 1149-59	12
460	Positron Emission Tomography. <b>2016</b> , 99-117	
459	Occupancy of pramipexole (Sifrol) at cerebral dopamine D2/3 receptors in Parkinson's disease patients. <b>2016</b> , 12, 41-6	14
458	Guidelines to PET measurements of the target occupancy in the brain for drug development. <b>2016</b> , 43, 2255-2262	18
457	Distinct roles for primate caudate dopamine D1 and D2 receptors in visual discrimination learning revealed using shRNA knockdown. <b>2016</b> , 6, 35809	10
456	Noninvasive bi-graphical analysis for the quantification of slowly reversible radioligand binding. <b>2016</b> , 61, 6770-6790	3
455	Endogenous opioidergic dysregulation of pain in fibromyalgia: a PET and fMRI study. <b>2016</b> , 157, 2217-2225	87
454	Comparative assessment of (18) F-Mefway as a serotonin 5-HT1A receptor PET imaging agent across species: Rodents, nonhuman primates, and humans. <b>2016</b> , 524, 1457-71	10
453	Parametric Binding Images of the TSPO Ligand 18F-DPA-714. <b>2016</b> , 57, 1543-1547	17

## (2016-2016)

452	Kinetics of the Tau PET Tracer 18F-AV-1451 (T807) in Subjects with Normal Cognitive Function, Mild Cognitive Impairment, and Alzheimer Disease. <b>2016</b> , 57, 1535-1542	72
451	Dopamine D2 receptor availability is linked to hippocampal-caudate functional connectivity and episodic memory. <b>2016</b> , 113, 7918-23	84
450	Investigation of Proposed Activity of Clarithromycin at GABAA Receptors Using [(11)C]Flumazenil PET. <b>2016</b> , 7, 746-50	3
449	Preclinical Characterization of the Phosphodiesterase 10A PET Tracer [(11)C]MK-8193. <b>2016</b> , 18, 579-87	10
448	Tracer Kinetic Analysis of (S)-IB-THK5117 as a PET Tracer for Assessing Tau Pathology. <b>2016</b> , 57, 574-81	41
447	PET Radioligands Reveal the Basis of Dementia in Parkinson's Disease and Dementia with Lewy Bodies. <b>2016</b> , 16, 118-24	32
446	Dynamic Changes in Striatal mGluR1 But Not mGluR5 during Pathological Progression of Parkinson's Disease in Human Alpha-Synuclein A53T Transgenic Rats: A Multi-PET Imaging Study. <b>2016</b> , 36, 375-84	24
445	Differential dopamine function in fibromyalgia. <b>2016</b> , 10, 829-39	31
444	In Vivo Imaging of Human Neuroinflammation. <b>2016</b> , 7, 470-83	121
443	Reduced sleep duration mediates decreases in striatal D2/D3 receptor availability in cocaine abusers. <b>2016</b> , 6, e752	26
442	Small-Animal PET Imaging of Tau Pathology with 18F-THK5117 in 2 Transgenic Mouse Models. <b>2016</b> , 57, 792-8	27
441	Diabetes, Gray Matter Loss, and Cognition in the Setting of Parkinson Disease. <b>2016</b> , 23, 577-81	18
440	The Role of Dopamine in Value-Based Attentional Orienting. <b>2016</b> , 26, 550-5	78
439	Socioeconomic status is associated with striatal dopamine D2/D3 receptors in healthy volunteers but not in cocaine abusers. <b>2016</b> , 617, 27-31	55
438	Eamyloid, hippocampal atrophy and their relation to longitudinal brain change in cognitively normal individuals. <b>2016</b> , 40, 173-180	22
437	Glial Activation and Glucose Metabolism in a Transgenic Amyloid Mouse Model: A Triple-Tracer PET Study. <b>2016</b> , 57, 954-60	86
436	Serotonin-to-dopamine transporter ratios in Parkinson disease: Relevance for dyskinesias. <b>2016</b> , 86, 1152-8	60
435	Tau PET patterns mirror clinical and neuroanatomical variability in Alzheimer's disease. <b>2016</b> , 139, 1551-67	57°

434	Optimal timing of [II]Mefway PET for imaging the serotonin 1A receptor in healthy male subjects. <b>2016</b> , 107, 127-132	2
433	Overlapping expression of serotonin transporters and neurokinin-1 receptors in posttraumatic stress disorder: a multi-tracer PET study. <b>2016</b> , 21, 1400-7	16
432	P-Glycoprotein, not BCRP, Limits the Brain Uptake of [(18)F]Mefway in Rodent Brain. 2016, 18, 267-73	4
431	Dual time-point imaging for post-dose binding potential estimation applied to a [C]raclopride PET dose occupancy study. <i>Journal of Cerebral Blood Flow and Metabolism</i> , <b>2017</b> , 37, 866-876	1
430	Quantitative longitudinal imaging of activated microglia as a marker of inflammation in the pilocarpine rat model of epilepsy using [C]-(R)-PK11195 PET and MRI. <i>Journal of Cerebral Blood Flow and Metabolism</i> , <b>2017</b> , 37, 1251-1263	19
429	Use of T1-weighted/T2-weighted magnetic resonance ratio to elucidate changes due to amyloid accumulation in cognitively normal subjects. <b>2017</b> , 13, 209-214	12
428	Neural correlates of apathy in late-life depression: a pilot [F]FDDNP positron emission tomography study. <b>2017</b> , 17, 186-193	18
427	Central Expioidergic System Activation Evoked by Heavy and Severe-Intensity Cycling Exercise in Humans: a Pilot Study Using Positron Emission Tomography with 11C-Carfentanil. <b>2017</b> , 38, 19-26	13
426	Sensory Processing in Rhesus Monkeys: Developmental Continuity, Prenatal Treatment, and Genetic Influences. <b>2017</b> , 88, 183-197	5
425	Mutual effect of cerebral amyloid land peripheral lymphocytes in cognitively normal older individuals. <b>2017</b> , 32, e93-e99	5
424	Binding of C-Pittsburgh compound-B correlated with white matter injury in hypertensive small vessel disease. <b>2017</b> , 31, 227-234	2
423	Initial Evaluation of an Adenosine A Receptor Ligand, C-Preladenant, in Healthy Human Subjects. <b>2017</b> , 58, 1464-1470	18
422	Neuroinflammation in Neurodegenerative Disorders-a Review. <b>2017</b> , 17, 25	155
421	Amyloid and tau PET demonstrate region-specific associations in normal older people. <b>2017</b> , 150, 191-199	49
420	GABA receptor subtypes in the mouse brain: Regional mapping and diazepam receptor occupancy by in vivo [F]flumazenil PET. <b>2017</b> , 150, 279-291	11
419	Dopamine in the medial amygdala network mediates human bonding. <b>2017</b> , 114, 2361-2366	68
418	New Repeat Polymorphism in the Gene Predicts Striatal Dopamine D2/D3 Receptor Availability and Stimulant-Induced Dopamine Release in the Healthy Human Brain. <b>2017</b> , 37, 4982-4991	13
417	Progressive Cortical Neuronal Damage and Extracranial-Intracranial Bypass Surgery in Patients with Misery Perfusion. <b>2017</b> , 38, 935-941	4

# (2017-2017)

416	Neuroimaging markers associated with maintenance of optimal memory performance in late-life. <b>2017</b> , 100, 164-170	23
415	Translocator positron-emission tomography and magnetic resonance spectroscopic imaging of brain glial cell activation in multiple sclerosis. <b>2017</b> , 23, 1469-1478	17
414	C-PBR28 and F-PBR111 Detect White Matter Inflammatory Heterogeneity in Multiple Sclerosis. <b>2017</b> , 58, 1477-1482	36
413	Dopamine D2/D3 imbalance during migraine attack and allodynia in vivo. <b>2017</b> , 88, 1634-1641	30
412	Density of available striatal dopamine receptors predicts trait impulsiveness during performance of an attention-demanding task. <b>2017</b> , 118, 64-68	4
411	In vivo tau PET imaging in dementia: Pathophysiology, radiotracer quantification, and a systematic review of clinical findings. <b>2017</b> , 36, 50-63	84
410	Serotonin and dopamine transporter PET changes in the premotor phase of LRRK2 parkinsonism: cross-sectional studies. <b>2017</b> , 16, 351-359	64
409	Generalized paired-agent kinetic model for in vivo quantification of cancer cell-surface receptors under receptor saturation conditions. <b>2017</b> , 62, 394-414	6
408	A single-scan protocol for absolute D receptor quantification with [I]IBZM SPECT. 2017, 147, 461-472	10
407	In vivo evaluation of [F]FECIMBI-36, an agonist 5-HT receptor PET radioligand in nonhuman primate. <b>2017</b> , 27, 21-23	10
406	. <b>2017</b> , 1, 128-135	3
405	Utility of Molecular and Structural Brain Imaging to Predict Progression from Mild Cognitive Impairment to Dementia. <b>2017</b> , 60, 939-947	4
404	Neuroinflammation and its relationship to changes in brain volume and white matter lesions in multiple sclerosis. <b>2017</b> , 140, 2927-2938	57
403	Human iPS cell-derived dopaminergic neurons function in a primate Parkinson's disease model. <b>2017</b> , 548, 592-596	364
402	Striatal dopamine D2/3 receptor-mediated neurotransmission in major depression: Implications for anhedonia, anxiety and treatment response. <b>2017</b> , 27, 977-986	41
401	Early synaptic dysfunction induced by Bynuclein in a rat model of Parkinson's disease. <b>2017</b> , 7, 6363	43
400	In Vivo Monitoring for Regional Changes of Metabotropic Glutamate Receptor Subtype 1 (mGluR1) in Pilocarpine-Induced Epileptic Rat Brain by Small-Animal PET. <b>2017</b> , 7, 14945	7
399	Whole-body biodistribution and the influence of body activity on brain kinetic analysis of the C-PiB PET scan. <b>2017</b> , 10, 464-474	

398	Striatal Dopamine D2/D3 Receptor Availability Varies Across Smoking Status. <b>2017</b> , 42, 2325-2332	19
397	Quantitative positron emission tomography in brain research. <b>2017</b> , 1670, 220-234	27
396	Associations between cerebral amyloid and changes in cognitive function and falls risk in subcortical ischemic vascular cognitive impairment. <b>2017</b> , 17, 133	3
395	Compartmental Modeling in PET Kinetics. <b>2017</b> , 323-352	
394	In Vivo Comparison of Tau Radioligands F-THK-5351 and F-THK-5317. <b>2017</b> , 58, 996-1002	43
393	Estimation of the binding potential BP without a reference region or blood samples for brain PET studies. <b>2017</b> , 146, 121-131	7
392	Preclinical in vivo and in vitro comparison of the translocator protein PET ligands [F]PBR102 and [F]PBR111. <b>2017</b> , 44, 296-307	17
391	Modeling Strategies for Quantification of In Vivo F-AV-1451 Binding in Patients with Tau Pathology. <b>2017</b> , 58, 623-631	46
390	Characterization of [C]Lu AE92686 as a PET radioligand for phosphodiesterase 10A in the nonhuman primate brain. <b>2017</b> , 44, 308-320	4
389	Reference Tissue-Based Kinetic Evaluation of 18F-AV-1451 for Tau Imaging. <b>2017</b> , 58, 332-338	66
388	Assessing neuronal density in peri-infarct cortex with PET: Effects of cortical topology and partial volume correction. <b>2017</b> , 38, 326-338	7
387	Pharmacokinetic Evaluation of the Tau PET Radiotracer F-T807 (F-AV-1451) in Human Subjects. <b>2017</b> , 58, 484-491	65
386	Longitudinal Small-Animal PET Imaging of the zQ175 Mouse Model of Huntington Disease Shows In Vivo Changes of Molecular Targets in the Striatum and Cerebral Cortex. <b>2017</b> , 58, 617-622	18
385	TSPO imaging using the novel PET ligand [F]GE-180: quantification approaches in patients with multiple sclerosis. <b>2017</b> , 7, 89	40
384	Parametric PET Image Reconstruction via Regional Spatial Bases and Pharmacokinetic Time Activity Model. <b>2017</b> , 19, 629	1
383	Revisiting the Logan plot to account for non-negligible blood volume in brain tissue. <b>2017</b> , 7, 66	7
382	In Vivo Characterization of Two F-Labeled PDE10A PET Radioligands in Nonhuman Primate Brains. <b>2018</b> , 9, 1066-1073	3
381	Reference tissue models in the assessment of C-DTBZ binding to the VMAT2 in rat striatum: A test-retest reproducibility study. <b>2018</b> , 72, e22029	4

380	Serotonin, 🖾 myloid, and cognition in Parkinson disease. <b>2018</b> , 83, 994-1002	27
379	Brain morphology, cognition, and 🗈 myloid in older adults with superior memory performance. <b>2018</b> , 67, 162-170	35
378	EAmyloid accumulation in the human brain after one night of sleep deprivation. 2018, 115, 4483-4488	333
377	Nigrostriatal proteasome inhibition impairs dopamine neurotransmission and motor function in minipigs. <b>2018</b> , 303, 142-152	20
376	Chronic ETHC in Rhesus Monkeys: Effects on Cognitive Performance and Dopamine D2/D3 Receptor Availability. <b>2018</b> , 364, 300-310	10
375	Longitudinal uncoupling of cerebral perfusion, glucose metabolism, and tau deposition in Alzheimer's disease. <b>2018</b> , 14, 652-663	11
374	Imaging Aland tau in early stage Alzheimer's disease with [F]AV45 and [F]AV1451. <b>2018</b> , 8, 19	10
373	Characterization of 3 Novel Tau Radiopharmaceuticals, C-RO-963, C-RO-643, and F-RO-948, in Healthy Controls and in Alzheimer Subjects. <b>2018</b> , 59, 1869-1876	61
372	Cardiovascular Risk Factor Burden in Veterans and Non-Veterans with Parkinson Disease. <b>2018</b> , 8, 153-160	5
371	Vascular-metabolic and GABAergic Inhibitory Correlates of Neural Variability Modulation. A Combined fMRI and PET Study. <b>2018</b> , 379, 142-151	3
370	D2/D3 dopamine receptor binding with [F-18]fallypride correlates of executive function in medication-nalle patients with schizophrenia. <b>2018</b> , 192, 442-456	12
369	Parametric Imaging of [C]Flumazenil Binding in the Rat Brain. 2018, 20, 114-123	4
368	Novel F-Labeled Expioid Receptor Antagonist as PET Radiotracer: Synthesis and In Vivo Evaluation of F-LY2459989 in Nonhuman Primates. <b>2018</b> , 59, 140-146	22
367	Latent-Profile Analysis Reveals Behavioral and Brain Correlates of Dopamine-Cognition Associations. <b>2018</b> , 28, 3894-3907	22
366	Local and distant relationships between amyloid, tau and neurodegeneration in Alzheimer's Disease. <b>2018</b> , 17, 452-464	83
365	Pseudoreference Regions for Glial Imaging with C-PBR28: Investigation in 2 Clinical Cohorts. <b>2018</b> , 59, 107-114	26
364	In Vivo Brain Plaque and Tangle Burden Mediates the Association Between Diastolic Blood Pressure and Cognitive Functioning in Nondemented Adults. <b>2018</b> , 26, 13-22	4
363	Human brain imaging of nicotinic acetylcholine 42* receptors using [F]Nifene: Selectivity, functional activity, toxicity, aging effects, gender effects, and extrathalamic pathways. 2018, 526, 80-95	14

362	Memory and Brain Amyloid and Tau Effects of a Bioavailable Form of Curcumin in Non-Demented Adults: A Double-Blind, Placebo-Controlled 18-Month Trial. <b>2018</b> , 26, 266-277	126
361	Associations Between Tau, EAmyloid, and Cognition in Parkinson Disease. <b>2018</b> , 75, 227-235	36
360	Entorhinal Tau Pathology, Episodic Memory Decline, and Neurodegeneration in Aging. 2018, 38, 530-543	126
359	A first-in-man PET study of [F]PSS232, a fluorinated ABP688 derivative for imaging metabotropic glutamate receptor subtype 5. <b>2018</b> , 45, 1041-1051	12
358	Association of genetic ancestry with striatal dopamine D2/D3 receptor availability. 2018, 23, 1711-1716	14
357	Adaptive Weighted Nonlinear Least Squares Method for Fluorodeoxyglucose Positron Emission Tomography Quantification. <b>2018</b> , 38, 63-75	2
356	Dopamine transporter imaging with [F]FE-PE2I PET and [I]FP-CIT SPECT-a clinical comparison. <b>2018</b> , 8, 100	32
355	Reproducible quantification of cardiac sympathetic innervation using graphical modeling of carbon-11-meta-hydroxyephedrine kinetics with dynamic PET-CT imaging. <b>2018</b> , 8, 63	7
354	Association between aromatase in human brains and personality traits. 2018, 8, 16841	10
353	Quantification of Contrast Kinetics in Clinical Imaging. 2018,	1
352	Longer TOMM40 poly-T variants associated with higher FDDNP-PET medial temporal tau and amyloid binding. <b>2018</b> , 13, e0208358	3
351	Comparison of two different methods of image analysis for the assessment of microglial activation in patients with multiple sclerosis using (R)-[N-methyl-carbon-11]PK11195. <b>2018</b> , 13, e0201289	6
350	Advances in PET Methodology. <b>2018</b> , 141, 3-30	3
349	Imaging biomarkers of behavioral impairments: A pilot micro-positron emission tomographic study in a rat electrical post-status epilepticus model. <b>2018</b> , 59, 2194-2205	12
348	Habitual exercisers versus sedentary subjects with Parkinson's Disease: Multimodal PET and fMRI study. <b>2018</b> , 33, 1945-1950	18
347	Investigation of the quantitative accuracy of low-dose amyloid and tau PET imaging. 2018, 11, 451-459	O
346	Validation of diffusion tensor imaging measures of nigrostriatal neurons in macaques. <b>2018</b> , 13, e0202201	9

344 Tracer Kinetics in Radionanomedicine. **2018**, 293-310

343	Dual tracer tau PET imaging reveals different molecular targets for C-THK5351 and C-PBB3 in the Alzheimer brain. <b>2018</b> , 45, 1605-1617	27
342	Utilizing the Centiloid scale in cross-sectional and longitudinal PiB PET studies. 2018, 19, 406-416	37
341	Early Detection of A Deposition in the 5xFAD Mouse by Amyloid PET. <b>2018</b> , 2018, 5272014	13
340	Imaging correlates of behavioral impairments: An experimental PET study in the rat pilocarpine epilepsy model. <b>2018</b> , 118, 9-21	15
339	PBB3 binding in a patient with corticobasal syndrome. <b>2018</b> , 33, 1359-1360	5
338	FDDNP-PET Tau Brain Protein Binding Patterns in Military Personnel with Suspected Chronic Traumatic Encephalopathy1. <b>2018</b> , 65, 79-88	10
337	Investigation of the influence of sampling schemes on quantitative dynamic fluorescence imaging. <b>2018</b> , 9, 1859-1870	3
336	The Impact of Preprocessing Pipeline Choice in Univariate and Multivariate Analyses of PET Data. <b>2018</b> ,	1
335	Molecular Imaging of Sirtuin1 Expression-Activity in Rat Brain Using Positron-Emission Tomography-Magnetic-Resonance Imaging with [F]-2-Fluorobenzoylaminohexanoicanilide. <b>2018</b> , 61, 7116-7130	2
334	Methylation of the dopamine transporter gene in blood is associated with striatal dopamine transporter availability in ADHD: A preliminary study. <b>2018</b> , 48, 1884-1895	17
333	Self-rated intensity of habitual physical activities is positively associated with dopamine D receptor availability and cognition. <b>2018</b> , 181, 605-616	13
332	In vivo quantification of neurofibrillary tangles with [F]MK-6240. <b>2018</b> , 10, 74	69
331	In vivo quantification of glial activation in minipigs overexpressing human	9
330	The correlation between striatal and cortical binding ratio of C-PiB-PET in amyloid-uptake-positive patients. <b>2018</b> , 32, 398-403	5
329	Noninvasive PK11195-PET Image Analysis Techniques Can Detect Abnormal Cerebral Microglial Activation in Parkinson's Disease. <b>2018</b> , 28, 496-505	17
328	Selective D2 receptor PET in manganese-exposed workers. <b>2018</b> , 91, e1022-e1030	23
327	Evaluation of F-RO-948 PET for Quantitative Assessment of Tau Accumulation in the Human Brain. <b>2018</b> , 59, 1877-1884	44

326	Imaging Brain Metabolism in the Newborn. <b>2018</b> , 33, 851-860	15
325	Are dopamine receptor and transporter changes in Rett syndrome reflected in Mecp2-deficient mice?. <b>2018</b> , 307, 74-81	11
324	Reduced striatal dopamine release during motor skill acquisition in Parkinson's disease. <b>2018</b> , 13, e0196661	6
323	Brain Imaging of Alzheimer Dementia Patients and Elderly Controls with F-MK-6240, a PET Tracer Targeting Neurofibrillary Tangles. <b>2019</b> , 60, 107-114	63
322	Regional times to equilibria and their impact on semi-quantification of [F]AV-1451 uptake. <i>Journal of Cerebral Blood Flow and Metabolism</i> , <b>2019</b> , 39, 2223-2232	5
321	In Vivo Characterization and Quantification of Neurofibrillary Tau PET Radioligand F-MK-6240 in Humans from Alzheimer Disease Dementia to Young Controls. <b>2019</b> , 60, 93-99	106
320	QModeling: a Multiplatform, Easy-to-Use and Open-Source Toolbox for PET Kinetic Analysis. <b>2019</b> , 17, 103-114	2
319	Quantifying SV2A density and drug occupancy in the human brain using [C]UCB-J PET imaging and subcortical white matter as reference tissue. <b>2019</b> , 46, 396-406	45
318	Spatially Adaptive Varying Correlation Analysis for Multimodal Neuroimaging Data. <b>2019</b> , 38, 113-123	2
317	The Value of In Vitro Binding as Predictor of In Vivo Results: A Case for [F]FDDNP PET. <b>2019</b> , 21, 25-34	7
316	Essentials of Quantitative Imaging with PET. <b>2019</b> , 219-233	1
315	Optimized dual-time-window protocols for quantitative [F]flutemetamol and [F]florbetaben PET studies. <b>2019</b> , 9, 32	19
314	Amyloid Ideposition in subcortical stroke patients and effects of educational achievement: A pilot study. <b>2019</b> , 34, 1651-1657	6
313	Evaluation of pharmacokinetic modeling strategies for in-vivo quantification of tau with the radiotracer [F]MK6240 in human subjects. <b>2019</b> , 46, 2099-2111	13
312	The Influence of Hippocampal Dopamine D2 Receptors on Episodic Memory Is Modulated by and Polymorphisms. <b>2019</b> , 31, 1422-1429	2
311	Impact of chronic migraine attacks and their severity on the endogenous Eppioid neurotransmission in the limbic system. <b>2019</b> , 23, 101905	11
310	Multi-Modal Signatures of Tau Pathology, Neuronal Fiber Integrity, and Functional Connectivity in Traumatic Brain Injury. <b>2019</b> , 36, 3233-3243	16
309	Tau deposition is associated with functional isolation of the hippocampus in aging. <b>2019</b> , 10, 4900	39

308	Exercise increases caudate dopamine release and ventral striatal activation in Parkinson's disease. <b>2019</b> , 34, 1891-1900	41
307	PET Measures of D1, D2, and DAT Binding Are Associated With Heightened Tactile Responsivity in Rhesus Macaques: Implications for Sensory Processing Disorder. <b>2019</b> , 13, 29	1
306	Cardiovascular factors are related to dopamine integrity and cognition in aging. 2019, 6, 2291-2303	5
305	AD molecular: Imaging tau aggregates with positron emissions tomography. <b>2019</b> , 165, 107-138	7
304	Mapping the landscape of human dopamine D2/3 receptors with [C]raclopride. 2019, 224, 2871-2882	15
303	A pitfall of white matter reference regions used in [F] florbetapir PET: a consideration of kinetics. <b>2019</b> , 33, 848-854	6
302	μ-Opioid Activity in Chronic TMD Pain Is Associated with COMT Polymorphism. <b>2019</b> , 98, 1324-1331	8
301	Predicting PET-derived demyelination from multimodal MRI using sketcher-refiner adversarial training for multiple sclerosis. <b>2019</b> , 58, 101546	17
300	Optimal timing of tau pathology imaging and automatic extraction of a reference region using dynamic [F]THK5317 PET. <b>2019</b> , 22, 101681	2
299	Accuracy and reliability of [C]PBR28 specific binding estimated without the use of a reference region. <b>2019</b> , 188, 102-110	16
298	Sleep as a Potential Biomarker of Tau and EAmyloid Burden in the Human Brain. <b>2019</b> , 39, 6315-6324	70
297	Human Positron Emission Tomography Neuroimaging. <b>2019</b> , 21, 551-581	24
296	Optimization of preprocessing strategies in Positron Emission Tomography (PET) neuroimaging: A [C]DASB PET study. <b>2019</b> , 199, 466-479	12
295	Alzheimer's pathology targets distinct memory networks in the ageing brain. <b>2019</b> , 142, 2492-2509	56
294	Selective neuronal damage and blood pressure in atherosclerotic major cerebral artery disease. <b>2019</b> , 90, 975-980	2
293	Network Patterns of Beta-Amyloid Deposition in Parkinson's Disease. <b>2019</b> , 56, 7731-7740	9
292	Tau covariance patterns in Alzheimer's disease patients match intrinsic connectivity networks in the healthy brain. <b>2019</b> , 23, 101848	39
291	Kinetic Modeling of Radiotracers. <b>2019</b> , 501-514	1

290	Misery perfusion and amyloid deposition in atherosclerotic major cerebral artery disease. <b>2019</b> , 22, 101762	4
289	Molecular imaging HDACs class IIa expression-activity and pharmacologic inhibition in intracerebral glioma models in rats using PET/CT/(MRI) with [F]TFAHA. <b>2019</b> , 9, 3595	16
288	Effect of Off-Target Binding on F-Flortaucipir Variability in Healthy Controls Across the Life Span. <b>2019</b> , 60, 1444-1451	49
287	Cognitive Control as a 5-HT-Based Domain That Is Disrupted in Major Depressive Disorder. <b>2019</b> , 10, 691	11
286	Expectation effects on brain dopamine responses to methylphenidate in cocaine use disorder. <b>2019</b> , 9, 93	12
285	Measuring longitudinal cognition: Individual tests versus composites. <b>2019</b> , 11, 74-84	27
284	Imaging metabotropic glutamate receptor system: Application of positron emission tomography technology in drug development. <b>2019</b> , 39, 1892-1922	9
283	Vascular Burden Score Impacts Cognition Independent of Amyloid PET and MRI Measures of Alzheimer's Disease and Vascular Brain Injury. <b>2019</b> , 68, 187-196	14
282	Sucrose intake lowers Eppioid and dopamine D2/3 receptor availability in porcine brain. <b>2019</b> , 9, 16918	13
281	Positron emission tomography probes targeting bromodomain and extra-terminal (BET) domains to enable in vivo neuroepigenetic imaging. <b>2019</b> , 55, 12932-12935	11
280	Expression and co-expression of serotonin and dopamine transporters in social anxiety disorder: a multitracer positron emission tomography study. <b>2021</b> , 26, 3970-3979	21
279	Reduced acquisition time PET pharmacokinetic modelling using simultaneous ASL-MRI: proof of concept. <i>Journal of Cerebral Blood Flow and Metabolism</i> , <b>2019</b> , 39, 2419-2432	7
278	Discrepancies in Kappa Opioid Agonist Binding Revealed through PET Imaging. <b>2019</b> , 10, 384-395	16
277	Dorsal striatal dopamine D1 receptor availability predicts an instrumental bias in action learning. <b>2019</b> , 116, 261-270	21
276	Longitudinal tau accumulation and atrophy in aging and alzheimer disease. <b>2019</b> , 85, 229-240	116
275	C957T-mediated Variation in Ligand Affinity Affects the Association between C-raclopride Binding Potential and Cognition. <b>2019</b> , 31, 314-325	11
274	Longitudinal tau and metabolic PET imaging in relation to novel CSF tau measures in Alzheimer's disease. <b>2019</b> , 46, 1152-1163	23
273	A non-human primate model for stable chronic Parkinson's disease induced by MPTP administration based on individual behavioral quantification. <b>2019</b> , 311, 277-287	19

272	Rhesus Macaque Brain Atlas Regions Aligned to an MRI Template. <b>2019</b> , 17, 295-306	7
271	Quantitative PET Imaging in Drug Development: Estimation of Target Occupancy. <b>2019</b> , 81, 3508-3541	10
270	Cerebral serotonin transporter measurements with [C]DASB: A review on acquisition and preprocessing across 21 PET centres. <i>Journal of Cerebral Blood Flow and Metabolism</i> , <b>2019</b> , 39, 210-222 <sup>7.3</sup>	21
269	Dopamine receptor density and white mater integrity: F-fallypride positron emission tomography and diffusion tensor imaging study in healthy and schizophrenia subjects. <b>2020</b> , 14, 736-752	8
268	Validation of Parametric Methods for [C]UCB-J PET Imaging Using Subcortical White Matter as Reference Tissue. <b>2020</b> , 22, 444-452	15
267	Quantitative parametric maps of O-(2-[F]fluoroethyl)-L-tyrosine kinetics in diffuse glioma. <i>Journal of Cerebral Blood Flow and Metabolism</i> , <b>2020</b> , 40, 895-903	4
266	Simultaneous Covariance Inference for Multimodal Integrative Analysis. <b>2020</b> , 115, 1279-1291	3
265	Parametric Imaging With PET and SPECT. <b>2020</b> , 4, 1-23	25
264	Parametric methods for [F]flortaucipir PET. <i>Journal of Cerebral Blood Flow and Metabolism</i> , <b>2020</b> , 40, 365-373	11
263	F-FIBT may expand PET for Emyloid imaging in neurodegenerative diseases. <b>2020</b> , 25, 2608-2619	7
262	High long-term test-retest reliability for extrastriatal C-raclopride binding in healthy older adults. <i>Journal of Cerebral Blood Flow and Metabolism</i> , <b>2020</b> , 40, 1859-1868  7-3	6
261	Different preprocessing strategies lead to different conclusions: A [C]DASB-PET reproducibility study. <i>Journal of Cerebral Blood Flow and Metabolism</i> , <b>2020</b> , 40, 1902-1911	2
260	Test-retest repeatability of [F]Flortaucipir PET in Alzheimer's disease and cognitively normal individuals. <i>Journal of Cerebral Blood Flow and Metabolism</i> , <b>2020</b> , 40, 2464-2474	13
259	Positive association between cerebral grey matter metabolism and dopamine D/D receptor availability in healthy and schizophrenia subjects: An F-fluorodeoxyglucose and F-fallypride positron emission tomography study. <b>2020</b> , 21, 368-382	7
258	Head-to-head comparison of tau positron emission tomography tracers [F]flortaucipir and [F]RO948. <b>2020</b> , 47, 342-354	33
257	The pro-psychotic metabotropic glutamate receptor compounds fenobam and AZD9272 share binding sites with monoamine oxidase-B inhibitors in humans. <b>2020</b> , 162, 107809	7
256	PET Imaging of Pancreatic Dopamine D and D Receptor Density with C-(+)-PHNO in Type 1 Diabetes. <b>2020</b> , 61, 570-576	11

254	Balance between Transmitter Availability and Dopamine D2 Receptors in Prefrontal Cortex Influences Memory Functioning. <b>2020</b> , 30, 989-1000		14
253	Image-based biomedical data modeling and parametric imaging. <b>2020</b> , 461-521		
252	Repurposing radiotracers for myelin imaging: a study comparing 18F-florbetaben, 18F-florbetapir, 18F-flutemetamol,11C-MeDAS, and 11C-PiB. <b>2020</b> , 47, 490-501		16
251	Cholinergic denervation in patients with idiopathic rapid eye movement sleep behaviour disorder. <b>2020</b> , 27, 644-652		12
250	Molecular imaging in biology and pharmacology. <b>2020</b> , 523-560		
249	Spatial patterns of tau deposition are associated with amyloid, ApoE, sex, and cognitive decline in older adults. <b>2020</b> , 47, 2155-2164		5
248	Breast Cancer F-ISO-1 Uptake as a Marker of Proliferation Status. <b>2020</b> , 61, 665-670		15
247	Automatic delineation algorithm of reference region for amyloid imaging based on kinetics. <b>2020</b> , 34, 102-107		2
246	Ethnic disparities in pain processing among healthy adults: Ebpioid receptor binding potential as a putative mechanism. <b>2020</b> , 161, 810-820		6
245	[11C]dihydrotetrabenazine Positron Emission Tomography in Manganese-Exposed Workers. <b>2020</b> , 62, 788-794		3
244	Proper names from story recall are associated with beta-amyloid in cognitively unimpaired adults at risk for Alzheimer's disease. <b>2020</b> , 131, 137-150		8
243	Predicting PET-derived myelin content from multisequence MRI for individual longitudinal analysis in multiple sclerosis. <b>2020</b> , 223, 117308		9
242	Functional genomic analyses uncover APOE-mediated regulation of brain and cerebrospinal fluid beta-amyloid levels in Parkinson disease. <b>2020</b> , 8, 196		4
241	False positive rates in positron emission tomography (PET) voxelwise analyses. <i>Journal of Cerebral Blood Flow and Metabolism</i> , <b>2021</b> , 41, 1647-1657	7.3	4
240	Cortical cholinergic dysfunction correlates with microglial activation in the substantia innominata in REM sleep behavior disorder. <b>2020</b> , 81, 89-93		6
239	Identification and Development of a New Positron Emission Tomography Ligand 4-(2-Fluoro-4-[C]methoxyphenyl)-5-((1-methyl-1-pyrazol-3-yl)methoxy)picolinamide for Imaging Metabotropic Glutamate Receptor Subtype 2 (mGlu). <b>2020</b> , 63, 11469-11483		2
238	Evaluation of the neuroprotective effect of taurine in Alzheimer's disease using functional molecular imaging. <b>2020</b> , 10, 15551		4
237	Quantification of aromatase binding in the female human brain using [C]cetrozole positron emission tomography. <b>2020</b> , 98, 2208-2218		2

236	Sleep Disturbance Forecasts EAmyloid Accumulation across Subsequent Years. 2020, 30, 4291-4298.e3	36
235	PET Imaging of Mitochondrial Function in the Living Brain. 2020,	1
234	Reduced Expression of Cerebral Metabotropic Glutamate Receptor Subtype 5 in Men with Fragile X Syndrome. <b>2020</b> , 10,	8
233	ADORA2A variation and adenosine A receptor availability in the human brain with a focus on anxiety-related brain regions: modulation by ADORA1 variation. <b>2020</b> , 10, 406	3
232	Noninvasive Measurement of [C]PiB Distribution Volume Using Integrated PET/MRI. 2020, 10,	1
231	Distinct effects of beta-amyloid and tau on cortical thickness in cognitively healthy older adults. <b>2021</b> , 17, 1085-1096	8
230	A Multi-Ligand Imaging Study Exploring GABAergic Receptor Expression and Inflammation in Multiple Sclerosis. <b>2020</b> , 22, 1600-1608	2
229	Corticostriatal White Matter Integrity and Dopamine D1 Receptor Availability Predict Age Differences in Prefrontal Value Signaling during Reward Learning. <b>2020</b> , 30, 5270-5280	2
228	Neurophysiological Biomarkers of Parkinson's Disease. <b>2020</b> , 10, 471-480	9
227	Clinical evaluation of [F] JNJ-64326067, a novel candidate PET tracer for the detection of tau pathology in Alzheimer's disease. <b>2020</b> , 47, 3176-3185	10
226	PET technology for drug development in psychiatry. <b>2020</b> , 40, 114-121	9
225	Neurophysiological signatures in Alzheimer's disease are distinctly associated with TAU, amyloid-[] accumulation, and cognitive decline. <b>2020</b> , 12,	28
224	The Effects of Intramuscular Naloxone Dose on Mu Receptor Displacement of Carfentanil in Rhesus Monkeys. <b>2020</b> , 25,	4
223	Evaluation of the Neuroprotective Effect of Microglial Depletion by CSF-1R Inhibition in a Parkinson's Animal Model. <b>2020</b> , 22, 1031-1042	8
222	A strategy to account for noise in the X-variable to reduce underestimation in Logan graphical analysis for quantifying receptor density in positron emission tomography. <b>2020</b> , 20, 15	2
221	Deep Brain Stimulation of the Medial Forebrain Bundle in a Rodent Model of Depression: Exploring Dopaminergic Mechanisms with Raclopride and Micro-PET. <b>2020</b> , 98, 8-20	6
220	Visualization of AMPA receptors in living human brain with positron emission tomography. <b>2020</b> , 26, 281-288	24
219	Characterization of F-PM-PBB3 (F-APN-1607) Uptake in the rTg4510 Mouse Model of Tauopathy. <b>2020</b> , 25,	12

218	Repeatability of parametric methods for [F]florbetapir imaging in Alzheimer's disease and healthy controls: A test-retest study. <i>Journal of Cerebral Blood Flow and Metabolism</i> , <b>2021</b> , 41, 569-578	.3	3
217	Simulating the effect of cerebral blood flow changes on regional quantification of [F]flutemetamol and [F]florbetaben studies. <i>Journal of Cerebral Blood Flow and Metabolism</i> , <b>2021</b> , 41, 579-589	.3	7
216	Chemokine Receptor 2-targeted Molecular Imaging in Pulmonary Fibrosis. A Clinical Trial. <b>2021</b> , 203, 78-89		15
215	Brain 5-HT1A Receptor Binding in Multiple System Atrophy: An [F]-MPPF PET Study. <b>2021</b> , 36, 246-251		4
214	Regional Tau Effects on Prospective Cognitive Change in Cognitively Normal Older Adults. <b>2021</b> , 41, 366-375		7
213	Analysis of Four-Dimensional Data for Total Body PET Imaging. <b>2021</b> , 16, 55-64		1
212	Kinetic Modelling and Test-Retest Reproducibility for the Dopamine DR Radioligand [C]SCH23390 in Healthy and Diseased Mice. <b>2021</b> , 23, 208-219		3
211	Quantification of SV2A Binding in Rodent Brain Using [F]SynVesT-1 and PET Imaging. <b>2021</b> , 23, 372-381		6
<b>21</b> 0	Serotonergic System Impacts Levodopa Response in Early Parkinson's and Future Risk of Dyskinesia. <b>2021</b> , 36, 389-397		6
209	Dopaminergic Nigrostriatal Connectivity in Early Parkinson Disease: In Vivo Neuroimaging Study of C-DTBZ PET Combined with Correlational Tractography. <b>2021</b> , 62, 545-552		7
208	New PET radiopharmaceuticals for imaging CNS diseases. <b>2021</b> ,		
207	Pharmacokinetic Modeling. 2021, 1625-1631		O
206	Regional amyloid accumulation predicts memory decline in initially cognitively unimpaired individuals. <b>2021</b> , 13, e12216		1
205	Optimized Methodology for Reference Region and Image-Derived Input Function Kinetic Modeling in Preclinical PET. <b>2021</b> , 1-1		О
204	Preliminary Investigation of a Novel 18F Radiopharmaceutical for Imaging CB2 Receptors in a SOD Mouse Model. <b>2021</b> , 74, 443		2
203	Pharmacokinetic neuroimaging to study the dose-related brain kinetics and target engagement of buprenorphine in vivo. <b>2021</b> , 46, 1220-1228		1
202	PET imaging reveals early and progressive dopaminergic deficits after intra-striatal injection of preformed alpha-synuclein fibrils in rats. <b>2021</b> , 149, 105229		14
201	Spatially constrained kinetic modeling with dual reference tissues improves F-flortaucipir PET in studies of Alzheimer disease. <b>2021</b> , 48, 3172-3186		1

200	Association of Memory Impairment With Concomitant Tau Pathology in Patients With Cerebral Amyloid Angiopathy. <b>2021</b> , 96, e1975-e1986	2
199	Molecular Imaging Approaches in Dementia. <b>2021</b> , 298, 517-530	8
198	Uses of Human MR and PET Imaging in Research of Neurodegenerative Brain Diseases. <b>2021</b> , 18, 661-672	1
197	Improving contrast between gray and white matter of Logan graphical analysis' parametric images in positron emission tomography through least-squares cubic regression and principal component analysis. <b>2021</b> ,	2
196	Dopaminergic Regulation of Reward System Connectivity Underpins Pain and Emotional Suffering in Migraine. <b>2021</b> , 14, 631-643	3
195	Principal Component Analysis of Striatal and Extrastriatal D2 Dopamine Receptor Positron Emission Tomography in Manganese-Exposed Workers. <b>2021</b> , 182, 132-141	1
194	Kinetic and static analysis of poly-(adenosine diphosphate-ribose) polymerase-1 (PARP-1) targeted F-FluorThanatrace (F-FTT) PET images of ovarian cancer. <b>2021</b> ,	3
193	Strategies to reduce sample sizes in Alzheimer's disease primary and secondary prevention trials using longitudinal amyloid PET imaging. <b>2021</b> , 13, 82	3
192	Reproducibility of findings in modern PET neuroimaging: insight from the NRM2018 grand challenge. <i>Journal of Cerebral Blood Flow and Metabolism</i> , <b>2021</b> , 41, 2778-2796	4
191	A high-resolution in vivo atlas of the human brain's benzodiazepine binding site of GABA receptors. <b>2021</b> , 232, 117878	10
191		10
Í	2021, 232, 117878  Alzheimer's Pathology Is Associated with Dedifferentiation of Intrinsic Functional Memory	
190	2021, 232, 117878  Alzheimer's Pathology Is Associated with Dedifferentiation of Intrinsic Functional Memory Networks in Aging. 2021, 31, 4781-4793	4
190 189	Alzheimer's Pathology Is Associated with Dedifferentiation of Intrinsic Functional Memory Networks in Aging. 2021, 31, 4781-4793  Parametric imaging of dual-time window [F]flutemetamol and [F]florbetaben studies. 2021, 234, 117953	2
190 189 188	Alzheimer's Pathology Is Associated with Dedifferentiation of Intrinsic Functional Memory Networks in Aging. 2021, 31, 4781-4793  Parametric imaging of dual-time window [F] flutemetamol and [F] florbetaben studies. 2021, 234, 117953  Longitudinal change in TSPO PET imaging in progressive multiple sclerosis. 2021, 8, 1755-1759  F-florbetapir PET/MRI for quantitatively monitoring myelin loss and recovery in patients with	2
190 189 188	Alzheimer's Pathology Is Associated with Dedifferentiation of Intrinsic Functional Memory Networks in Aging. 2021, 31, 4781-4793  Parametric imaging of dual-time window [F] flutemetamol and [F] florbetaben studies. 2021, 234, 117953  Longitudinal change in TSPO PET imaging in progressive multiple sclerosis. 2021, 8, 1755-1759  F-florbetapir PET/MRI for quantitatively monitoring myelin loss and recovery in patients with multiple sclerosis: A longitudinal study. 2021, 37, 100982  Astrocyte activation imaging with 11C-acetate and amyloid PET in mild cognitive impairment due to	4 2 2
190 189 188 187	Alzheimer's Pathology Is Associated with Dedifferentiation of Intrinsic Functional Memory Networks in Aging. 2021, 31, 4781-4793  Parametric imaging of dual-time window [F]flutemetamol and [F]florbetaben studies. 2021, 234, 117953  Longitudinal change in TSPO PET imaging in progressive multiple sclerosis. 2021, 8, 1755-1759  F-florbetapir PET/MRI for quantitatively monitoring myelin loss and recovery in patients with multiple sclerosis: A longitudinal study. 2021, 37, 100982  Astrocyte activation imaging with 11C-acetate and amyloid PET in mild cognitive impairment due to Alzheimer pathology. 2021, 42, 1261-1269  Preclinical and clinical study on [F]DRKXH1: a novel Emyloid PET tracer for Alzheimer's disease.	4 2 2 0

182	Evaluation of [F]-JNJ-64326067-AAA tau PET tracer in humans. <i>Journal of Cerebral Blood Flow and Metabolism</i> , <b>2021</b> , 41, 3302-3313	7.3	3
181	Molecular imaging of the serotonin transporter availability and occupancy by antidepressant treatment in late-life depression. <b>2021</b> , 194, 108447		2
180	Different Alterations of Agonist and Antagonist Binding to 5-HT1A Receptor in a Rat Model of Parkinson's Disease and Levodopa-Induced Dyskinesia: A MicroPET Study. <b>2021</b> , 11, 1257-1269		1
179	Sex differences in dopamine integrity and brain structure among healthy older adults: Relationships to episodic memory. <b>2021</b> , 105, 272-279		1
178	Positron emission tomography imaging of serotonin degeneration and beta-amyloid deposition in late-life depression evaluated with multi-modal partial least squares. <b>2021</b> , 11, 473		0
177	Test-retest reproducibility of cerebral adenosine A receptor quantification using [C]preladenant. <b>2021</b> , 1		
176	Rapid high-quality PET Patlak parametric image generation based on direct reconstruction and temporal nonlocal neural network. <b>2021</b> , 240, 118380		1
175	Dopamine release during psychological stress in euthymic bipolar I disorder: a Positron Emission Tomography study with [C]raclopride. <b>2021</b> , 295, 724-732		
174	Concepts for design and analysis of receptor radiopharmaceuticals: The Receptor-Binding Radiotracers series of meetings provided the foundation. <b>2021</b> , 92, 5-23		2
173	4D deep image prior: dynamic PET image denoising using an unsupervised four-dimensional branch convolutional neural network. <b>2021</b> , 66, 015006		18
172	Tau aggregation and increased neuroinflammation in athletes after sports-related concussions and in traumatic brain injury patients - A PET/MR study. <b>2021</b> , 30, 102665		5
171	Tracer Kinetic Modeling: Basics and Concepts. <b>2021</b> , 531-549		
170	Quantification of Tau Load in Alzheimer's Disease Clinical Trials Using Positron Emission Tomography. <b>2018</b> , 1750, 221-229		1
169	Quantitative approaches to amyloid imaging. <b>2011</b> , 680, 201-25		3
168	Exact Parameter Determination for Parkinson Disease Diagnosis with PET Using an Algebraic Approach. <b>2007</b> , 110-124		3
167	Compartmental Modeling in Emission Tomography. <b>2012</b> , 1065-1081		1
166	Ligand Tracer Kinetics: Theory and Application. <b>2004</b> , 75-93		4
165	Serotonin Synthesis Studied with Positron Emission Tomography (PET). <b>2014</b> , 687-709		1

#### (2020-1998)

164	Limitations of Binding Potential as a Measure of Receptor Function: A Two-Point Correction for the Effects of Mass. <b>1998</b> , 407-413	2
163	Estimation of Binding Potential for the 5HT2 Receptor Ligand [18F]Setoperone by a Noninvasive Reference Region Graphical Method. <b>1998</b> , 421-426	1
162	Effect of Population k2 Values in Graphical Estimation of DV Ratios of Reversible Ligands. 2001, 127-129	2
161	Comparison of multiple tau-PET measures as biomarkers in aging and Alzheimer's disease. <b>2017</b> , 157, 448-463	228
160	Conscientiousness is associated with less amyloid deposition in cognitively normal aging. <b>2020</b> , 35, 993-999	2
159	Positron Emission Tomography Compartmental Models: A Basis Pursuit Strategy for Kinetic Modeling. <i>Journal of Cerebral Blood Flow and Metabolism</i> , <b>2002</b> , 1425-1439	73
158	In Vivo Measurement of Receptor Density and Affinity: Comparison of the Routine Sequential Method With a Nonsequential Method in Studies of Dopamine D2 Receptors With [11C]Raclopride.  Journal of Cerebral Blood Flow and Metabolism, 2003, 280-284	5
157	OASIS-3: Longitudinal Neuroimaging, Clinical, and Cognitive Dataset for Normal Aging and Alzheimer Disease.	81
156	Kinfitr han open source tool for reproducible PET modelling: validation and evaluation of test-retest reliability.	2
155	Chemokine receptor 2-targeted molecular imaging in pulmonary fibrosis.	0
154	A High-Resolution In Vivo Atlas of the Human Brain Benzodiazepine Binding Site of GABAA Receptors.	3
153	In vivo characterization and quantification of neurofibrillary tau PET radioligand [18F]MK-6240 in humans from Alzheimer∄ disease dementia to young controls.	3
152	kinfitr: Reproducible PET Pharmacokinetic Modelling in R.	4
151	CT-guided PET parametric image reconstruction using deep neural network without prior training data. <b>2019</b> ,	7
150	PET imaging of brain macrophages using the peripheral benzodiazepine receptor in a macaque model of neuroAIDS. <b>2004</b> , 113, 981-989	34
149	PET imaging of brain macrophages using the peripheral benzodiazepine receptor in a macaque model of neuroAIDS. <b>2004</b> , 113, 981-9	30
148	Quantification and reliability of [C]VC - 002 binding to muscarinic acetylcholine receptors in the human lung - a test-retest PET study in control subjects. <b>2020</b> , 10, 59	3
147	Kinfitr´-´an open-source tool for reproducible PET modelling: validation and evaluation of test-retest reliability. <b>2020</b> , 10, 77	7

146	[C]PIB amyloid quantification: effect of reference region selection. <b>2020</b> , 10, 123	4
145	Levodopa effects on [ (11)C]raclopride binding in the resting human brain. <b>2015</b> , 4, 23	14
144	Serotonin transporter occupancy of SKL10406 in humans: comparison of pharmacokinetic-pharmacodynamic modeling methods for estimation of occupancy parameters. <b>2014</b> , 22, 83	1
143	Detection of pancreatic carcinomas by imaging lactose-binding protein expression in peritumoral pancreas using [18F]fluoroethyl-deoxylactose PET/CT. <b>2009</b> , 4, e7977	19
142	Adenosine A(2A) receptors measured with [C]TMSX PET in the striata of Parkinson's disease patients. <b>2011</b> , 6, e17338	105
141	Genotype and ancestry modulate brain's DAT availability in healthy humans. <b>2011</b> , 6, e22754	46
140	Changes in striatal dopamine release associated with human motor-skill acquisition. <b>2012</b> , 7, e31728	22
139	The role of serotonin in sleep disordered breathing associated with Parkinson disease: a correlative [11C]DASB PET imaging study. <b>2012</b> , 7, e40166	28
138	Brain imaging of vesicular monoamine transporter type 2 in healthy aging subjects by 18F-FP-(+)-DTBZ PET. <b>2013</b> , 8, e75952	19
137	Building up analgesia in humans via the endogenous Eppioid system by combining placebo and active tDCS: a preliminary report. <b>2014</b> , 9, e102350	54
136	Automated movement correction for dynamic PET/CT images: evaluation with phantom and patient data. <b>2014</b> , 9, e103745	16
135	18F-Mefway PET imaging of serotonin 1A receptors in humans: a comparison with 18F-FCWAY. <b>2015</b> , 10, e0121342	9
134	Striatal Dopamine D2/D3 Receptor Availability Is Associated with Executive Function in Healthy Controls but Not Methamphetamine Users. <b>2015</b> , 10, e0143510	7
133	In Vivo Evaluation of Blood Based and Reference Tissue Based PET Quantifications of [11C]DASB in the Canine Brain. <b>2016</b> , 11, e0148943	3
132	Normal Striatal Vesicular Acetylcholine Transporter Expression in Tourette Syndrome. 2017, 4,	11
131	tacmagic: Positron emission tomography analysis in R. <b>2019</b> , 4, 1281	1
130	Dexmethylphenidate hydrochloride in the treatment of attention deficit hyperactivity disorder. <b>2006</b> , 2, 467-73	5
129	Considerations in the Development of Reversibly Binding PET Radioligands for Brain Imaging. <b>2016</b> , 23, 1818-69	110

128	Unidirectional Influx and Net Accumulation of PIB. 2008, 2, 114-25	44
127	[German Society of Nuclear Medicine procedure guideline on beta-amyloid brain PET imaging]. <b>2016</b> , 55, 129-37	3
126	Occupancy of A Nicotinic Acetylcholine Receptors in the Brain by Tropisetron: A Positron Emission Tomography Study Using [(11)C]CHIBA-1001 in Healthy Human Subjects. <b>2011</b> , 9, 111-6	21
125	Direct Reconstruction of Linear Parametric Images from Dynamic PET Using Nonlocal Deep Image Prior. <b>2021</b> , PP,	3
124	Comparison of Invasive and Non-invasive Estimation of [C]PBR28 Binding in Non-human Primates. <b>2021</b> , 1	
123	[F](2,4)-4-Fluoroglutamine as a New Positron Emission Tomography Tracer in Myeloma. <b>2021</b> , 11, 760732	2
122	In vivo staging of regional amyloid progression in healthy middle-aged to older people at risk of Alzheimer's disease. <b>2021</b> , 13, 178	1
121	Measuring the BP of Four Dopaminergic Tracers Utilizing a Tissue Input Function. <b>2001</b> , 131-137	
120	A New Linear Parametric Imaging Algorithm Derived from a Simplified Reference Tissue Model for Ligand-Receptor Dynamic PET Studies. <b>2002</b> , 33-39	
119	Comparison between Bolus and Infusion [11C]Raclopride Delivery for the Quantification of Dopamine Release. <b>2002</b> , 71-75	
118	Quantification of Expioid Receptor Binding with [11C]Carfentanil. 2002, 27-32	
117	Wavelet Methods for the Mathematical and Statistical Modeling of PET Images. <b>2002</b> , 101-106	
116	61. Analysis of 123I-FPCIT (DATSCANTM) binding in normal volunteers and in patients with Parkinson disease. <b>2002</b> , 23, 401-402	
115	Techniques for Parametric Imaging. <b>2008</b> , 137-IX	1
114	Molecular Imaging in Biology and Pharmacology. 2008, 457-XLV	
113	Tracer Kinetic Modeling: Basics and Concepts. <b>2010</b> , 333-351	1
112	Imaging in Neurology Research III: Focus on Neurotransmitter Imaging. <b>2011</b> , 515-541	
111	Imaging in Drug Development. <b>2014</b> , 731-746	

110	Imaging of Central Benzodiazepine Receptors in Chronic Cerebral Ischemia. 2014, 213-227	
109	Imaging Histamine Receptors Using PET and SPECT. <b>2014</b> , 331-376	
108	Tracer Kinetic Modelling. <b>2014</b> , 59-73	
107	Intra-bone Marrow Transplant (IBMT) of Cord Blood (CB) Cells: A Transplant Approach that Tries to Optimize Seeding Efficiency and Trafficking of Hematopoietic Stem Cells (HSCs). <b>2014</b> , 203-210	
106	Encyclopedia of Computational Neuroscience. <b>2014</b> , 1-14	
105	Kinetic Modeling: Achieving Computer Platform Independence with Java. 1998, 353-356	
104	Computational Methods for Molecular Imaging. <b>2015</b> , 3-14	
103	Hybrid Imaging in Cerebrovascular Disease: Ischemic Stroke. <b>2016</b> , 251-262	
102	Enhanced detection of early photons in time-domain optical tomography using dead-time characteristics of SPADs. <b>2016</b> ,	
101	Dynamic PET imaging. <b>2017</b> , 321-335	
101	Dynamic PET imaging. 2017, 321-335  Molecular Contrast Agents. 2018, 131-184	
		1
100	Molecular Contrast Agents. 2018, 131-184  First in-human PET study of 3 novel tau radiopharmaceuticals: [11C]RO6924963, [11C]RO6931643,	1
100	Molecular Contrast Agents. 2018, 131-184  First in-human PET study of 3 novel tau radiopharmaceuticals: [11C]RO6924963, [11C]RO6931643, and [18F]RO6958948.  Observation of magnetic susceptibility changes within the thalamus: a comparative study between	1
100 99 98	Molecular Contrast Agents. 2018, 131-184  First in-human PET study of 3 novel tau radiopharmaceuticals: [11C]RO6924963, [11C]RO6931643, and [18F]RO6958948.  Observation of magnetic susceptibility changes within the thalamus: a comparative study between healthy and Parkinson® disease afflicted cynomolgus monkeys using 7 T MRI. 2019, 10,	
<ul><li>100</li><li>99</li><li>98</li><li>97</li></ul>	Molecular Contrast Agents. 2018, 131-184  First in-human PET study of 3 novel tau radiopharmaceuticals: [11C]RO6924963, [11C]RO6931643, and [18F]RO6958948.  Observation of magnetic susceptibility changes within the thalamus: a comparative study between healthy and Parkinson® disease afflicted cynomolgus monkeys using 7 T MRI. 2019, 10,  Sex differences in methylphenidate-induced dopamine increases in ventral striatum. 2021,  Fronto-striatal dopamine D2 receptor availability is associated with cognitive variability in older	
100 99 98 97 96	Molecular Contrast Agents. 2018, 131-184  First in-human PET study of 3 novel tau radiopharmaceuticals: [11C]RO6924963, [11C]RO6931643, and [18F]RO6958948.  Observation of magnetic susceptibility changes within the thalamus: a comparative study between healthy and Parkinson disease afflicted cynomolgus monkeys using 7 T MRI. 2019, 10,  Sex differences in methylphenidate-induced dopamine increases in ventral striatum. 2021,  Fronto-striatal dopamine D2 receptor availability is associated with cognitive variability in older individuals with low dopamine integrity. 2021, 11, 21089  Effects of placebo administration on immune mechanisms and relationships with central	1

92 Compartmental Modeling in Emission Tomography. **2020**, 1-20

91	Expectancy effects on serotonin and dopamine transporters during SSRI treatment of social anxiety disorder: a randomized clinical trial. <b>2021</b> , 11, 559	5
90	Maternal Dopamine Encodes Affective Signals of Human Infants. 2021,	O
89	Reading abilities and dopamine D/D receptor availability: An inverted U-shaped association in subjects with schizophrenia. <b>2021</b> , 223, 105046	O
88	A common polymorphism in the dopamine transporter gene predicts working memory performance and in vivo dopamine integrity in aging. <b>2021</b> , 245, 118707	О
87	Genome-wide association, Mendelian Randomization and polygenic risk score studies converge on a role of Emyloid and APOE locus in Parkinson disease.	
86	Quantitative Analysis of Amyloid [Deposition in Patients with Alzheimer Disease Using Positron Emission Tomography. 220-230	1
85	[F]MPPF and [F]FDG <b>B</b> ET imaging in rats: impact of transport and restraint stress. <b>2020</b> , 10, 112	2
84	Alzheimer pathology is associated with dedifferentiation of functional memory networks in aging.	
83	Tracer Kinetic Modelling. <b>2021</b> , 37-52	
82	The Use of Small Animal Molecular Imaging (PET) Exemplified in a Neurobiological Pathology. <b>2021</b> , 57-92	
81	Imaging of Central Benzodiazepine Receptors in Chronic Cerebral Ischemia. <b>2021</b> , 245-264	
80	18F-AV-1451 positron emission tomography in neuropathological substrates of corticobasal syndrome. <b>2021</b> , 144, 266-277	1
79	Imaging the serotonin transporter during major depressive disorder and antidepressant treatment. <b>2007</b> , 32, 86-102	188
78	Serotonin2A receptor binding potential in people with aggressive and violent behaviour. <b>2008</b> , 33, 499-508	35
77	Role of Kinetic Modeling in Biomedical Imaging. <b>2008</b> , 28, 57-63	3
76	FDG- and amyloid-PET in Alzheimer's disease: is the whole greater than the sum of the parts?. <b>2011</b> , 55, 250-64	29
75	Limitations of SRTM, Logan graphical method, and equilibrium analysis for measuring transient dopamine release with [(11)C]raclopride PET. <b>2013</b> , 3, 247-60	13

74	How to design PET experiments to study neurochemistry: application to alcoholism. 2014, 87, 33-54	7
73	Positron Emission Tomography (PET) and Graphical Kinetic Data Analysis of the Dopamine Neurotransmitter System: An Exercise for an Undergraduate Laboratory Course. <b>2014</b> , 12, A114-22	
72	PET brain kinetics studies of (11)C-ITMM and (11)C-ITDM,radioprobes for metabotropic glutamate receptor type 1, in a nonhuman primate. <b>2014</b> , 4, 260-9	14
71	Comparison of Kinetic Models for Dual-Tracer Receptor Concentration Imaging in Tumors. <b>2014</b> , 1,	12
7º	Simplified estimation of binding parameters based on image-derived reference tissue models for dopamine transporter bindings in non-human primates using [F]FE-PE2I and PET. <b>2017</b> , 7, 246-254	3
69	Quantification methods comparison in brain F-FDOPA PET. <b>2019</b> , 9, 274-281	1
68	Evaluation of quantitative modeling methods in whole-body, dynamic [C]-erlotinib PET. <b>2021</b> , 11, 143-153	O
67	Compartmental Modeling in Emission Tomography. <b>2021</b> , 1431-1450	
66	Four-modality imaging of unmedicated subjects with schizophrenia: F-fluorodeoxyglucose and F-fallypride PET, diffusion tensor imaging, and MRI <b>2021</b> , 320, 111428	1
65	The Aged Striatum: Evidence of Molecular and Structural Changes Using a Longitudinal Multimodal Approach in Mice <b>2022</b> , 14, 795132	O
64	Risk for opioid misuse in chronic pain patients is associated with endogenous opioid system dysregulation <b>2022</b> , 12, 20	О
63	Spatial and temporal dynamics of HDACs class IIa following mild traumatic brain injury in adult rats <b>2022</b> ,	О
62	Validation and test-retest repeatability performance of parametric methods for [C]UCB-J PET <b>2022</b> , 12, 3	
61	Upregulation of Striatal Metabotropic Glutamate Receptor Subtype 1 (mGluR1) in Rats with Excessive Glutamate Release Induced by N-Acetylcysteine <b>2022</b> , 40, 26	О
60	First-in-human evaluation of F-SMBT-1, a novel F-labeled MAO-B PET tracer for imaging reactive astrogliosis <b>2022</b> ,	5
59	Evaluation of the Bynuclein PET radiotracer (d3)-[11C]MODAG-001 in pigs.	
58	Spontaneous remyelination in lesions protects the integrity of surrounding tissues over time in multiple sclerosis <b>2022</b> ,	О
57	Epileptic discharges initiate from brain areas with elevated accumulation of Emino-3-hydroxy-5-methyl-4-isoxazole propionic acid receptors <b>2022</b> , 4, fcac023	O

56	Lack of association between bridging integrator 1 () rs744373 polymorphism and tau-PET load in cognitively intact older adults <b>2022</b> , 8, e12227	
55	Rates of Eamyloid deposition indicate widespread simultaneous accumulation throughout the brain <b>2022</b> , 115, 1-11	
54	Identifying Mild Alzheimer's Disease With First 30-Min C-PiB PET Scan 2022, 14, 785495	
53	Application of correlated component analysis to dynamic PET time-activity curves denoising. <b>2021</b> , 2021, 3680-3683	
52	NRM 2021 Abstract Booklet Journal of Cerebral Blood Flow and Metabolism, <b>2021</b> , 41, 11-309 7-3	
51	Brain opioid segments and striatal patterns of dopamine release induced by naloxone and morphine. <b>2021</b> ,	1
50	PET imaging of brain aromatase in humans and rhesus monkeys by C-labeled cetrozole analogs. <b>2021</b> , 11, 23623	O
49	Trapping of Nicotinic Acetylcholine Receptor Ligands Assayed by in vitro Cellular Studies and in vivo PET Imaging.	O
48	Simultaneous Multifactor Bayesian Analysis (SiMBA) of PET Time Activity Curve Data 2022, 256, 119195	1
47	Beyond monoamines: I. Novel targets and radiotracers for Positron emission tomography imaging in psychiatric disorders <b>2022</b> ,	1
46	Dynamic regulation of neural variability during working memory reflects dopamine, functional integration, and decision-making.	1
45	Continuous but not intermittent theta burst stimulation decreases striatal dopamine release and cortical excitability <b>2022</b> , 354, 114106	
44	Cortical D1 and D2 dopamine receptor availability modulate methylphenidate-induced changes in brain activity and functional connectivity. <b>2022</b> , 5,	
43	Imaging the fetal nonhuman primate brain with SV2A positron emission tomography (PET).	
42	Rejection sensitivity and mu opioid receptor dynamics associated with mood alterations in response to social feedback. <b>2022</b> , 111505	O
41	Design and Synthesis of Aryl-Piperidine Derivatives as Potent and Selective PET Tracers for Cholesterol 24-Hydroxylase (CH24H).	
40	Unsupervised PET Logan Parametric Image Estimation Using Conditional Deep Image Prior. <b>2022</b> , 102519	1
39	Mu Opioid Receptor Dynamics in Healthy Volunteers with a History of Childhood Maltreatment.	

38 Kinetic Models for PET/SPECT Imaging. **2022**, 1753-1763

37	Metacognition, cortical thickness, and tauopathy in aging. <b>2022</b> ,	
36	Longitudinal Dopamine D2 Receptor Changes and Cerebrovascular Health in Aging. 10.1212/WNL.0000	000000200891
35	Neuronal Alterations in Secondary Thalamic Degeneration Due to Cerebral Infarction: A 11 C-Flumazenil Positron Emission Tomography Study.	O
34	A quantitative in vivo imaging platform for tracking pathological tau depositions and resultant neuronal death in a mouse model.	0
33	Measurement of Striatal Dopamine Release Induced by Neuropsychological Stimulation in Positron Emission Tomography With Dual Injections of [11C]Raclopride. 13,	
32	Design and synthesis of aryl-piperidine derivatives as potent and selective PET tracers for cholesterol 24-hydroxylase (CH24H). <b>2022</b> , 240, 114612	0
31	Practical considerations for navigating the regulatory landscape of non-clinical studies for clinical translation of radiopharmaceuticals. <b>2022</b> , 7,	O
30	Multi-method investigation of factors influencing amyloid onset and impairment in three cohorts.	4
29	Dopamine D 2/3 receptor availabilities in striatal and extrastriatal regions of the adult human brain: Comparison of four methods of analysis.	
28	Trapping of Nicotinic Acetylcholine Receptor Ligands Assayed by in vitro Cellular Studies and in vivo PET Imaging. JN-RM-2484-21	
27	Evaluation of an image-derived input function for kinetic modeling of nicotinic acetylcholine receptor-binding PET ligands.	
26	Evaluation of the Bynuclein PET radiotracer (d3)-[11C]MODAG-001 in pigs. <b>2022</b> ,	1
25	Four decades of mapping and quantifying neuroreceptors at work in vivo by positron emission tomography. 16,	O
24	Preliminary evidence for the sequentially mediated effect of racism-related stress on pain sensitivity through sleep disturbance and corticolimbic opioid receptor function. <b>2022</b> ,	0
23	Serotonin and dopamine transporter availability in social anxiety disorder after combined treatment with escitalopram and cognitive-behavioral therapy. <b>2022</b> , 12,	O
22	Assessment of cholesterol homeostasis in the living human brain. 2022, 14,	0
21	A pilot study comparing myelin measurements from myelin water imaging and 11C-PIB PET in multiple sclerosis. <b>2022</b> , 68, 104238	O

20	Advances in molecular neuroimaging methodology. 2023, 53-66	О
19	Kinetic evaluation and assessment of longitudinal changes in reference region and extracerebral [18F]MK-6240 PET uptake. 0271678X2211421	1
18	Dosimetry and efficacy of a tau PET tracer [18F]MK-6240 in Japanese healthy elderly and patients with Alzheimer disease.	0
17	Noninvasive Quantitative PET Imaging in Humans of the Pancreatic Beta-Cell Mass Biomarkers VMAT2 and Dopamine D2/D3 Receptors In Vivo. <b>2023</b> , 61-74	O
16	Reduced D 2 / D 3 Receptor Binding and Glucose Metabolism in a Macaque Model of Huntington's Disease.	О
15	Dopamine D2/3 Receptor Availabilities in Striatal and Extrastriatal Regions of the Adult Human Brain: Comparison of Four Methods of Analysis.	O
14	Molecular Imaging of the Association between Serotonin Degeneration and Beta-Amyloid Deposition in Mild Cognitive Impairment. <b>2023</b> , 103322	0
13	Serotonin transporter availability in physically aggressive personality disordered patients: associations with trait and state aggression, and response to fluoxetine.	Ο
12	Automated production of [11C]butyrate for keto body PET imaging. 2023, 108315	0
11	NiftyPAD - Novel Python Package for Quantitative Analysis of Dynamic PET Data.	O
10	Methods to Verify Expression and Function of DREADDs Using PET. 2023, 263-273	0
9	Synthesis and Biological Evaluation of Enantiomerically Pure (R)- and (S)-[18F]OF-NB1 for Imaging the GluN2B Subunit-Containing NMDA receptors.	O
8	Acute nicotine exposure blocks aromatase in the limbic brain of healthy women: A [11C]cetrozole PET study. <b>2023</b> , 123, 152381	0
7	Discontinuation of methylphenidate after long-term exposure in nonhuman primates. <b>2023</b> , 97, 107173	O
6	Small-animal PET study for noninvasive quantification of transmembrane AMPA receptor regulatory protein B (TARP B) in the brain. 0271678X2311520	O
5	An empirical measure of resilience explains individual differences in the effect of tau pathology on memory change in aging. <b>2023</b> , 3, 229-237	O
4	In vivo Brain Estrogen Receptor Expression By Neuroendocrine Aging And Relationships With Gray Matter Volume, Bio-Energetics, and Clinical Symptomatology.	О
3	Development of near-infrared paired-agent imaging for in vivo quantification of drug receptor occupancy in tumor. 2023,	O

2 Parkinson's disease. **2023**, 337-361

Ο

Dynamics of AMPA receptors regulate epileptogenesis in patients with epilepsy. **2023**, 101020

О